Ph.D. Thesis

"Tailoring Magnetic, Mechanical and Dielectric Properties of Magnetorheological Elastomers based on Natural Rubber and Iron by Magnetic Field Assisted Curing for Possible Applications"

Submitted to Cochin University of Science and Technology
in partial fulfillment of the requirements
for the award of the degree of

Doctor of Philosophy

by

M. P. Vasudevan Nambudiry

COCHIN UNIVERSITY OF
SCIENCE AND TECHNOLOGY

Department of Physics
Cochin University of Science & Technology
Cochin- 682 022, India.

October 2015

Tailoring Magnetic, Mechanical and Dielectric Properties of Magnetorheological Elastomers based on Natural Rubber and Iron by Magnetic Field Assisted Curing for Possible Applications

Author
M. P. Vasudevan Nambudiry
Moovidathu Mecheri Mana
GRA 42-A, West Kadungalloor
Aluva – 683 110
Kerala, India

Supervising Guide
Prof. M. R. Anantharaman
Department of Physics
Cochin University of Science & Technology
Cochin – 682 022, India.

October 2015

Cover page illustration
Front Cover: Schematic of MRE based Dynamic Vibration Absorber.
Back Cover: SEM image of MRE sheets based on Carbonyl Iron and Natural Rubber under field assisted curing.

Dedicated to all who have showered great support, strength and solace………..

Department of Physics
Cochin University of Science and Technology
Cochin − 682022

Certificate

Certified that the present Ph.D. thesis work entitled **"Tailoring Magnetic, Mechanical and Dielectric Properties of Magnetorheological Elastomers based on Natural Rubber and Iron by Magnetic Field Assisted Curing for Possible Applications"** submitted by **Mr. M. P. Vasudevan Nambudiry** is an authentic record of research work carried out by him under my supervision in the Department of Physics in partial fulfillment of the requirements for the Degree of Doctor of Philosophy of Cochin University of Science and Technology, and has not been included in any other thesis submitted previously for the award of any degree.
.

October 2015
Cochin -22

Prof. M. R. Anantharaman

Supervising Guide
Department of Physics
Cochin University of Science and Technology

Department of Physics
Cochin University of Science and Technology
Cochin − 682022

Certificate

Certified that all the relevant corrections and modifications suggested by the audience during the Pre-synopsis seminar and recommended by the Doctoral Committee of the candidate has been incorporated in the thesis.

October 2015
Cochin -22

Prof. M. R. Anantharaman

Supervising Guide
Department of Physics
Cochin University of Science and Technology

Declaration

I hereby declare that the work presented in this thesis entitled **"Tailoring Magnetic, Mechanical and Dielectric Properties of Magnetorheological Elastomers based on Natural Rubber and Iron by Magnetic Field Assisted Curing for Possible Applications"** is based on the original research work carried out by me under the guidance and supervision of Prof. M R Anantharaman, Department of Physics, Cochin University of Science and Technology, Cochin-682 022 and no part of the work reported in this thesis has been presented for the award of any other degree from any other institution.

October 2015
Cochin-22

M. P. Vasudevan Nambudiry

ACKNOWLEDGEMENT

PREFACE

If magnetism is universal in nature, magnetic materials are ubiquitous. A life without magnetism is unthinkable and a day without the influence of a magnetic material is unimaginable. They find innumerable applications in the form of many passive and active devices namely, compass, electric motor, generator, microphone, loud speaker, maglev train, magnetic resonance imaging, data recording and reading, hadron collider etc. The list is endless. Such is the influence of magnetism and magnetic materials in ones day to day life. With the advent of nanoscience and nanotechnology, along with the emergence of new areas/fields such as spintronics, multiferroics and magnetic refrigeration, the importance of magnetism is ever increasing and attracting the attention of researchers worldwide. The search for a fluid which exhibits magnetism has been on for quite some time. However nature has not bestowed us with a magnetic fluid and hence it has been the dream of many researchers to synthesize a magnetic fluid which is thought to revolutionize many applications based on magnetism. The discovery of a magnetic fluid by Jacob Rabinow in the year 1952 paved the way for a new branch of Physics/Engineering which later became magnetic fluids. This gave birth to a new class of material called magnetorheological materials. Magnetorheological materials are considered superior to electrorheological materials in that magnetorheology is a contactless operation and often inexpensive.

Most of the studies in the past on magnetorheological materials were based on magnetic fluids. Recently the focus has been on the solid state analogue of magnetic fluids which are called Magnetorheological Elastomers (MREs). The very word magnetorheological elastomer implies that the rheological properties of these materials can be altered by the influence of an external applied magnetic field and this process is reversible. If the application of an external magnetic field modifies the viscosity of a magnetic fluid, the effect of external magnetic stimuli on a magnetorheological elastomer is in the modification of its stiffness. They are reversible too. Magnetorheological materials exhibit variable stiffness and find applications in adaptive structures of aerospace, automotive civil and electrical engineering applications. The major advantage of MRE is that the particles are not able to settle with time and hence there is no need of a vessel to hold it. The possibility of hazardous waste leakage is no more with a solid MRE. Moreover, the particles in a solid MRE will not affect the performance and durability of the equipment. Usually MR solids work only in the pre yield region while MR fluids, typically work in the post yield state.

The application of an external magnetic field modifies the stiffness constant, shear modulus and loss modulus which are complex quantities. In viscoelastic materials a part of the input energy is stored and released during each cycle and a part is dissipated as heat. The storage modulus G' represents the capacity of the material to store energy of deformation, which contribute to material stiffness. The loss modulus

G'' represents the ability of the material to dissipate the energy of deformation. Such materials can find applications in the form of adaptive vibration absorbers (ATVAs), stiffness tunable mounts and variable impedance surfaces. MREs are an important material for automobile giants and became the focus of this research for eventual automatic vibration control, sound isolation, brakes, clutches and suspension systems.

Since magnetorheological elastomers are essentially composites consisting of magnetic filler hosted in matrices like Natural Rubber or silicone rubber, their crosslinking during curing is critical. In a similar manner, the application of an external magnetic field during curing, determines whether the resultant properties are isotropic or anisotropic. Anisotropy is an essential criteria leading to magnetorheology and can be achieved by the application of an external magnetic field during curing of these samples.

Usually magnetically soft particles are used as fillers in MRE to produce magneto mechanical coupling. Magnetic field induced stiffness is due to magnetic dipolar interaction. The attraction between two magnetic dipoles could lead to an increase in the shear modulus of the material. Stiffness also depends on the volume fraction of the particle, magnitude and frequency of the strain. By measuring the magnetic interaction energy between two dipoles, the strength of magnetic interaction can be calculated and the magnetic interaction energy depends on the dipole moment as well as the chain geometry. From a fundamental perspective minimization of Zeeman energy during these processes are of relevance. The mechanism by which

anisotropy modifies stiffness is a rich area in Physics and warrants thorough investigation.

MREs are also of interest as composite magnetostrictive materials when made in the form of a rod and can be employed as actuators. Fabrication of MRE rods for actuator applications is one of the objectives of this investigation. MRE rods with various loading fraction of fillers will be fabricated and tested. For this a mould with appropriate dimension will be designed and fabricated. This mould will be employed to fabricate rods having appropriate dimensions. Studying the effect of an external magnetic field during curing of the rods is also an intended motivation of the present study. An appropriate set up for field assisted curing of MRE rods also will be fabricated which will be complete with housing and the required power supply. The fabrication of the mould for MRE rods, designing and preparation of magnetic field curing assembly also form one of the objectives of the present study. Having fabricated MRE rods, demonstrating them as actuators is necessary. For this a contact less technique called Laser Doppler Vibrometry will be employed.

A complete experimental setup for this study together with a power amplifier will be assembled. The effect of field curing on the actuation and amplitude of vibration and their dependence on the frequency of applied AC magnetic field during actuation will be investigated. For this MRE rods based on Natural Rubber and iron fillers will be employed. Both field cured samples and pristine rods will be used for the study.

The application of an external magnetic field during curing aligns the magnetic particles along the direction of the magnetic field and carves channels within the matrix creating voids inside the matrix. The morphology of the composite can thus be transformed which in turn modifies the mechanical properties of the MRE. A field cured MRE is thus a potential magneto dielectric material whose dielectric properties can be altered by the application of a magnetic field. The changes in the dielectric properties manifests as magneto capacitative effects. So evaluation of the magneto capacitative effects of these MRE sheets is yet another motive of the present study.

The focus of this thesis is on the fabrication of MRE materials and to tailor its magnetic, mechanical and dielectric properties by field assisted curing for possible applications. Various matrices are available which can be made into composite MRE by impregnating ferromagnetic fillers like iron or Carbonyl Iron which is available commercially, and are in micrometric dimensions embedded in isoprene. Matrices such as silicone rubber, polyurethane or Natural Rubber can play the host. In this work host matrix is Natural Rubber and the fillers chosen are pure and high energy ball milled iron powders and commercially available Carbonyl Iron.

High energy ball milling of pure iron powders result in the reduction of particle size. MRE composites will be fabricated with various loadings of fillers according to a specific recipe. Cross linking is essential when fillers are incorporated and thus the formulation of a recipe is necessary. This is achieved by trial and error

methods. The incorporation of nanometric sized iron powders in a Natural Rubber matrix provides an opportunity to study the size effect on various properties.

Some applications dictate that MREs are in the form of sheets. So fabrication of MRE sheets under the application of an external magnetic field during curing is envisaged. This requires the proper design of a coil system. The design and fabrication of a complete infield curing system is another objective of the present work.

The alignment of particles and carving chains in directions along the surface of the sheet and normal to the sheet affect the morphology and mechanical property as well. For this, two separate magnetic field curing assemblies are required. For creating a field perpendicular to the surface, a coil assembly will be fabricated and for in plane, an assembly consisting of permanent magnets will be fabricated. A mould for the production of MRE sheets having provisions for applying magnetic field in any direction (in plane or out of plane to the surface of the sheet) is to be designed and fabricated. This is another motivation. The surface properties will be investigated using Scanning Electron Microscopy.

Evaluation of magnetic properties of these MRE sheets are all the more important; Hysteresis loop parameters for both in field and out of field cured samples will be evaluated by employing vibrating sample magnetometry. The influence of field curing in creating anisotropy will be studied. Evaluation of magneto-dielectric

properties of these MR sheets is of significance. For this an assembly which will produce an appropriate field during dielectric measurement is to be fabricated. So a setup for this also will be fabricated. The shear modulus and loss modulus of these MRE sheets will also be estimated by subjecting them to Dynamic Mechanical Analyzer studies. The mechanical properties of rods fabricated with and without the application of a magnetic field will be estimated by subjecting the rods to Instron Mechanical Analyser studies in the compression mode.

From a fundamental perspective, an investigation on magnetorheological elastomers can possibly lead to elucidation of mechanisms for the modification of stiffness and enhanced storage modulus. From an application point of view magnetorheological elastomers can be made available for various applications such as adaptive structures of aerospace, automotive, civil and electrical engineering fields by tailoring morphology and mechanical properties.

The objectives of the present investigation are as follows.

1) Design and fabrication of experimental set ups for the preparation of Magnetorheological Elastomer rods as well as sheets.

2) Fabrication of Magnetorheological Elastomer rods and sheets with various loading of iron powders according to a specific recipe.

3) Investigations on the actuating properties of Magnetorheological Elastomer rods by employing Laser Doppler Vibrometry.

4) Evaluation of structural, magnetic, mechanical and dielectric properties of magnetorheological sheets and rods.

5) Correlation of Results.

The proposed thesis is entitled *"Tailoring Magnetic, Mechanical and Dielectric Properties of Magnetorheological Elastomers based on Natural Rubber and Iron by Magnetic Field Assisted Curing for Possible Applications"* and consists of eight chapters.

Chapter 1 gives an introduction to Electrorheology and Magnetorheology. An introduction to magnetic materials and properties of polymer matrices are also discussed.

Chapter 2 describes the design and fabrication of various accessories, moulds, magnet assembly required for the preparation of magnetorheological sheets and rods. Other experimental techniques utilized for characterization of these samples are also dealt with in this chapter. A concise description of Laser Doppler Vibrometric (LDV) technique used for the current study is also given in this chapter.

Chapter 3 briefly discusses the enhanced micro actuation of Magnetorheological Elastomer Rods based on Natural Rubber and Iron under field curing. Effect of Particle size and Loading of magnetic filler on microactuation is also discussed.

In **Chapter 4**, Micro actuation of Magneto Rheological Elastomer rods based on Natural Rubber and Carbonyl Iron is evaluated using Laser Doppler Vibrometry and the details are reported.

Chapter 5 Deals with the mechanical properties of Magneto Rheological Elastomer rods and sheets based on Natural Rubber and milled iron.

Mechanical properties of Magneto Rheological Elastomer rods and sheets based on Carbonyl Iron and Natural Rubber are presented in **Chapter 6.**

Chapter 7 is on the magnetocapacitative effects exhibited by Magnetorheological Elastomer sheets under the influence of a magnetic field.

In **Chapter 8**, the salient observations and the inferences drawn out of these investigations are presented. The scope for improvement and possible future investigations based on these materials are listed in this chapter.

Publication resulted during the course of this PhD programme

Peer reviewed journals

- Enhanced microactuation with magnetic field curing of magnetorheological elastomers based on iron-natural rubber nanocomposites **M.P.Vasudevan**, P.M.Sudeep, I. A. Al-Omari, Philip Kurian, P.M.Ajayan, T.N.Narayanan, M. R. Anantharaman, Bulletin of Materials Science 2015,38:919

- Effect of particle size and loading of magnetic filler on microactuation of magnetorheological rods based on natural rubber and pure iron, **M P Vasudevan**, T N Narayanan, P M Sudeep, Philip Kurian, P M Ajayan, I.A Omari, D Sakthikumar, M R Anantharaman; (Ready for communication)

- Mechanical analysis of magnetorheological elastomers based on carbonyl iron-rubber nanocomposites, **M P Vasudevan**, T N Narayanan, P M Sudeep, Philip Kurian, P M Ajayan, M R Anantharaman (Ready for communication)

- On the dielectric and magnetic properties of magnetorheological elastomers based on carbonyl iron-rubber nanocomposites, **M P Vasudevan**, T N Narayanan, P M Sudeep, Philip Kurian, P M Ajayan, M R Anantharaman (Ready for communication)

Conference Presentations

- **A Smart magnetorheological nanocomposite based on iron and natural rubber**
  National Conference on New horizons in Theoretical and Experimental Physics, Oct 8-10, 2007, Cochin University of Science and Technology, Cochin.

- **Magnetorheological elastomers based on rare earth magnets**
  National Seminar on Recent trends in Conducting Polymers and Polymer Nanostructures, Aug 29-30, 2013, Aquinas College, Cochin

- **Microactuation and mechanical studies of magnetorheological elastomers based on NdFeB-rubber composites**
  National Conference on Emerging Technologies for Processing and Utilization of Beach Sand Minerals, March 1-2, 2013, Cochin

- **Effect of field assisted curing on microactuation of magnetorheological elastomer rods based on natural rubber and micro fine iron**
  National Seminar on Frontiers of Nanotechnology, March 6-7, 2014, Sree Sankara Vidyapeetom College, Valayanchirangara, Perumbavoor.

- **On Rheological Properties of Magneto Rheological Elastomers based on Carbonyl Iron powders and Natural Rubber**

  National Seminar on Current Trends in Material Science ,August 13-14,2014,Aquinas College,Edacochin.

- **Effect of Particle size and Loading of α-Iron on Micro actuation of Magneto Rheological Elastomer Rods based on Natural Rubber and pure Iron**
  International Conference on Magnetic Materials and Applications 2014(ICMAGMA-2014), September 15-17, 2014, Pondicherry University,Pondicherry, India.

Contents

CHAPTER 1

INTRODUCTION

Magneto Rheological Elastomers (MRE) have been the subject of intense research during the past few decades. They exhibit novel properties and are potential materials for new generation devices [1, 2]. These elastomers are new engineering materials included in the category of active materials whose mechanical properties can be controlled by an external magnetic field [3]. They can be utilized in transduction and vice versa. These two important properties of magneto rheological (MR) elastomers give rise to many potential applications in the form of actuators, transducers, automobile suspension systems, clutches, breaks, vibration isolators and dampers [4,5]. This is analogous to the behavior of an MR fluid system or an electro rheological (ER) system [6]. The cross-linked chains of magnetically coupled particles are thought to be responsible for enhancement of its elastic shear modulus under the influence of an external magnetic field [7]. The rheological properties of MR elastomers can be changed continuously, rapidly and reversibly by applying a varying electric or magnetic field [8]. By the use of suitable control mechanism and feedback system they can be thoroughly utilized to sense external perturbations [9].

MREs are the solid state analogues of MR fluids. MRE can provide dynamic stiffness elements capable of operation over a wide range of conditions [10,11]. This controllability in response to an applied magnetic field is achieved by embedding magnetic particles into a cross linked polymeric rubber matrix. During cross linking or curing each particle in MRE is held in position until magnetic or mechanical perturbations induce changes in the configuration of the embedded particles [12,13].

The filler element used in MRE is magnetic in nature. An added advantage of incorporating nanosized fillers in an elastomer matrix is that they reinforce the matrix and improve the mechanical properties. Magnetic field assisted curing of MR

1

elastomers can produce an alignment of magnetic particles in the field direction creating a chain like structure in the host matrix. This can modify the stiffness of the rod and a change in natural frequency of the material is expected. Other than this, addition of filler to a polymer matrix can change the viscosity of the material by therelation

$$\eta F = \eta U (1 + 2.5C) \qquad (1.1)$$

where ηF is the viscosity of the filled sample , ηU is the viscosity of the unfilled sample and C is the volume concentration of the filler [14].

MREs require an elastomer matrix which can be polar or non-polar. Ferromagnetic fillers are incorporated in the matrix according to an operatic recipe. The alignment of particles in the matrix and the formation of chain like structure inside the matrix aids in modifying the stiffness of MRE. This can be achieved by polling the magnetic particles by applying an external magnetic field during curing.

This chapter describes the basic properties of elastomers such as storage modulus, loss modulus and loss factor ($tan\,\delta$). The motivation of the present work is also brought out together with the objectives of the present investigation.

1.1. POLYMER

Elastomers are polymers with special elastic property known as viscoelasticity and having low Young's Modulus and high failure strain when compared to other materials. The term elastomer arises from elastic polymer and sometimes used instead of rubber like substances. The monomers of these polymers are made of carbon,hydrogen,oxygen, and silicon. They are amorphous in nature and their existence is always above the glass transition temperature which facilitates segmental motion in elastomers[15].

Elastomers are also known as thermo sets, which require vulcanization or curing, and at the same time, they are thermoplastic. The linking of polymer chains during vulcanization/curing is known as cross-linking. The cross-linked polymer chains distribute the applied stress and attain the property of elasticity to regain its size and shape on the withdrawal of the deforming force. These cross linkages between monomers actually convert a polymer into an elastomer. In the absence of this linkage, application of stress on a polymer will produce permanent set of deformation having zero elasticity or maximum plasticity [16].

1.2. RHEOLOGY

Rheology is the study of flow or deformation of matter not particularly in the liquid state,but also in the case of soft solids/ solid in the plastic flow region and other similar materialsknown as soft matter. Rheological properties are exhibited by substances having a complex micro structure such as polymers,mud, suspensionlike substances, food and additives, bodily fluids other bio materials coming under the category of soft matter [17].

Fluids with a constant value of viscosity for a specific temperature come under the category of Newtonian fluids. Here the viscosity changes with temperature but does not vary with strain rate. Only few fluids have this constant viscosityand they are known as Newtonian fluids.However, for the other large group of fluids, the viscosity changes with strain rate and are called non Newtonian fluids. Usually viscoelastic properties of elastomers (polymer) are defined on the basis of different parameters including temperature, pressure and time. Other important variables affecting viscoelasticity of a polymer are molecular weight and weight distribution, chemical composition, degree of hardening and crystallinity, types of component concentration, dilution with solvents or plasticizers and mixture with other materials to form composites[18]. The above dependence of viscoelasticity of polymers with such variables can be explained on the basis of molecular theory. This is made possible by

introducing new concepts like free volume,the monomeric friction coefficient and spacing between entanglement loci.These factors can be manipulated to tailorthe physical and chemical properties by altering the microstructure. Viscoelasticity indicates the combined response via, viscous and elastic properties of the materials, which is under strain.

Viscoelasticity of a material is due to motions of flexible polymer molecules and their entanglements and network junctions. Thus,the rearrangement of these polymer molecules for a short range is very rapid while for a long range namely it is very slow. Morethan that,under stress a new assortment of configuration can be obtained. The nature and rates of change of the configurational rearrangements and the nature of the molecular interactions over a wide range of time scales can be obtained by studying viscoelastic properties [19].

The word 'Rheo' is a Greek word which meansflow and 'Ology' means study of. Scientists who study the properties of non-Newtonian fluids are called Rheologists.

1.3. ELETRO AND MAGNETO RHEOLOGY

Electrorheological and Magnetorheological fluids are also known as controllable fluids[20]. They are used in rotary brake of aerobic equipmentand in a linear damper for lorry seat suspensions to enhance the comfort of drivers.Another important application of MR fluid is in magneto rheological finishing of optical components.

They are very much useful in stress transfer and damping devices. Electro and magneto Rheological fluids show a novel property, in that their rheological properties are dramatically altered by applying external electric and magnetic fields respectively. A typical scheme is shown below (Figure 1.1).
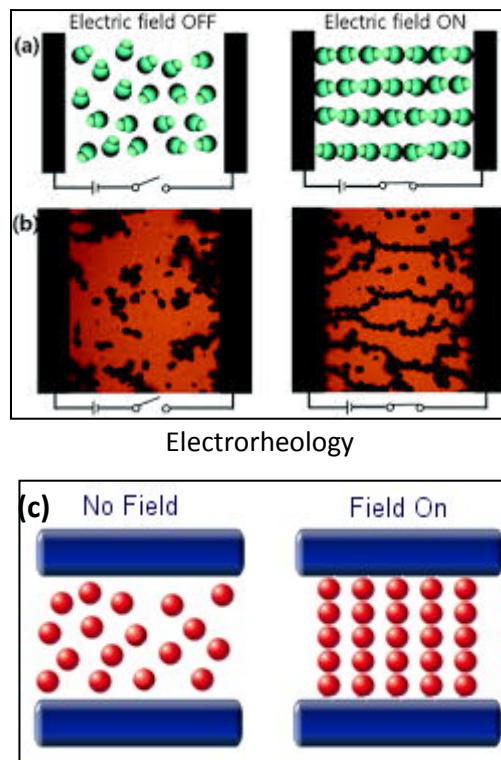
Electrorheology

Figure1.1-(a) Electorheology-schematic (b)Electoreheology- actual case electric field on and off (c)Magnetorheology- schematic

Electrically Active Polymers (EAP) is the solid-state analogue of an Electro Rheological liquid. EAP can be used as sensors, actuators, and artificial muscles. A change in applied voltage changes the molecular composition or structure of the polymer which results in its expansion,contraction or bending (Figure1.2). This motion of EAP is smoother than that and produced bymechanical devices. But energy consumption of EAP is very high and its lifespan is also very short. Artificial muscles fabricated using EAP's can produce natural movements to biomedical and robotic devices[21].
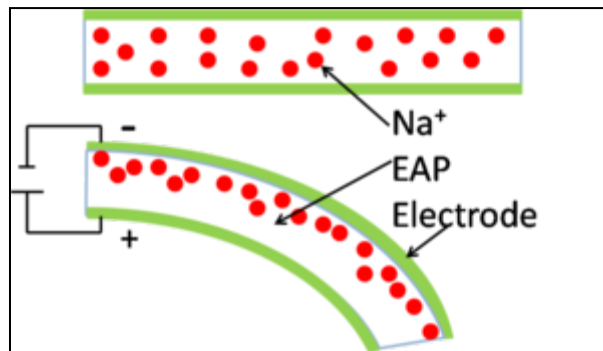
Figure 1.2.Electrically Active Polymer with Na+

1.4. FERROFLUIDS

Ferrofluids are rheological fluids and find innumerable engineering applications. They usually contain ferrite particles that are less than 10 nanometer in diameter and exhibit only weak field dependent rheology.It is also known as a liquid magnet and is a colloidal mixture of magnetic nano particles. A Surfactant locked in the magnetic particles prevents the magnetic particles from being stuck together. Ferrofluids can be synthesized with hydrocarbon as carriers or they can be aqueous based. Hydrocarbon based ferrofluids find engineering applications while aqueous based fluids are known for their biomedical applications [22].
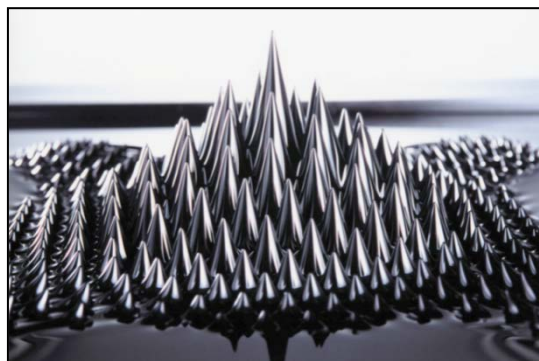
Figure1.3 Effect of magnetic field on a ferrofluid

They are used in high-end speakers and in the laser heads of CD and DVD players. Their important uses are in low friction seals for rotating shaft motors, computer disk driveseals, study of magnetic domain structure in magnetic tapes, rigid and floating disk, geological rocks, magneto optical discs, crystalline and amorphous alloys, garnets, steels, drug delivery etc. In the absence of a magnetic field, all the magnetic particles in ferrofluidare oriented in random directions. By applying a magnetic field, all the suspended magnetic particles align in the direction of the magnetic field producing spikes in the field direction (Figure.1.3). Withdrawal of the field will restore the random orientation of magnetic particles in the carrier fluid [23].

1.5. MAGNETORHEOLOGICAL FLUIDS

As the particle size of the suspended particle in a Ferro fluid is 10nm, its magnetic properties are inferior to its bulk counterparts. So it cannot be used in damper, clutches and brakes. For that, we have to prepare MR liquids using micron size particles as filler.
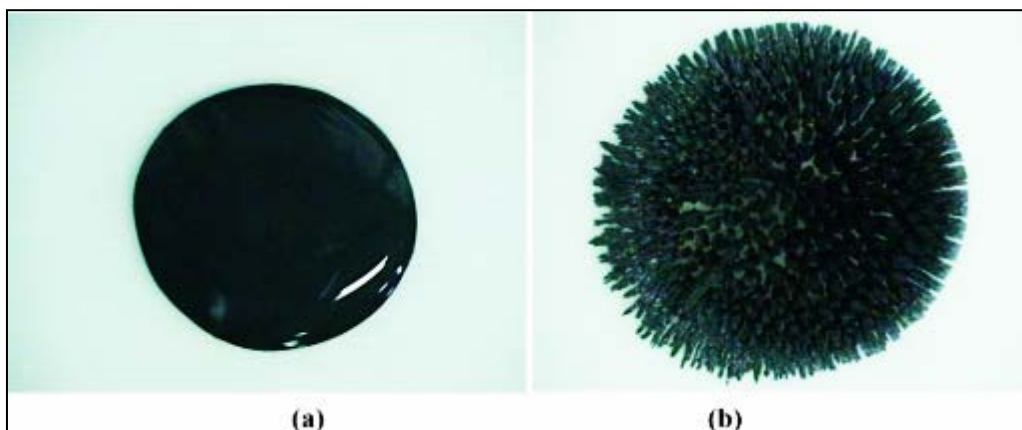
Figure 1.4.MR Fluid (a)magnetic field off(b)magnetic field on

Application of MR fluids are of relevance to engineers and can be used in many damping devices. Here ferrofluids are not preferred [24]. The reason for this is simple. There is a huge difference in the yield shear stress of the MR and ferrofluids,

which affects the maximum force the fluid can provide.MR fluids are more efficient than ER fluids because they possess high field induced inter particle forces and having high yield stress than ER fluids(figure 1.4).

1.6. MAGNETO RHEOLOGICAL ELASTOMERS

MR materials exhibit variable stiffness/multiple stiffness and find applications in adaptive structures of aerospace,automotive civil and electrical engineering applications.MR elastomers (MRE) show excellent mechanical properties.Their rheological properties vary in accordance with the change in applied magnetic field. They are equivalent to MR fluids but are solid state analogues of MR fluids. In MRE,magnetostrictive/ magneto active particles are fixed in the polymer matrix during the curing process. This matrix withstands high strains so as to get the shape of element.The magneto rheological effect of these elastomers depends on dipole interactions between ferromagnetic particles.Under the influence of a magnetic field,particles try to align themselves parallel to the magnetic field. This will produce a strain on aligned chain like microstructures inside the polymer matrix [25] and hence produce a change in dimension of the elastomer as shown in Figure 1.5.
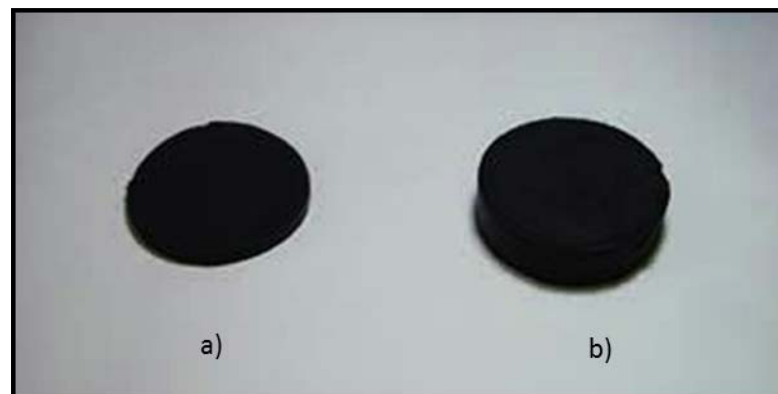
Figure 1.5.M R elastomer a) without field and b) with field

Vulcanization keeps the alignment of particles intact inside the matrix as such and after the completion of curing process elastomers is ready for test or use. It can be

shown that MR rods with aligned microstructure exhibit enhanced MR effect than that with isotropic microstructure.

1.7. FUNDAMENTALS OF MAGNETISM

The earliest experiments with magnetism involved the lodestone, which was magnetite, known for its ability to attract bits of iron. Therefore, magnetism began with ferrites. Now we must explain how a spontaneously magnetized substance exhibits the magnetic properties familiar to us. If all the moments in a macroscopic sample were aligned, a very strong external magnetic field would be produced. This magnetic field represents a great deal of energy. If the moments were rearranged to reduce this external field, then the overall free energy would be reduced and render a more stable state. Magnets play an important role in our daily life. As we are familiar, a variety of devices are employed in the electromagnetic industry [26].

1.7.1. Classes of Magnetic materials

The origin of magnetism is based on orbital and spin motions of electrons and how they interact with one another. Different types of magnetism can be defined on the basis of response of these materials to magnetic fields. It can be seen that matter is magnetic in nature but with some difference in their magnetic properties. In some materials, there is no collective interaction of atomic magnetic moments, whereas other materials exhibit strong magnetic interaction. They are classified into

(1) Diamagnetism
(2) Paramagnetism
(3) Ferromagnetism
(4) Antiferromagnetism
(5) Ferrimagnetism

9

The first two in the group have no collective magnetic interaction and are not magnetically ordered. However, in the last three groups, materials exhibit long-range magnetic order below a certain critical temperature. Ferromagnetic and ferrimagnetic materials are usually considered as "magnetic." The rest are weakly magnetic and considered as "nonmagnetic".

(1) Diamagnetism: It is a fundamental property of all materials, although it is usually very weak. It is due to non-ordering behavior of orbital electrons when placed in a magnetic field [27]. Diamagnetic materials are made up of atoms, which have net magnetic moments. This is because all the orbital shells are filled and no free electrons exist. However, when exposed to a magnetic field, a negative magnetism is produced and therefore susceptibility of these kinds of materials is negative. In zero field, magnetization is also zero. Susceptibility of a diamagnetic substance is temperature dependent. Examples of diamagnetic materials are quartz, calcite and water. A typical diamagnetic material under the influence of a magnetic field is shown below. (Figure 1.6)
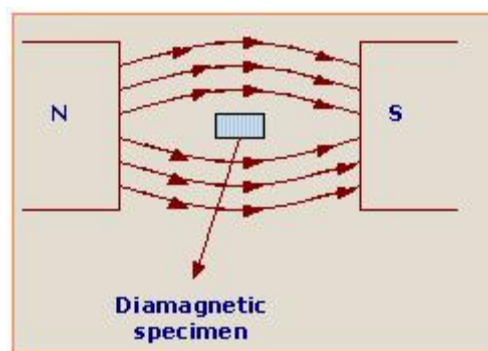
Figure.1.6.Dia magnetism

(2) Paramagnetism: In this type of materials, some of the atom or ions have a net magnetic moment due to unpaired electrons in their partially filled orbits. Like diamagnetism, in this case also individual magnetic moments do not interact magnetically. Thus when the field is removed magnetization is reduced to zero. However, in the presence of a magnetic field, there is a partial alignment

of the atomic magnetic moments in the direction of the field resulting in a net positive magnetization and positive susceptibility of a paramagnetic substance is temperature dependent and based on Curie's Law[28]. Under normal temperature and moderate field, the paramagnetic susceptibility is small. But for very low temperatures and high field it is independent of applied field but depends on total Iron content in it.
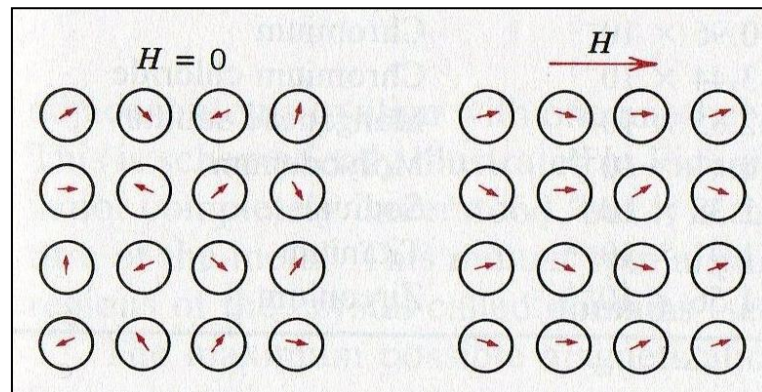
Figure1.7. Paramagnetism

Many minerals containing iron are paramagnetic in nature at room temperature. Some examples are Monotmorillonite(clay),Pyrite (sulphide),Nontronite(Fe rich clay), Biotite (silicate), Siderite (Carbonate). The arrangement of individual magnetic moment under zero and applied field are shown in Figure 1.7.

(3) Ferromagnetism:Unlike paramagnetic materials, the atomic moments in these materials exhibit very strong interactions. They are produced by the electronic exchange forces and result in parallel and antiparallel alignment of atomic moments. The magnitude of these exchange forces are very high and is of the order of 1000 Tesla. The exchange force is a quantum mechanical phenomenon arising out of the relative orientation of the spins of free electrons. Ferromagnetic materials usually show parallel alignment of moments resulting in large net magnetization even in the absence of a magnetic field. A typical ferromagnet in the magnetized and unmagnetized

11

state is shown in figure 1.8. Fe, Co,Ni and many of their alloys exhibit ferromagnetism at room temperature.

Two important characteristics of ferromagnetic materials are (1) spontaneous magnetization and (2) existence of magnetic ordering temperature[29]. The spontaneous magnetization is the net magnetization that existsin a uniformly magnetized microscopic volume in the absence of a field. Its magnitude depends on the spin magnetic moments of electrons.The saturation magnetization of a ferromagnetic material is the maximum induced magnetic moment that can be acquired by it in a magnetizing field. Beyond this field, magnetization remains a constant and hence it is called as saturation magnetization. Saturation magnetization is an intrinsic property, independent of particle size but dependent on temperature. When compared to paramagnetic susceptibility, ferromagnetic susceptibility is very high value. Even if the electronic exchange forces in ferromagnetic material are very large, thermal energy supersedes the exchange and produces a randomizing effect. This happens at a particular temperature called Curie temperature. Below Curie temperature, the ferromagnetic material is ordered and above it they are in disordered state.
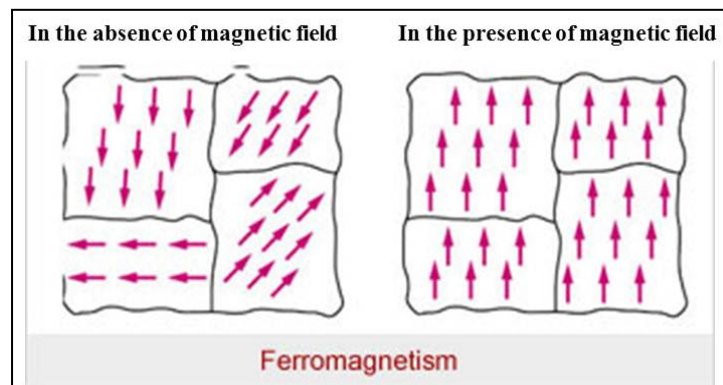
Figure.1.8 Ferromagnetism

Saturation magnetization is the maximum possible magnetization of a material. Remanence is the remaining magnetization when magnetizing field

is removed.Coercivity is the strength of the magnetizing field that is to be applied to the ferromagnetic material in the opposite direction so that remanence becomes zero.

(4) Ferrimagnetism: More complex forms of ordering of magnetic moments can be seen in ionic compounds like oxides. One such magnetic ordering is called ferrimagnetism. In this material, the magnetic structure is composed of two magnetic sub lattices separated by Oxygen. The exchange interactions are mediated by an oxygen anion. These interactions are called indirect or super exchange interactions[29]. The strongest super exchange interactions results in an antiparallel alignment of spins between two sub lattices. In ferrimagnetic materials, these magnetic moments of sub lattices are not equal and result in a net magnetic moment (Figure.1.9). So it is quite similar to ferromagnetism and characterized by spontaneous magnetization, Curie temperature, hysteresis and remanence. Howeverthey possess very different magnetic ordering. Figure 1.9 is the arrangement of moments. Magnetite is a well-known ferrimagnet.
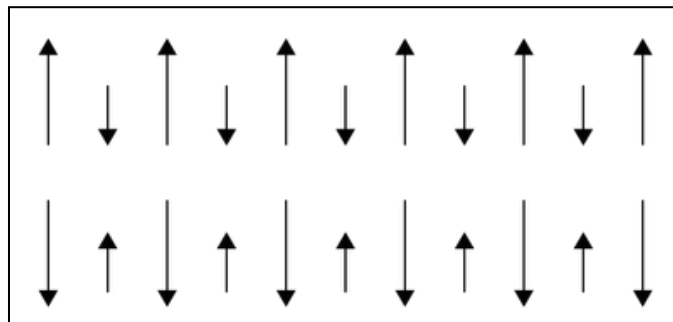
Figure 1.9.Ferrimagnetism

(5) Antiferromagnetism: When magnetic moments of the two sub lattices in a magnetic structure are equal and opposite, the net magnetic moment is zero (figure 1.10). This type of magnetic ordering is called antiferromagnetism. Antiferro magnetic materials also have zero remanence, no hysteresis but a small positive value for susceptibility that varies with temperature. In the case of antiferromagnetism, there is a critical temperature called Neel temperature,

above which the susceptibility obeys the Curie–Weiss Law for paramagnetic materials but with a negative intercept showing negative exchange interactions [30].If the spins in the two sub lattices are slightly tilted or canted, a very small net magnetization can be produced. This is called canted antiferromagnetism. Hematite is a well-known example.
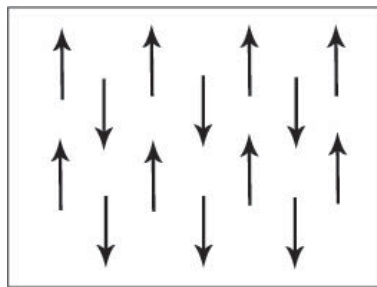
Figure1.10.Antiferromagnetism

1.7.2. Magnetic Anisotropy

Ferromagnetic materials can be divided into a large number of sub volumes called domains. Each domain is spontaneously magnetized to saturation but the direction of magnetization varies from domain to domain. The net vector sum of all moments therefore produces a total magnetization of near zero. The dependence of magnetic properties on a specific direction is called magnetic anisotropy. There are different types of anisotropy. They are magneto crystalline anisotropy which depends on the crystal structure, shape anisotropy is dependent on grain size and stress anisotropy is related to the applied or residual stresses.

Magnetic anisotropy affects the shape of hysteresis loops and controls the value of coercivity and remanence. Anisotropy is of utmost importance in technology because Material Engineers use this for commercial applications.

Magneto crystalline anisotropy: It is the energy required to deflect the magnetic moment in a single crystal from the easy to the hard direction. The easy and hard

directions arise from the interaction of the spin magnetic moment with crystal lattice known as spin orbit coupling [31].

Stress Anisotropy: Another effect of spin orbit coupling is magnetostriction. Magnetostriction originates from the strain dependence of anisotropy constants. Upon magnetization, a previously demagnetized crystal experience a strain that can be measured as a function of applied field along the principal crystallographic axis. A magnetic material therefore changes its dimension when magnetized. In the reverse process, the application of a suitable stress can produce a change in magnetization. A uniaxial stress can produce a unique easy axis of magnetization, if the stress is sufficient to overcome all other anisotropy. Magnitude of stress anisotropy is described by two more empirical constants known as magnetostriction constant and level of stress.

Shape anisotropy: It is due to the shape of grain. A magnetized body will produce magnetic poles at the surface. This surface charge distribution, acting in isolation, is itself another source of magnetic field called the demagnetizing field. It is called so because it acts in opposite direction to the magnetization producing the same.

1.7.3 Domain Theory

A magnetic material is actually composed of small regions called magnetic domains within each of which the local magnetization is saturated but not necessarily parallel. Domains are small but much larger than atomic distances. The existence of domains is quite important because some magnetic properties especially coercivity and remanence vary with grain size.

The maximum coercivity for a given material occurs within its single domain range. For larger grain sizes, coercivity decreases as the grains subdivides into domains. For smaller grain sizes, coercivity again decreases, but this time due to randomizing of thermal energy.

Multi-domain grains are magnetically soft and having low values of coercivity and remanence.

As the particle size continuously decreases within single domain range, another critical point is reached, at which remanence and coercivity go to zero. At this stage particle becomes super paramagnetic.

1.8. MAGNETOSTRICTION

The deformation produced in a magnetorheological elastomer under an applied magnetic field iscalled Magnetostriction.Magnetostrictive materials are typically mechanically biased in normal operation. A compressive load is applied to a material, which is due to magneto elastic coupling, forces the domain structure to orient perpendicular to the applied force. When a magnetic field is applied, the domain structure rotates producing the maximum possible strain in the material. A tensile preload should orient the domain structure parallel to the applied force. This has not yet been observed due to the brittleness of the material.

Magnetostriction can be measured by noting the small changes in the length of the elastomer rod when an external magnetic field is applied. This change in length of the rod is called longitudinal magnetostriction $\lambda = \Delta L / L$. In the absence of saturation magnetization the combined effect of longitudinal and transverse magnetostriction causes no net change in the volume of the material. When a sufficient magnetic field is applied to saturate the magnetization, both longitudinal and transverse magnetostrictions have the same sign, the resulting change in the volume of the rod is called volume magnetostriction (Barrett effect). As volume magnetostriction is always much smaller than longitudinal magnetostriction, the term magnetostriction generally refers to longitudinal or linear magnetostriction[32].

For an MRE, dimension changes are due to interactive coupling between the applied magnetic field and the magnetic moments of the material's individual domain. All these magnetic domains get aligned in the direction of the magnetic field. Schematic of the above phenomena is shown below (Figure 1.11)
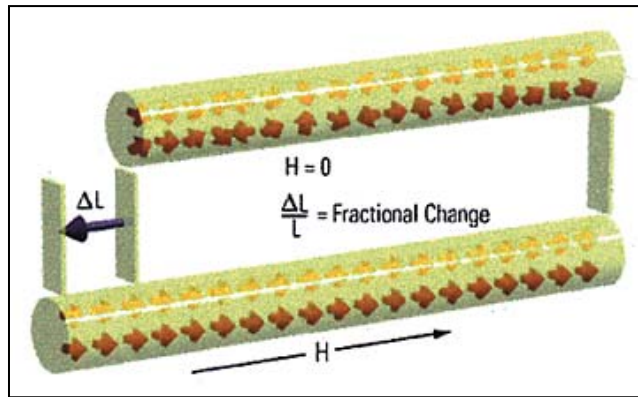
Figure 1.11.Effect of magnetic field on a Magnetorheological elastomer rod

The anisotropy of a magnetic material varies with strain and correspondingly the magnetic material lattice will distort /strain spontaneously if the resultant strain lowers the anisotropy energy.

The magnetostriction between the demagnetized state and saturation is structure sensitive so general constitutive relations for the magnetostriction are not possible. However, an explicit solution exists for cases when the strains are due primarily to 90° domain rotations. In practice, these rotations occur in a single crystal with uniaxial anisotropy in which the field is applied in a direction perpendicular to the easy axis ora polycrystalline material in which the magnetic moments have been brought to complete alignment in a direction perpendicular to the applied. The latter case implies that the perpendicular stress energy is sufficient to dominate the crystal anisotropy.

$$\lambda = \frac{3}{2}\lambda_s \cos^2 \varphi$$

(1.2)

Where λ is magnetostriction , λ_s is saturation magnetostriction and $\emptyset$ is the angle between the Ms vectors and the field direction. Recognizing that the bulk magnetization along the field direction is given by

17

$M = M_s \cos\varphi$, where M is magnetisation and M_S is saturation magnetisation above equation becomes

$$\lambda = \frac{3}{2}\lambda_s \left(M \middle/ M_s \right)^2 \qquad (1.3)$$

This provides a quadratic relation between the magnetization and magnetostriction[33].

The major advantage of MRE's is that particles are not able to settle with time and there is no need of a vessel to contain them. The possibility of hazardous waste leakage is no more with a solid MRE. Secondly, the particles in a solid MR will not affect the performance and durability of a piece of equipment as much as the interaction of particles in MR fluid. Usually MR solids work only in the pre yield region while MR fluid, typically work in the post yield state.

MR elastomers normally work in the pre yield regime of linear viscoelastic region. In viscoelastic materials a part of the deforming force or corresponding input energyis stored and released during each cycle and some is dissipated as heat. The storage modulus G' represents the capacity of the material to store energy of deformation, which contribute to material stiffness. The loss modulus G'' represents the ability of the material to dissipate the energy of deformation.

Usually magnetically soft particles are used as fillers in an appropriate matrix to produce magneto mechanical coupling. Magnetic field induced stiffening is due to magnetic dipolar interaction .The attraction between two magnetic dipoles could increase the shear modulus of the material. Stiffness change also depends on the volume fraction of the particle, magnitude, and frequency of the strain[34].

By measuring magnetic interaction energy between two dipoles, the strength of magnetic interaction can be calculated. If the field applied is along the aligned chains and in the vertical direction, the magnetic interaction energy is given by

$$U = \frac{\mu_0 m^2}{4\pi r^3 (1 - 3\cos^2\theta)} \qquad (1.4)$$

18

Where, μ_0 is the magnetic constant, θ is the angle between the line connecting the two dipoles and the direction of magnetization. The magnetic interaction energy depends on the dipole moment as well as the chain geometry.

1.9. LINEAR VISCOELASTIC THEORY

Figure 1.12 shows relation connecting stresses and strains of three group of materials, perfectly elastic, purely viscous and viscoelastic. For an elastic material, stress response is in phase with strain.
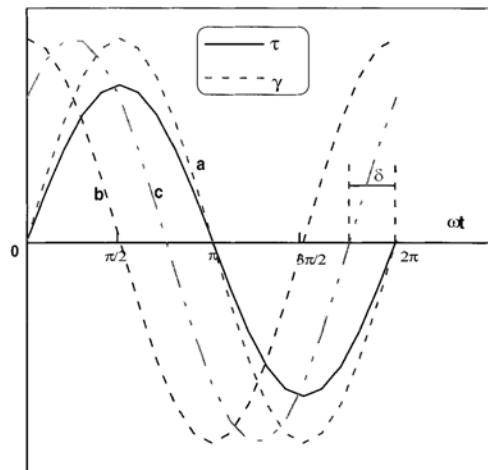
Figure 1.12. Relation connecting stresses and strains of three group of materials, (a)perfectly elastic, (b)purely viscous and (c)viscoelastic

The general equation related to sinusoidal deformation γ of small amplitude γ_0 at fixed pulse ω is given by

$$\gamma = \gamma_0 \sin \omega t. \qquad (1.5)$$

For a purely viscous material stress is 90^0 out of phase with strain and a viscoelastic material would yield a stress having components both in phase and out of phase. Thus viscoelasticity of the material can be described by a complex modulus G^*.

19

$$G^* = G' + iG'' \qquad\qquad (1.6)$$

where G' is the storage modulus and G'' is the loss (out of phase) modulus.

Loss factor tanδof the material is given by the relation

$$tan\delta = \frac{G''}{G'} \qquad\qquad (1.7)$$

The loss factor of a material is the ratio of energy dissipated from the material per radian to the stored energy during a study state sinusoidal excitation. Magneto rheological materials in the form of fluids, foams, and elastic come under the category of smart materials and functional materials. Application of an external magnetic field can tune their rheological properties. MR fluids are liquids whose shear flow properties can be controlled for applications in torque transfer and vibration control devices. MR foams are high-end application of MR fluids with maximum efficiency. MR elastomers are solid-state analogues of MR fluids whose stiffness can be controlled to provide suspension devices and tunable mounts. At the US 'National Bureau of standards, JacobRabinow carried out an initial study on MR fluids. At the same period, William Winslow was concentrating on the work associated with electro rheological fluids. Bingham plastic model gave a satisfactory explanation to the field depend behavior of MR fluids[35]. Micron sized MR particles will support several hundreds of magnetic domains. Domain dipole rotation in the presence of a field causes interparticle attraction and thus maximum magneto rheological effect.

1.10. POLYMER MATRIX

In the present study polymer matrix selected is natural rubber. Sulphur is added for the vulcanisation of natural rubber. It brings cross linking and converts rubber to create bound structure. Usually 0.5 to 5phr (part per hundred rubber by weight) Sulphur is added. Certain chemicals, termed accelerators, after we used with

Sulphur shorten the time of vulcanisation and improve the physical properties of rubber. Despite the fact that inorganic accelerators, like white lead, lead monoxide, lime and magnesia are used as accelerators, the organic accelerators are found to be additional active. Some examples are MercaptoBenzoThiazoleDisulphide(MBTS), TetramethyThiuramDisulphide(TMTD), CyclohexylBenzthiazylSulphenamide (CBS), ZincDibutyl Carbonates (ZDC) etc. The proportion needed is comparatively tiny, usually 0.5 to 1.0 part per 100 gm of rubber being spare. Most accelerators need the presence of zinc oxide to exert their full effectiveness, and a few need an organic acid, like stearic acid [36].

1.11. FILLERS

The filler materials appropriate for MR solids are pure Iron and Carbonyl Iron. Thanks to their high porosity and low remnant magnetism and high saturation magnetization. High porosity and high saturation magnetization provides high inter particle interaction and there by high MR effect[37].

1.12. MOTIVATION

As has been described earlier, the importance of MREs lies in its ability to react to external stimuli to modify parameters like stiffness constant, resonant absorption, viscosity etc. The incorporation of ferromagnetic fillers in the matrix for various loadings of the filler necessitates that they are impregnated into the matrix according to a specific recipe. They are to be moulded into rods as well as sheets. The recipe has to be worked out on a trial and error means. The moulded sheets/rods must be homogeneous, where the particles are uniformly distributed. In this investigation, it is intended to incorporate two types of fillers namely Iron and Carbonyl Iron.

In the case of iron containing MREs, the effect of particle size on its different properties is also to be investigated. For this, commercially available iron is milled to

make nanosized powders. In the first phase of the investigation, both micro and nanosized fillers will be incorporated and rods and sheets will be moulded with and without the application of external magnetic field. For this a complete setup for moulding sheets and rods are to be designed. This has to be designed and fabricated. This forms a part of the objectives of the present work. Evaluation of magnetostriction of these MREs is of importance for micro actuator applications. A non-contact method of LDV will be employed for this. Necessary accessories for the estimation of micro actuation under different magnetic fields will also be fabricated. They include magnetic assemblies, power amplifiers. A complete automated system with laser, power amplifier, Dynamic Signal Analyzer (DSA), Vibration controllerwill be assembled for this purpose. This is yet another objective of the present work

A second type of MREs consisting of Carbonyl Iron of different particle size also will be made and tested for its micro actuation. The evaluation of magnetic properties especially its loop parameters are also necessary, for this, Vibrating Sample Magnetometry(VSM) will be used. The various mechanical properties namely, Young's Modulus, Storage Modulus, Loss Modulus and Stiffness are also to be evaluated by employing DMA and Instron Mechanical Analyzer. The magnetodielectric properties of MREs are seldom studied thoroughly. The magnetodielectric properties of MREs will be evaluated at various frequencies.Finally the results are to be correlated.

So, the objectives of the present work can be listed as follows.

- Design and fabrication of a set up for curing MRE rods in an applied magnetic field.

- Design and fabrication of a set up for curing MRE sheets in an applied magnetic field(1)Normal (2) horizontal to the plane of the sample.

- Preparing iron powders of different crystallite sizes by high energy ball milling.

- Mixing and homogenizing of Fe and Carbonyl Iron powders in natural rubber matrix for the realization of MRE rods and sheets

- Structural characterization of the prepared samples using XRD.

- Structural characterization of the prepared samples using TEM.

- Morphological characterization of the prepared samples using SEM.

- Studying the mechanical properties of the prepared samples using Instron mechanical Analyser.

- Magnetic characterization using Vibrating Sample Magnetometer.

- Actuation measurements using Laser Doppler Vibrometer.

- Shear studies of MRE sheets using modified DMA.

- Studying the dielectric properties of these samples using an impedance analyzer.

REFERENCES

[1]. Daniel J. Klingenberg -AIChE Journal, **2**(2001) 47

[2]. Seung-Bok Choi-Front.Mater., **1** (2014)11

[3]. H. Bose and R. Roder-J. Phys.: Conference Series,**149**(2009) 012090

[4]. Constitutive Models for Rubber VII-Stephen Jerrams, Niall Murphy,CRC Press(2011)474

[5]. Bogdan Sapiñski-Mechanics **28**(2009)18

[6]. Dmitry Borin, David Gunther,Christian Hintze, Gert Heinrich, Stefan Odenbach-J. Magn.Magn.Mater.**324**(2012)3452

[7]. Miao Yu, BenxiangJu, Jie Fu, Xueqin Liu, Qi Yang- J. Magn.Magn.Mater.,**324** (2012) 2147

[8]. Weihua Li and Xianzhou Zhang - Recent Pat.Mech. Eng. **1**(2008)161

[9]. T. Bailey and J. E. Ubbard Jr, Journal of Guidance, Control, and Dynamics, 8(1985) 605

[10]. Zhu, XuliMeng, Yonggang Tian, Yu -Smart Mater. Struct., **19** (2010)0964

[11]. Kchit N, Bossis G.-J Phys: Condens Matter. **20** (2008)204136

[12]. Mietta JL, Ruiz MM, Antonel PS, Perez OE, Butera A, Jorge G, Negri RM-Langmuir, **28** (2012)6985

[13]. Jun-Tao Zhu, Zhao-Dong Xu and Ying-Qing Guo, Smart Mater. Struct.,**21**(2012) 7

[14]. Martin Bellander-Thesis-1998

[15]. V Koutsos ,ICE manual of construction materials, **2**(2009) 571

[16]. Tao Xie, Polymer,**52**(2011)4985

[17]. Thomas Voigtmann, Curr. Opin. Colloid Interface Sci., **19** (2014) 549

[18]. Composite materials handbook - Polymer matrix composites guidelines for characterization of structural materials, 1-5(2002).

[19]. Lipatov YS, Polymer reinforcement, Chem.Tec. Publishing (1995)

[20]. Ping Sheng and WeijiaWen ,Annu. Rev. Fluid Mech., **44**(2012)143

[21]. De Rossi, F. Carpi, A. Mazzoldi, Electrically responsive polymers as materials for artificial muscles- D., 2004

[22]. Dmitry Borin and Stefan Odenbach ,Int. J. Mod. Phys. B, **25**(2011), 963

[23]. C. Scherer and A. M. FigueiredoNeto, -Braz. J. Phys. **35**(2005)

[24]. H.Wang and W. H. Liao, Smart Mater. Struct.,**20**(2011) 023001

[25]. T F Tian, X Z Zhang , W H Li , G Alici and J Ding, J. Phys.**412**(2013) 012038

[26]. Handbook of Magnetism and Advanced Magnetic Materials,John Wiley & Sons, Inc - (1999-2015)

[27]. Carl Heck, Magnetic Materials and their Applications, Elsevier Ltd, 1974

[28]. Nicola A. Spaldin, Magnetic Materials: Fundamentals and Device Applications, **1**(2003)

[29]. Chih-Wen Chen , Magnetism and Metallurgy of Soft Magnetic Materials, 2011

[30]. Rainer Hilzinger, Werner Rodewald, Magnetic Materials 1st Edition, **1**(2013)

[31]. F. F. Mazda, Electronics Engineer's Reference Book, 1989

[32]. Deborah D. L. Chung , Functional Materials: Electrical, Dielectric, Electromagnetic, Optical and Magnetic Applications, World Scientific, 2010

[33]. Craig A. Grimes, Somnath C. Roy, Sanju Rani and QingyunCai, Sensors, **11**(2011) 2809

[34]. G Ligia, R Deodato , Viscoelastic Behaviour of Polymers, 2009

[35]. W H Li, G Z Yao, G Chen, S H Yeo and F F Yap, Smart Mater. Struct., 9 (2000) 95

[36]. Hofmann, Werner, Rubber technology handbook , 1989

[37]. K.A. Malini, E. M. Mohammed, S. Sindhu,P. A. Joy, S. K. Date, S. D. Kulkarni,P. Kurian,M. R. Anantharaman, J. Mater. Sci. **36**(2001) 5551

CHAPTER 2

EXPERIMENTAL TECHNIQUES

Synthesis and characterization of materials is an integral part of any research in Material Science. Appropriate synthesis route and exact characterization is vital to interpretation of results. Hence adoption of eco-friendly and inexpensive techniques for preparation of samples assume importance. Moreover, if the synthesis is carried out by the researcher rather outsourced, the history of sample preparation and a prior knowledge of impurities come very handy in the right interpretation of results. Characterization of samples at various stages of preparation is highly essential in order to have an idea of the mechanism of formation, the amount of impurities etc.

The present investigation being on Magnetorheological Elastomers requires extensive trial and error experiments to arrive at the exact recipe for compounding. So mixing and compounding is vital in order to fabricate homogeneous sheets or rods. Very often since some of the studies are unique, no commercial set ups are available off the shelf. So fabrication of experimental set up is another requirement. So set ups for applying a magnetic field during curing have been designed and fabricated in house. This is described in detail in this chapter. Similarly measurement of magnetostriction of MRE rods was yet another challenge. A complete unit based on Laser Doppler effect was made in the lab with power amplifier, vibration free platform and magnets. This description is also provided in this chapter. The mechanical properties of sheets and rods under the influence of an applied magnetic field are also to be determined. For this magnet assemblies are designed and made by the author. The details are described in this chapter. Commercial instruments like Scanning ElectronMicroscope(SEM),Tunneling Electron Microscope (TEM), Vibrating Sample Magnetometry (VSM), Laser Doppler Vibrometer (LDV), Dynamic Mechanical Analyser (DMA) are employed for characterization. Though their

descriptions are available elsewhere, a brief description of the first principle along with their layout and theory are detailed in this chapter for continuity.

2.1. SYNTHESIS METHODS

2.1.1. High energy ball milling (HEBM)

High energy ball mills are devices used to rapidly grind materials to nano size based on top down approach by developing high grinding energy via centrifugal and/or planetary action. In this study a planetary type ball milling unit (Fritsch Pulverisette 7) was used (Figure 2.1)[1,2].

A two station planetary mill consists of two bowls made of tungsten carbide fixed on a platform, the platform and bowls can rotate in opposite direction and therefore the name planetary ball mill. To grind a sample in this mill, take appropriate amount of materialsare taken in two bowls and then sufficient number of balls are added. Samples can be run wet. Here in this study toluene is used as a wetting medium. A lid is placed on the bowl with proper sealing and then the bowl is mounted in the machine. Once the bowls are mounted and secured, the cover of the ball milling unit is lowered and the machine can be operated.

In planetary action, centrifugal forces alternately add and subtract. The grinding balls roll halfway around the bowls and then are thrown across the bowls, hitting on the opposite walls at high speed as shown in the Figure **2.2**. The ball – bowl contact time is given by the relation

$$t = (1 + 1.2e)\sqrt{\frac{\pi m}{30YR}} \qquad (2.1)$$

where, Y is the yield strength of the bowl, R is the ball radius, e is the coefficient of restitution of the bowl's inner walls and m is the mass of the ball.

Grinding is further intensified by interaction of the balls and sample. Planetary action gives up to 20 g acceleration and reduces the grinding time to about 2/3 of a simple centrifugal mill (one that simply spins around).

Figure 2.1. Fritsch Pulverisette 7

The following parameters of a high energy ball milling unit determines the size reduction that can be achieved by milling

1) Type of mill
2) Milling atmosphere
3) Milling media
4) Intensity of milling
5) Ball to powder weight ratio (BPR)
6) Milling time
7) Milling temperature
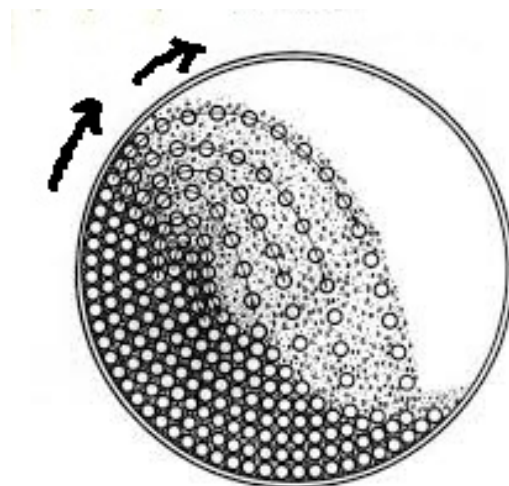
Figure 2.2. Schematic of the ball-movement

Grinding media are available in agate, sintered corundum, tungsten carbide, tempered chrome steel, stainless steel, zirconium oxide, and polyamide plastic. The exact type of bowl and balls that are used depends on the type of material being ground. For example, very hard samples might require tungsten carbide balls and bowls. For typical use, agate is good enough. As with any other methods of grinding, cross contamination of the sample with the grinding unit material can be a complication [3]. Samples of Iron powder of different particle size were prepared using HEBM by varying the milling time(1hr, 5hr, 10hr and 20 hr). They were kept inside vacuum desiccators to prevent oxidation.

2.1.2.Preparation of Magneto Rheological Elastomers (Rods and Sheets)

Sheets and rods of MRE are to be fabricated. A compounding recipe is to be formulated. A compounding recipe was arrived at after various trial and error experiments. The ingredients are Natural Rubber, Zinc Oxide, Stearic Acid, TQ (TrimethylQuinoline) CBS (CyclohexylBenzothiazoleSulfenamide), Sulphur and Filler Iron (Fe). The details are shown in the table. 2.1

Ingredients*	Blank NR	20 phr	30 phr	40 phr	80 phr
Natural Rubber	100	100	100	100	100
Zinc Oxide	4	4	4	4	4
Stearic acid	32	32	32	32	32
TQ	1	1	1	1	1
CBS	1	1	1	1	1
Sulphur	2.5	2.5	2.5	2.5	2.5
Filler	0	20	30	40	80

*weights are in phr

Table2.1. Recipe for mixing

2.1.3.Brabender Plasticorder

Brabender plasticorder is a torque rheometer [4]. In this study Brabender Plasticorder(PL 3S model) was utilized for mixing(Figure2.3).It has a volume of 40cc. There were horizontal rotors with protrusions in the mixing chamber. A dynamometer balance measures the resistance caused by the mixing and shearing of the test material against the rotating rotors. A mechanical measuring system attached to the dynamometer measures the torque.
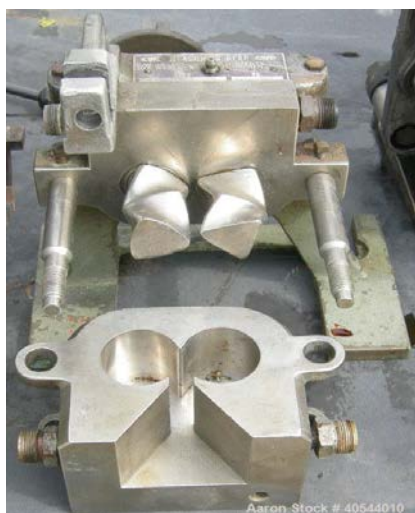
Figure 2.3. Brabender Plasticorder(PL 3S model)

A DC thyrister controlled drive was employed for controlling the speed of rotors (0 to 150 rpm). A thermocouple with a recorder was used for temperature measurements [5].

2.1.4.Two roll mill

Figure 2.4. Two roll mill

Homogenization of rubber was done on a two roll millof dimension 150mm×300mm(Figure 2.4). Mixing was carried out as per American Society for Testing and Materials (ASTM) standards in a brabender[6]. Finally the mixer was homogenised by passing through the tight nip of the mill for six times and sheeted out at a nip gap of 3mm.

2.1.5.Rubber Processing Analyser (RPA)

After the mixing of the elastomer with the magnetic filler according to a specific recipe, the resulting blend is to be vulcanized. For this, cure characteristics of the vulcanizable rubber compounds are to be estimated. Cure characteristics like minimum andmaximum torque,scorch time and cure time were determined using RPA-2000(Rubber Processing Analyzer)(Figure 2.5) at a temperature of 150ºC. Maximum torque is a measure of the stiffness or shear modulus of fully cured test specimen at the vulcanization temperature. Minimum torque is the stiffness of the unvulcanized test specimen at the lowest point of the cure curve. Cure time is the time required for 90% curing of the test specimen [7].The experiment is conducted as follows.
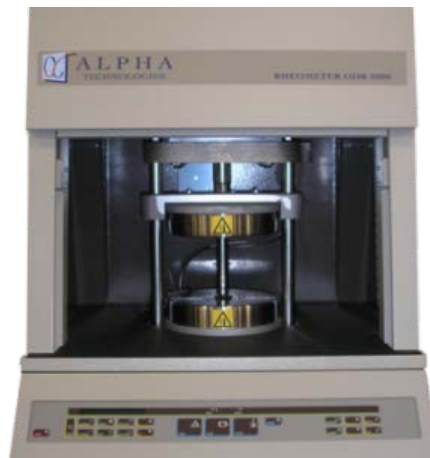
Figure 2.5. Rubber processing Analyser-2000

A test specimen of the mixed rubber compound is placed into the curometer test cavity and after a closure action it is contained in a sealed cavity under positive pressure. The cavity is maintained at some elevated vulcanization temperature. In the present case the temperature is maintained at 150ºC. The rubber totally surrounds the biconnial disc after the dies are closed. The disc is oscillated through small amplitude (1º or 3º) and this action exerts a shear strain on the test specimen. The force required to oscillate or rotate the disc to the maximum amplitude is continuously recorded as a function of time, with the force being proportional to the shear modulus or stiffness of the test specimen at the test temperature. This stiffness first decreases as it warms up and then increases as a result of vulcanization. The test is completed when recorded torque either reaches equilibrium or when predetermined time is elapsed. The time required to obtain the cure curve is a function of the characteristics of the rubber compound and of the test temperature. Thus from the cure curve obtained the cure parameters are extracted [8]. Using these parameters the compounds are then vulcanized at 150ºC on an electrically heated laboratory hydraulic press (450mm x 450mm) up to the respective cure time to make rods and sheets of the sample. The entire test is carried out according to the ASTM standards. A typical cure curve is shown in figure 2.6.
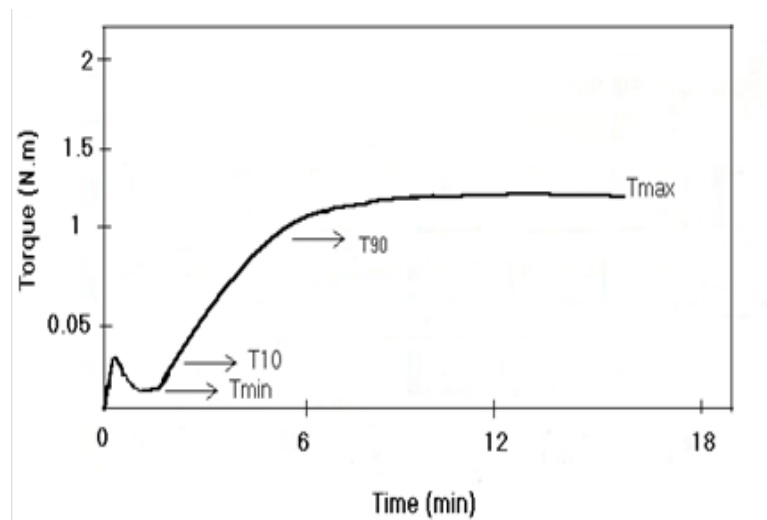
Figure 2.6.A typical cure curve

The following data can be obtained from the cure curve

Minimum torque (T_{min}): It is the lowest torque shown by the mix at the test temperature before the onset of cure.

Maximum torque (T_{max}): It is the maximum torque recorded when curing of the mix is completed.

Differential (Maximum – Minimum) torque: It is the difference between maximum torque and minimum torque during vulcanization. It represents improvement in the degree of crosslinking on vulcanization, it is a measure of final cross link density of the vulcanizate.

Scorch time (T10): It is taken as the time for 10% rise in torque from the minimum torque.

*The optimum cure time T90:*This corresponds to the time to achieve 90% of maximum cure which was calculated using the formula

$$\text{Torque at optimum cure} = 0.9\,(T_{max} - T_{min}) + T_{min}$$

where,T_{max} and T_{min} are the maximum and minimum torques, respectively [10].

34

2.1.6. Fabricationof rods and sheets

All the ingredients as per the formulated recipe were properly weighed and then added to a Brabender plasticorder in a prescribed order. After 15 minutes of mixing, the sample was taken out from the brabender and allowed to pass through a conventional two roll mill (150mm x 300mm) six times, for homogenization. It was then kept for 24 hours and a piece of it was cut and placed on an RPA for estimating the cure time. In the meantime, the remaining sample was once again passed through the roll mill and was rolled into the form of a cylinder. An appropriate portion was cut from it and weighed according to values obtained by trial moulding. An in house designed mould and an electromagnet was fabricated for field assisted curing of MREs and is shown in the Figure 2.7. The final piece was placed into the mould and properly closed with the lid. The coil magnet was placed over the mould and entire set up was moved into the pre-heated hydraulic press(Figure 2.8) maintained at a temperature of 150º C having an aerial dimension of (450mmx450mm). A very high pressure of ~200kgcc^{-1} and a suitable magnetic field was applied to the sample during the curing process. This process continued until the cure time was reached. After curing the rod was removed from the mould and immersed in water for cooling [11]. For ease of extracting the sample from the mould, a special type handle was employed.
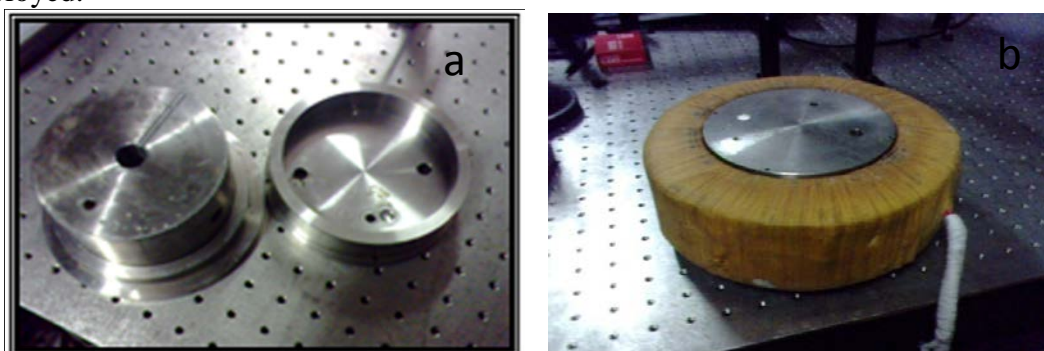
Figure 2.7. Photograph of a) Mould and b) Electro magnet for fabrication of MRE rods(Designed in house and fabricated by the author)

Figure 2.8. Photograph of Hydraulic press

For the preparation of MRE sheets with the same loading, another mould was designed and fabricated as shown in Figure 2.9. By employing this set up, three different types of sheets can be made. By using an electromagnet or set of permanent magnets, an appropriate field can be produced during curing. A suitable amount of mixture was placed at the centre of pre-heated mould at a temperature of 150ºC and it was then closed with the lid and electromagnet was placed around the mould for field curing. It was then pressed on a pre heated hydraulic press of same temperature by applying a high pressure.
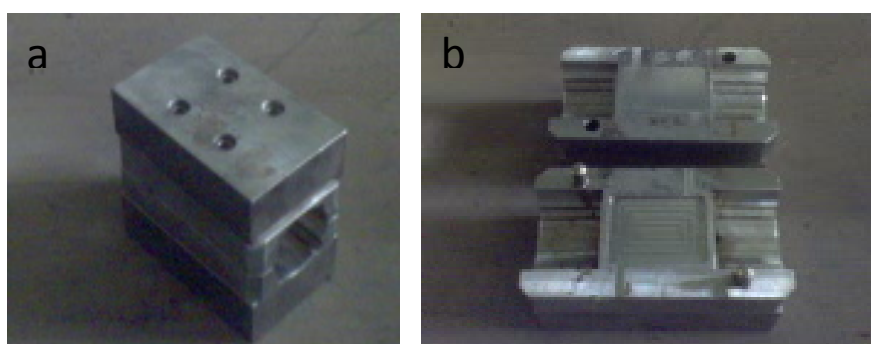
Figure 2.9. Photograph of Mould for MRE sheet fabrication(Field assisted) using permanent magnets and electromagnet

After curing it was immersed in water for sometime, for cooling. This was coded as WF(C)(with field coil) sample. Whole experiment was repeated with a set of permanent magnets producing a horizontal field and WF(M)(with field magnet) sample was prepared. By removing all the magnetic field components a WOF (without field) sample was also prepared. These sheets/rods are thus made available for further studies.

2.2. CHARACTERIZATION METHODS

2.2.1.Structural Analysis: X-Ray Diffractometer

X-ray diffraction offers an efficient and practical method for the structural characterization of crystals. It is useful in determining the arrangement and the spacing of atoms in a crystalline material. The basic X-ray diffractometer consists of an X-ray tube generating the necessary radiation; a collimator to prevent the scattering of the beam; a sample holder in which the specimen is heated or oriented, a goniometer on which a filter system and detector are mounted and rotated around the specimen and a detector for measuring intensity of diffracted X-rays[12]. The relation between the wavelengths λof the X-ray beam, the angle of diffraction $\theta$and the distance d between atomic planes of the crystal is given by the Bragg's equation

$$2d \sin \theta = n\lambda$$

(2.2)

where, n is the order of diffraction. In powder diffraction method, each particle of the powdered sample is a tiny crystallite oriented at random with respect to the incident X-ray beam and a good number of particles satisfy the Braggs diffraction condition.

The X-ray unit used in the present study is a fully automated Rigaku D max-C X-ray diffractometer. The X-ray tube produces monochromatic Cu kα radiation of wavelength 1.5418 Å, with an energy of 8.04 keV. An accelerating potential of 30 kV

is applied to the X-ray tube and the tube current is maintained at 20 mA. The scanning speed was adjusted to 5° per minute with a sampling interval of 0.05°.

From the diffractogram recorded, lattice parameter and crystallite size are evaluated. Lattice parameter a was calculated assuming cubic symmetry and planes were identified by matching inter planar spacing values (d) with ICDD(ASTM). Average grain size could be estimated using Debye-Scherrer's formulae

$$D = \frac{0.9\lambda}{\beta \cos\theta}$$

(2.3)

where, λ= Wave length of X-ray used in Å, β = FWHM in radians of the XRD peak with highest intensity, D = particle diameter in Å, θ= the angle of diffraction in radians.

$$\beta = \frac{FWHM}{180} \times \pi$$

FWHM is the Full Width at Half Maximum of the Gaussian peak [13].

2.2.2 Transmission Electron Microscope (TEM)

Transmission Electron Microscopy is a direct approach to determine the size and shape of the nano materials as well as to obtain structural information. In TEM, electrons are accelerated to 100keV or more and focussed on to a thin specimen by means of a condenser lens, and allowed to penetrate in to the sample. It uses transmitted and diffracted electrons which generates a two dimensional projection of the sample. The contrast in this projection or image is provided by diffracted electrons. In bright field images the transmitted electrons generate bright regions while the diffracted electrons produce dark regions. In dark field image the diffracted electrons preferentially form the image. In TEM, one can switch between imaging the sample and viewing its diffraction pattern by changing the strength of the intermediate

38

lens. The greatest advantage that TEM offers is its high magnification, ranging from 50 to 10^6 and its ability to provide both image and diffraction information from a single sample [14].

The high magnification or resolution of TEM is given by

$$L = \frac{h}{\sqrt{2mqV}}$$
(2.4)

where, m and q are the electron mass and charge, h the Planck's constant and V is the potential difference through which the electrons are accelerated.

The schematic of a transmission electron microscope is shown in figure 2.10. TEM consists of an emission source, which may be a tungsten filament, or a lanthanum hexaboride (LaB_6) source.
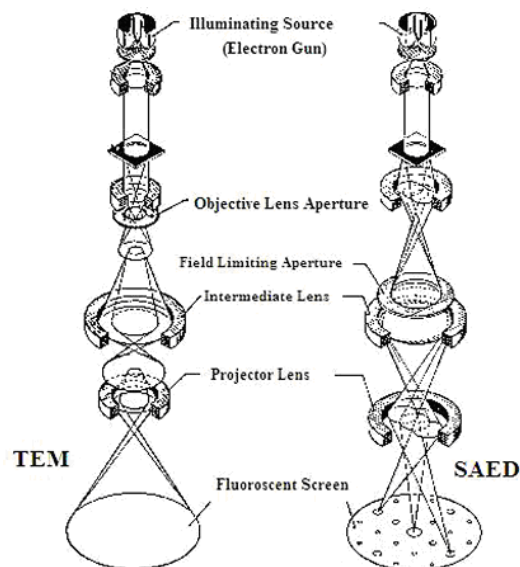
Figure 2.10. Transmission Electron Microscope for imaging and

Selected Area Diffraction Pattern

Typically a TEM consists of three stages of lensing. The different stages are the condenser lens, the objective lens, and the projector lens. The condenser lens is responsible for the primary beam formation, while the objective lenses focus the beam down onto the sample itself. The projector lenses are used to expand the beam onto the phosphor screen or other imaging device, such as a film. The magnification of the TEM is due to the ratio of the distances between the specimen and the objective lens' image plane. Imaging systems in a TEM consist of a phosphor screen, which may be made of fine (10-100μm) particulate Zinc Sulphide, for direct observation by the operator. Optionally, an image recording system such as film based or doped YAG screen coupled CCD's. High resolution transmission electron microscope (HRTEM) can generate lattice images of the crystalline material allowing the direct characterisation of the samples atomic structure. The resolution of the HRTEM is 1nm or smaller. However, the most difficult aspect of the TEM technique is the preparation of samples [15].

Joel JEM-2200 FS TEM was used here for carrying out the different electron microscopic studies.

2.2.3. Scanning Electron Microscope (SEM)

Scanning electron microscopy (SEM) is one of the most widely used techniques employed in the characterisation of nanomaterials and nanostructures. It provides morphology and microstructures of the bulk and nanostructured materials and devices. The resolution of SEM approaches a few nanometres and the magnification of the order of 10-30,000. The measurement is carried out by scanning an electron beam over the samples surface and detecting the yield of low energy electrons (secondary electrons) and high energy electrons (backscattered) according to the position of the primary beam. The secondary electrons which are responsible for the topological contrast provide information about the surface morphology. The backscattered electrons which are responsible for the atomic number contrast carry

information on the samples composition. A new generation of SEM-FESEM (Field Emission SEM) has emerged and is an important tool to characterize nanostructured materials. In this, Field Emission Gun provides the electron beam and the resolution is as high as 1nm [17].

JSM-6335 FESEM Scanning Electron Microscope was employed to study the morphology of the samples under test.

2.2.4. Magnetic Measurements-Vibrating Sample Magnetometry (VSM)

The magnetic hysteresis loop parameters of both rod samples (with field and without field) and sheets WF(C), WF (M) and WOF were evaluated using Vibrating Sample Magnetometer (VSM). Parameters like Saturation magnetization (M_s), Remnant magnetization (M_r), Coercivity (H_c) were estimated from these measurements. The broad principle is outlined here.

When a sample material is placed in a uniform magnetic field, a dipole moment is induced in the samplewhich is proportional to the susceptibility of the sample and the applied field. If the sample is vibrated periodically then it can induce an electrical signal in a pickup coil. The amount of magnetic flux linked to any coil placed in the vicinity of this magnetic moment is given by

$$\phi = \mu_o n \alpha M$$

(2.5)

Where μ_0 is the permeability of free space, n is the number of turns per unit length of the coil, M is the magnetic moment of the specimen and α is the Geometric moment decided by position of moment with respect to coil as well as shape of coil.

Anharmonic oscillator of the type $z = z_0 + Ae^{j\omega t}$ induces an emf in the stationary detection coil. The induced emf is given by

$$V = \frac{-d\phi}{dt} = -j\omega\mu_0 nMA \frac{\partial \alpha}{\partial Z} e^{j\omega t} \qquad (2.6)$$

If the amplitude of vibration and frequency ω is a constant over the sample zone, then the induced voltage is proportional to the magnetic moment of the sample [18]. This is the basic idea behind VSM. A simplified block diagram are given in figure 2.11.
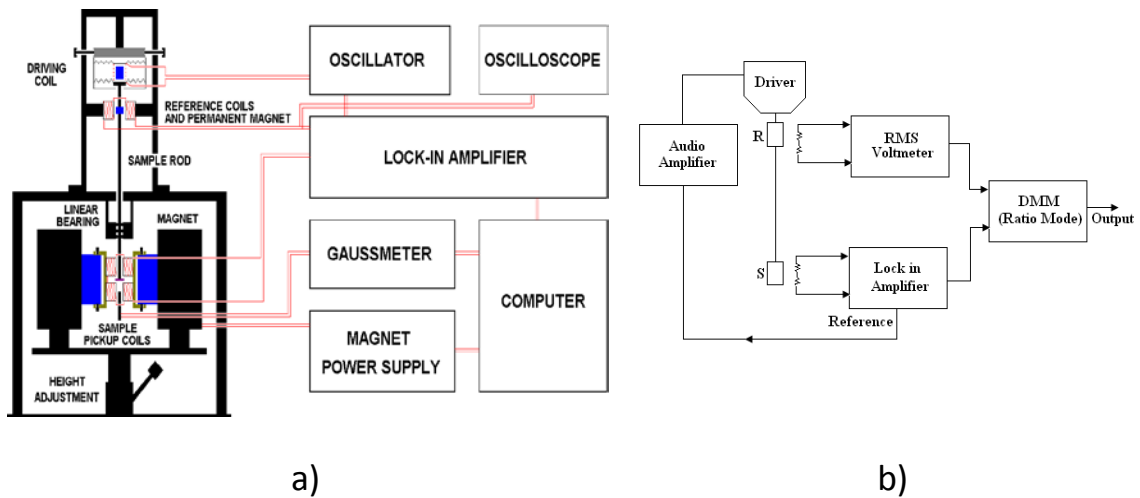
Figure 2.11.a) Main Parts and (b) Block Diagram of VSM.

The position of the pickup coil is adjusted in such a way as to give the maximum induction without much noise. The induced signal in the pickup coil will be proportional to the magnetic moment produced in the sample and the vibrating frequency of the sample. The material under study is loaded in the sample holder, and it is placed at the centre region of the pole pieces of an electromagnet. A slender vertically suspended sample rod connects the sample holder with a transducer assembly located above the magnet, which in turn supports the transducer assembly by means of sturdy adjustable support rods.

A transducer is used to convert the electrical oscillations into mechanical vibrations. An electronic oscillator circuit produces a constant frequency and it is

applied to the transducer to vibrate the sample rod. The vibrating sample in the uniform magnetic field induces a signal in the pickup coils mounted to it. The strength of the ac signal at the vibrating frequency is proportional to the magnetic moment induced in the sample. However, vibration amplitude and frequency also will have some contributions to the induced emf. A servomechanism is used to stabilize the amplitude and frequency of the drive so that the output accurately tracks the moment level without degradation due to variation in the amplitude and frequency of the oscillator [19].

This servo technique uses a vibrating capacitor located beneath the transducer to generate an ac control signal that varies solely with the vibration amplitude and frequency. The signal, which is at the vibration frequency, is fed back to the oscillator where it is compared with the drive signal so as to maintain constant drive output. It is also phase adjusted and routed to the signal demodulator where it functions as the reference drive signal. The signal developed in the pickup coils is then buffered, amplified and applied to the demodulator. There it is synchronously demodulated with respect to the reference signal derived from the moving capacitor assembly. The resulting dc output is an analog signal, which depends only on the magnitude of the magnetic moment, and not influenced by the amplitude and frequency drift. A cryogenic setup can be attached to the sample assembly and can be used to study the magnetization of samples at low temperatures. The resulting dc output is an analog of the moment magnitude alone, uninfluenced by vibration amplitude changes and frequency drifts [20].

2.2.5. Dielectric measurements

The dielectric properties of samples are studied by using a dielectric cell, figure 2.12 and an impedance analyzer (Model HP 4285A) in the frequency range of 100 kHz to 8 MHz [21]. The samples were made in to pellets having a diameter of 12mm and were loaded onto the spring loaded sample holder assembly. The

capacitance values at different frequencies ranging from 100 kHz to 5 MHz were noted. Figure2.12 shows the schematic representation of dielectric cell.

An electrical conductor charged with a quantity of electricity q at a potential V is said to have a capacitance. The capacitance of a simple parallel plate capacitor is given by

$$C = \frac{\varepsilon A}{d}$$ (2.7)

where A is the area of the parallel plates, d is the distance between the plates and ε is the ratio of dielectric constant of the medium between the plates to that of free space. This equation is utilised in calculating the dielectric constant of samples from the sheets.

A specially made sample holder is used to apply magnetic field normal to the sample. The capacitance values at different frequencies ranging from 100 kHz to 5 MHz were noted. The dielectric constant was calculated using the formula

$$C = \frac{\varepsilon_o \varepsilon_r A}{d}$$ (2.8)

where A is the area of the sample pieces used and d their thickness ε_o and ε_r are the dielectric constants of the air and medium respectively and C is the capacitance of the sample.
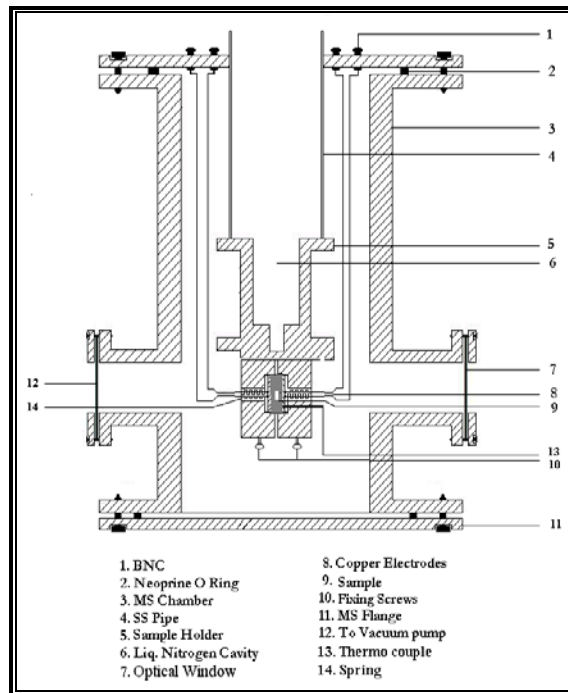
Figure 2.12. Experimental Set-up for Dielectric Measurements

The entire data acquisition and evaluation of the dielectric constant were automated by using a package called LabVIEW which in turn is based on G programming. LabVIEW is a programming language for data acquisition, analysis and simulation or computer control of instruments, techniques or processes. LabVIEW is an acronym for Laboratory Virtual Instrument Engineering Workbench and is a proprietary item owned by National Instruments.

Appropriate modifications were incorporated in the software so as to enable the data acquisition automatic and visual observation of the graph on the computer screen. It has been possible to acquire 20,000 data points or more in a matter of 5 to 10 minutes by using the modified package.

2.3. LASER DOPPLER VIBROMETER (LDV)

Laser Doppler Vibrometer measures velocity and absolute displacement of a point on a vibrating structure in a completely non-contact manner. A typical laser vibrometer system comprises of an optical interferometric sensor head and Vibrometer Controller. The controller demodulates signals from the optical head and provides analog voltage proportional to the velocity or displacement of the surface.

In PolyTec'sVibrometer, the velocity and displacement measurement is carried out using a modified Mach-Zehnder Interferometer. The optical configuration in the sensor head OFV-303 is shown schematically in Figure 2.13.
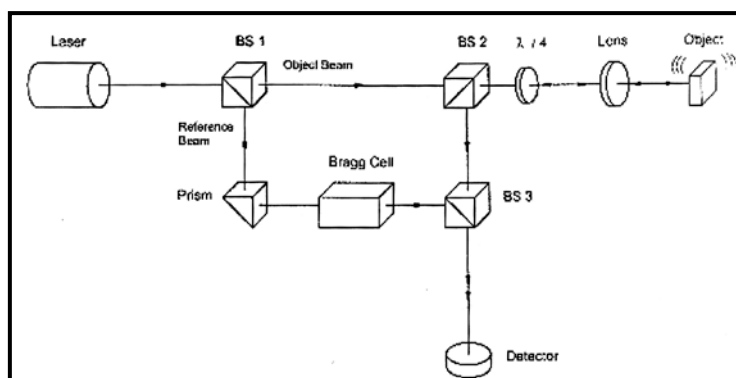
Figure 2.13. Optical configuration in the sensor head OFV-303

The light source is a helium neon laser which provides a linear polarized beam. The polarizing beam splitter BS1 splits the beam into the object beam and the reference. The object beam passes through the polarizing beam splitter BS2 as well as $\lambda/4$ plate, is then focused by the lens on the object and scattered back from there. The polarizing beam splitter BS2 then functions as an optical directional coupler together with the $\lambda/4$ plate, and deflects the object beam to the beam splitter BS3.As both arms of the internal interferometer are symmetrical, the optical path difference between the object beam and the reference beam vanishes within the interferometer. The resulting path difference is equal to twice of the distance between the beam splitter BS2 and the

object. The Bragg cell in the reference arm of the interferometer generates the additional frequency offset to determine the sign of the velocity [22].

The signal path in the vibrometer is shown schematically in the Figure 2.14. The beam of a helium-neon laser is focused on the object under investigation, scattered back from there and coupled back into the interferometer in the sensor head. The interferometer compares the phase ω_{mod} and frequency f_{mod} of the object beam with those of the internal reference beam ω_0 and f_0. The frequency difference is proportional to the instantaneous velocity and the phase difference is proportional the instantaneous position of the object.
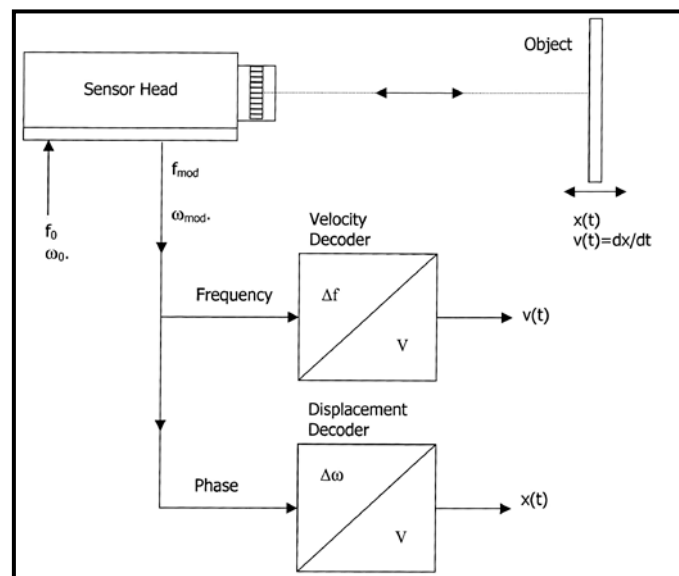
Figure 2.14. Displacement and Velocity measurement

In the controller, the resulting signal is decoded using the velocity decoder and optionally using displacement decoder. Two voltage signals are generated which are respectively proportional to the instantaneous velocity and to the instantaneous displacement of the object. Both signals are available at the front of the controller as an analog voltage and can be processed further externally.

2.3.1. Principle of Laser Doppler Vibrometry

Velocity Measurement

The principle relies on the detection of Doppler frequency shift in coherent light scattered by a moving object. Demodulation of this Doppler frequency shift enables a time-resolved measurement of the target velocity. The relationship between the frequency at which the wave is beamed and frequency at which the wave reflects back is outlined below.

1) If the object is approaching the source, the reflected frequency is higher that emitted frequency.

2) If the object is receding from the source, the reflected frequency is lower that of emitted frequency.

On scattering from the object, beam is subjected to a small frequency shift which is called Doppler shift (f_D). This is a function of the velocity component in the direction of the object beam. Superimposing object beam and internal reference beam ie, two electromagnetic waves with slightly different frequencies, generate a beat frequency at the detector which is equal to the Doppler shift. The direction of velocity can be measured by introducing a fixed frequency shift f_B in the interferometer to which the Doppler shift is added with the correct sign.

Displacement Measurement

The classical technique to measure displacement is the fringe counting technique. This technique is used in PolyTec'sVibrometer. Displacement is electronically derived by measuring the phase change at the detector as the surface motion of the object changes the total path length of the beam. The resulting intensity varies with the phase difference $\phi(t)$ between the two beams according to the equation,

$$I(t) = I_M I_R R + 2K\sqrt{I_R I_M R}\cos\left[2\pi(f_B - f_D)t + \varphi(t)\right] \qquad (2.9)$$

The phase difference $\phi(t)$ is function of the path difference $\Delta L(t)$ between the two beams according to the relation,

$$\phi(t) = 4\pi\Delta L(t)/\lambda \qquad (2.10)$$

where, λ is the laser wavelength .

If one of the two beams is scattered back from a moving object (object beam), the path difference becomes a function of time $\Delta L = L(t)$. As displacement by half the wave length changes the phase by 360º, by counting the zero crossing of fringes, the vibrometer measures how far the object has moved. With D/A converted the digital information is changed into voltage and time resolved output proportional to the surface displacement is measured. i.e., the interference fringe pattern moves on the detector and the displacement of the object can be determined using directionally sensitive counting of the passing fringe pattern.

2.3.2.Experimental set up

Schematic of the experimental set up used for the magnetostrictive measurements using LDV is depicted in figure2.15. Figure 2.16 is the photograph of the LDV integrated system. A brief description on the main parts of the system is given below.

Function Generator: A signal generator which can serve as a multipurpose signal generator from which square wave signal, sine wave signals and triangular wave signals can be obtained either simultaneously through separate output system or selectively through single out put system, is commonly called Function generator. In such a configuration the triangular wave may be considered as the integral of square wave, while shaping of the triangular wave gives a sine wave as an approximation. They are used to provide a known signal i.e., ac voltage (Sine Wave) at various

frequencies and driving voltages to energize the coil. Output of the function generator is amplified by the power amplifier.
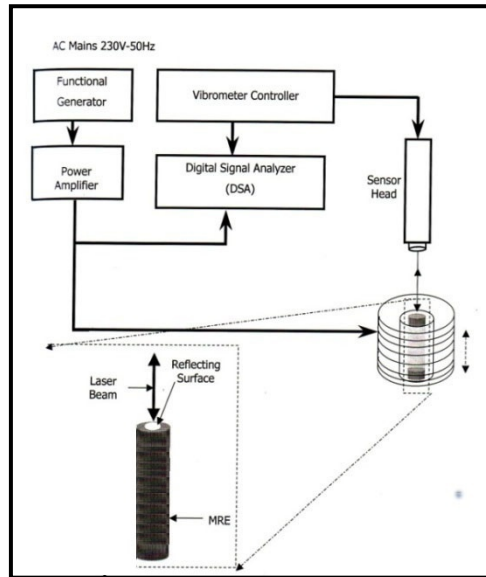
Figure2.15. Experimental Set-up for Magnetostrictive Measurements
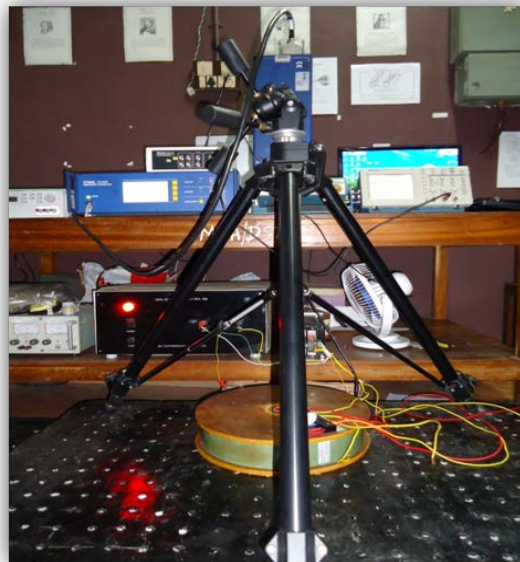
Figure 2.16. Photograph of the LDV integrated system

Power Amplifier: It is used to amplify the output from the function generator and output is fed to AC winding. The turn ratio of the output amplifier may be selected with switch to match various loads. The amplifier section consists of a pre amplifier, the output amplifier, damper circuits, the output transformer, a load matching switching device and output protective and monitoring circuits.

Digital Signal Analyzer (DSA):DSA is a spectrum analyzer used for studying frequency domain behavior of signal. Here the function of DSA is to analyze the signals from the Vibrometer controller. Signal processing extracts information concerning magnitude and phase of each parameter makes it a complicated and sophisticated device. It measures simultaneously all the frequency component present in complex time varying signal. The object of digital signal processing is to estimate Fourier Transform, which are supplied as inputs. One way of visualizing the Fourier Transform is to see it as a continuous set of fixed-width narrow band filters. ie, Discrete Fourier Transform or DFT. For evaluating DFT, digital spectrum analyzers use algorithm known as FFT or Fast Fourier Transform which can be easily implemented on a computer.

Frequency domain analysis of the output of the Vibrometer controller and time domain analysis of output of the power amplifier were performed using DSA. Peak amplitude of the voltage (i.e., output of the vibrometer controller) proportional to the displacement of the rod was noted for each exciting frequency.

**Coil:** Coil used has 2000 turns of insulated copper wire of gauge 20. Coil is wounded on a non magnetic bobbin case of inner diameter of the coil 20mm and length of the solenoid is 60mm. AC voltage is given to the coil ends connected to the output of the power amplifier.

The sensor head is aligned to an optimal position, focusing the laser beam on to the reflecting film on the surface of the elastomer rod. For magnetostrictive

measurements, the elastomer rod is placed inside a solenoid. The input signal is provided by a signal generator which is further amplified by the power amplifier and connected to the solenoid. An analog signal proportional to the velocity and displacement is obtained which is fed to the Dynamic Signal Analyser. The sensor head and the solenoid-elastomer rod arrangement are adjusted until a maximum signal is acquired. The experiment is repeated for various frequencies and driving voltage of the input signal.

2.4. DYNAMIC MECHANICAL ANALYSER (DMA)

Dynamic Mechanical Analysis is a technique that measures the properties of materials as they are deformed under periodic stress. Usually, in DMA a variable sinusoidal stress is applied, and the resultant sinusoidal strain is measured. If the sample under evaluation is purely elastic, the phase difference between the stress and strain sine waves is $0°$ (i.e. they are in phase). If the material is purely viscous, the phase difference is $90°$. But in real world situation materials including polymers are viscoelastic and exhibit a phase difference between those extremes [25].This phase difference, together with the amplitudes of the stress and strain waves, is used to determine a variety of fundamental material parameters, including storage and loss modulus, tanδ, complex and dynamic viscosity, storage and loss compliance, transition temperatures, creep, and stress relaxation, as well as related performance attributes such as rate and degree of cure, sound absorption and impact.
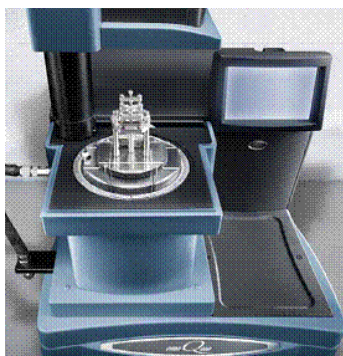
Figure 2.17. Dynamic Mechanical Analyser

2.4.1. Instrumentation

There are several components to design a dynamic mechanical analyzer. Those components are the drive motor which supplies the sinusoidal deformation force to the sample material, the drive shaft support and guidance system which transfers the force from the drive motor to the clamps that hold the sample, the displacement sensor which measures the sample deformation that occurs under an applied force, the temperature control system (furnace), and the sample clamps. The DMA Q800 dynamic mechanical analyzer (TA Instruments, Inc.)(Figure 2.17) is based on a design that optimizes the combination of these critical components. Important among are the analyzer incorporates a noncontact direct drive motor to deliver reproducible stresses over a wide dynamic range of 0.001–18 N; an air bearing shaft support and guidance system to provide frictionless continuous travel over 25 mm for evaluating large samples (e.g., fibers as long as 30 mm) or for evaluating polymers at large oscillation amplitudes(±0.5–10,000 mm); an optical encoder displacement sensor to provide high resolution (one part in 25million) of oscillation amplitude, which results in excellent modulus precision (±1%) and tan δ sensitivity(0.0001); and a bifilar-wound furnace complemented by a gas cooling accessory to allow a broad temperature range (–150 to 600 °C) to be covered [26]. The DMA Q800 also features a variety of clamping configurations to accommodate rigid bars, fibers, thin films, and viscous liquids (e.g., thermo sets) in bending, compression, shear, and tension modes of deformation.
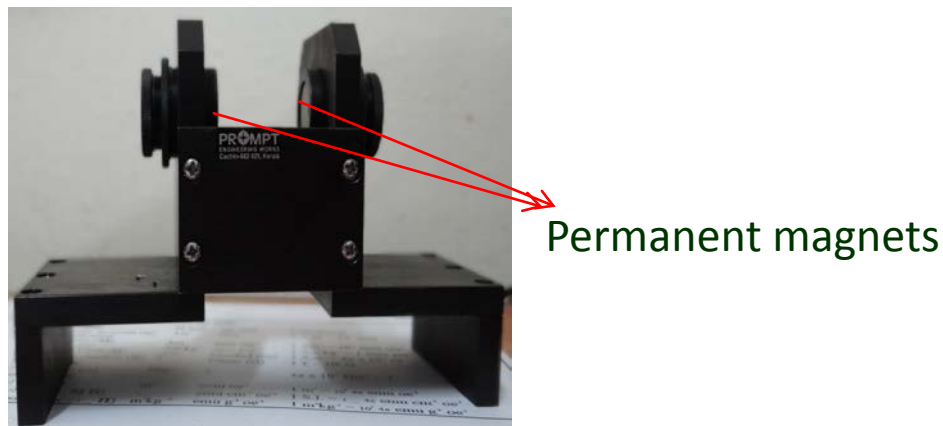
Figure.2.18. Set up for field induced DMA measurements

In this study a modified homemade set up was used for field induced DMA measurements. The photograph is shown in the figure 2.18.Two sets of permanent magnets producing high field were used. The strength of the magnetic field can be varied by changing the position of the magnets. The influence of magnetic field on storage modulus, loss modulus and tan δof MRE sheets were investigated by this new setup.

2.5. INSTRON MECHANICAL ANALYZER

Instron Mechanical Analyzercan be fully utilised for determining the compressive properties of rigid cellular materials, particularly expanded plastics. Suitable systems for this application include 3300 and 5900 series electromechanical testing machines equipped with compression plates (Figure2.19). The parallelism of the compression plates is important and it is recommended that a spherical seating style compression plate is utilized along with a rigid plates. The self-aligning nature of this fixture will maximize the contact area between the plate and the specimen. Swivel seating can be placed on the plate attached to the instrument's base or load cell in the moving crosshead. To reduce the possible affects from off-center loading, it is preferred to place the swivel seat in the base [27].
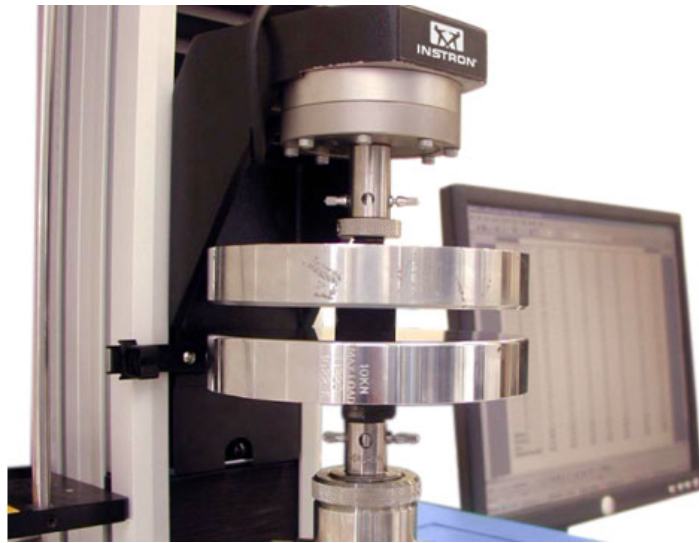
Figure 2.19. Instron Mechanical Analyzer

When two rigid compression plates are used, it is recommended that a strain gauge device, such as a linear variable displacement transformer (LVDT), is used to minimize error due to compliance from the system. However, by using Bluehill Software, which incorporates a load frame compliance correction calculation, a deflectometer is not required unless stated so in testing standard.

To make the testing easier, leave a 10 to 30 mm gap between the specimens that allow you to quickly and easily remove the tested specimens and position new ones. The Bluehill preload function automatically moves the upper compression plate down to precisely touch the specimen at a pre-defined load [28]. The preload function reduces the amount of operator interaction, saving time and improving accuracy.

REFERENCES

[1]. C.C. Koch, Y.S. Cho-Nanostruct. Mater. **1**, (1992)207

[2]. M. L. Trudeau, R. Schulz, D. Dussault, and A. Van Neste, Phys. Rev. Lett. **64**, (1990) 99

[3]. Fritch pulverisette7 Operation manual

[4]. M. G. Rogers-Ind. Eng. Chem. Process Des. Dev., **9** (1970) 49

[5]. Moshe Narkis and Joseph Miltz, -J.Appl. Polym. Sci. **12** (1968) 1031

[6]. James L. White and Sug Hun Bumm, Polymer Blend Compounding and Processing – Encyclopedia of Polymer Blends, **2**(2011)

[7]. John S. Dick , Clair Harmon, Alek Vare- Polym. Test. **18** (1999) 327

[8]. TianmingGao, RuihongXie, Linghong Zhang, HongxingGui, and Maofang Huang- Int. J. Polym. Sci.2015 (2015)

[9]. Mohammad Karrabi, SomayyehMohammadian-Gezaz- J. Vinyl Add. Tech.- **16** (2010) 209

[10]. K.A. Malini, P. Kurian, M.R. Anantharaman- Mater. Lett. **57** (2003) 3381

[11]. Shinzo Kohjiya, Yuko Ikeda-Chemistry, Manufacture and Applications of Natural Rubber – (2014) - Technology & Engineering

[12]. M. Arroyo, M.A. López-Manchado, J.L. Valentín, J. Carretero- Compos. Sci. Technol. **67** (2007) 1330

[13]. Ravi Sharma, D.P. Bisen, Usha Shukl and B.G. Sharma- Recent Res. Sci. Technol. **4** (2012) 77

[14]. David B Williams, C Barry Carter, Transmission Electron Microscopy-A Textbook for Materials Science- Plenum Press New York and London, **5**(1999)452

[15]. Ludwig Reimer, Transmission Electron Microscopy: Physics of Image Formation and Micro analysis, Springer ,**45**(1998)529

[16]. Handbook of Surfaces and Interfaces of Materials, - Hari Singh Nalwa- Academic Press,**1-5**(2001)2911

[17]. Simon Foner, Versatile and Sensitive vibrating-sample magnetometer, Rev.Sc.Instr, **30**(1959)548

[18]. W E Case ,R D Harrington-J. Res. Nat. Bur. Stand.Eng. Instrum.,**70**(1966) 236

[19]. Ekta Gupta, R R Yadav, Manish Sharma-Int. J. Software and Hard ware Res.Eng. **2**(2014)

[20]. TomášŽák, OldřichSchneeweiss-J. Electr. Eng. **59** (2008) 44

[21]. S. Saravanan, C. Joseph Mathai, M. R. Anantharaman, S. Venkatachalam, P. V. Prabhakaran-J. Appl. Polym. Sci., **91** (2004) 2529

[22]. Hani H. Nassif , MayraiGindy, , Joe Davis-NDT & E International, **38** (2005) 213

[23]. Enrico Esposito, Laser Doppler Vibrometry – Text Book (http://www.science4heritage.org)

[24]. Polytec Laser Doppler Vibrometers- Manual

[25]. Kevin P. Menard, Dynamic Mechanical Analysis: A Practical Introduction, CRC Press, **2**(2008)240

[26]. P.S. Gill,J.D. Lear,J.N. Leckenby-Polym. Test. **4** (1984) 131

[27]. P. Cheremisinoff, Handbook of Engineering Polymeric Materials-1997 CRC Press

[28]. Instron Electro mechanical Test Frame TestResources – info@testresources.com

CHAPTER 3

ENHANCED MICROACTUATION WITH MAGNETIC FIELD CURING OF MAGNETORHEOLOGICAL ELASTOMERS BASED ON IRON–NATURAL RUBBER

3.1. INTRODUCTION

Magneto rheological elastomers(MREs), which are solid state analogues of more familiar MR fluids, have been the subject of intensive research for the last few years in the leading automobile research laboratories all over the world [1-3]. MR elastomers represent a new class of engineering materials known as smart materials, and are viscoelastic solids whose material properties can be tuned by an external magnetic field. The important properties of MR elastomers are actuation, sensing and the change in shear modulus in an external field. Thus these materials have potential applications in the form of actuators, transducers,automobile suspension systems, clutches, breaks, vibration isolators and dampers [4].Rubber based MR elastomers are thought to be important because composites of rubber are already employed as bushing and engine mounts [5].

The apparent stiffness and damping of the composite containing rubber and magnetic filler can be tuned by applying an external magnetic field. The variable stiffness property of MR elastomers makes them unique for elastomer based engine parts and devices [6]. The applied magnetic field can produce magnetic dipolar interaction between the magnetic particles and hence induce changes in the stiffness and damping [7-8]. By varying the magnetic field, the stiffness of the composite canbe altered. Such MR devices in a feed back control mechanism can serve as an active

----

vibration arrestor.It is well known that incorporation of ferromagnetic/ferrimagnetic fillers impart magnetic properties to a matrix and the performance characteristics of the composite can then be tailored by controlling the volume fraction.

With the advent of nanoscience and nanotechnology,nano sized fillers are extensively being used which not only imparts the required magnetic properties but also enhance the mechanical properties of the composite. This is called the size effect on the mechanical properties when compared to the micron sized counterparts [9].Pure Iron belongs to the ferromagnetic class of materials and are metallic in nature. They are inexpensive. These iron powders can be pulverised using a top down approach to produce nanosized iron powders. They can be incorporated in the required weight percentages in an appropriate matrix, say,natural rubber to fabricate nanocomposites with the desired mechanical and rheological properties. Literature pertaining to nanocomposites based on Iron and natural rubber are rather scarce. Moreover an attempt to fabricate a MR microactuator with nano sized Iron as filler assumes significance since this is a low cost alternative to metals like Cobalt and Nickel. The incorporation of nanosized fillers results in flexible and mouldable components and is attractive from a practical point of view. From a fundamental perspective the modification of stiffness and micro actuation with respect to field curing also assumes significance. This is the motivation of the present investigation.

In the recent past, several reports have been published on MR materials based on synthetic rubber [10-12]. Natural rubber has advantages over other synthetic materials due to its abundant availability here in the state of Kerala and inexpensive production techniques. Moreover, casting and moulding of natural rubber into complex shapes is easy. The nature and amount (loading) of magnetic filler materials have unique roles in the resulting properties of MR elastomers. Considering the key parameters for a good quality MR elastomer, the assortment (soft/hard) of the magnetic filler is also important in designing an MR based device. Various

microactuators based on Silicon, Ti-Ni thin films and carbon nanotubes were realised in the recent past for various micro-electro mechanical devices [14-17]. These devices were fabricated using sophisticated lithographic and other deposition techniques. Most of them work in the 'contact-mode'. Attempts to make MR elastomer based micro actuator devices had met with only little success [18]. Because of high magnetic permeability, low remanent magnetisation and high saturation magnetisation, iron particles are used as fillers for MR elastomers and thus it provides high inter particle attraction and produce large MR effect. In the present investigation, iron based MR elastomers have been fabricated using a modified curing technique. Iron powder was milled in a high energy ball milling unit to reduce size. A non-contact method employing Laser Doppler Vibrometric(LDV) technique has been adopted to investigate the microactuation of polymer rod. A micro actuator based on these MR rods has been realized and tested. The effect of applied voltage and frequency on microactuation of MR elastomer rods is also investigated.In this chapter, a comprehensive study on the effect of field assisted curing of MRE rods is described.The influence of particle size and loading of the magnetic filler in the polymer matrix on the microactuation behaviour of the composite is also examined. The response of external stimuli in the form of an alternating magnetic field on MRE is analyzed for samples with field assisted curing as well as zero field curing.

3.2. EXPERIMENTAL

Micron sized Iron of 300 mesh size(53µm) (*Laboratory Rasayan (s.d. fine-CHEM LTD BOISAR 401501), Iron (metal) powder, electrolitic-300 mesh LR, Product No.38601*) was ball milled using a High Energy Ball Milling unit(Fritsch Pulverisette -7) as explained in the experimental chapter, for 1hour (hr), 5hr, 10hr and 20hr in toluene base at a milling speed of 500 rpm for a powder to ball ratio of 1:10. Mixing of Natural Rubber with magnetic filler and other curing agents was carried out in accordance with a recipe using a Brabender Plasticoder (PL 3S model).Recipe

details are described in Chapter 2. It was then homogenized by passing through a Two Roll Mill for six times. Sample was kept for 24 hours and its cure characteristics were determined. A rubber processing analyzer (RPA (2000)) gives the value of cure time (T 90) which is the time taken to complete 90% of curing of the sample [18].Cure characteristics was also plotted for each loading and important cure parameters like minimum torque, maximum torque, scorch time and cure time were found .
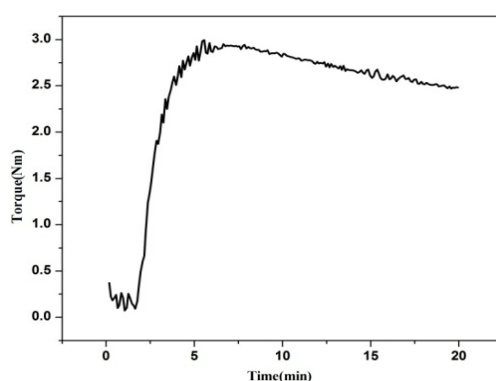
Figure 3.1. Cure characteristics of 20 phr MRE composite with 10 hr ball milled Fe

A homemade set up was employed for the fabrication of MR elastomers. For field assisted curing, an electromagnet is placed around the mould. A regulated power supply is used to maintain a constant current through the coil during curing. MRE rods of loading corresponding to20phr(parts per hundred grams of rubber), 30phr and 40phr of ball milled iron of different milling time were fabricated for both field assisted and zero field curing. The structural characterization of the samples was carried out using X-ray powder diffraction (XRD, RigakuDmax-C), with Cu Kα radiation λ=1.5418Å and the scanning speed was fixed at 5ºmin^{-1} with a sampling interval of 0.05. The morphology was examined using Scanning Electron Microscope (FEI Quanta 400 ESEM). Transmission Electron Microscopy (joel TEM 2200FS) was used to determine the size of the Fe particles. Vibrating Sample Magnetometry (VSM, model: DMS 1660) was employed for the magnetization studies of the

samples. For verifying the alignment of magnetic particles in the matrix, measurement was carried out in two different ways; by applying a field parallel and perpendicular to the sample. Micro actuation of MR elastomers was studied by incorporating a specially designed LDV (OFV-5000 with OFV-505 Sensor Head, PolyTec) setup. An alternating magnetic field generated by this set up produce actuation of the sample. Displacement of the rod during the vibration of MR elastomer rods for various frequencies of AC magnetic field was determined[9]. Doppler effect of light is employed here in LDV for the measurement of displacement of the MR rods [14, 15].

3.3. RESULTS AND DISCUSSION

3.3.1. Structural studies

The crystalline properties of Fe powder and iron filled rubber composites were analyzed by an X-ray powder diffraction technique.A typical X-ray diffraction pattern is shown in the Figure 3.2
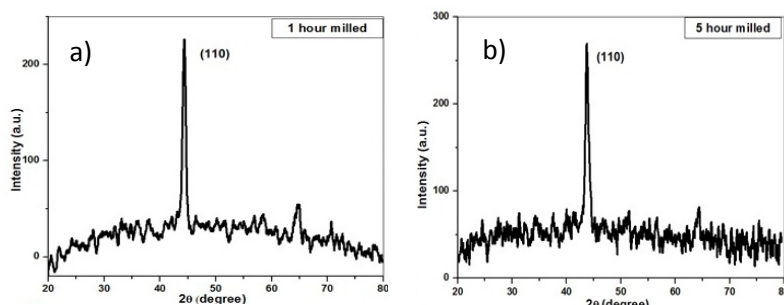

Figure 3.2. XRD pattern for ball milled Fe for a) 1 hr and b) 5 hour milling time
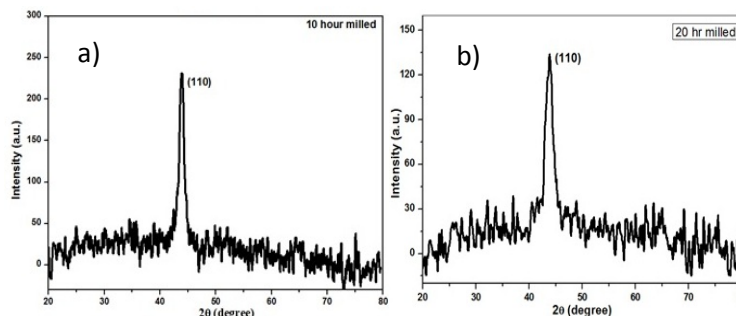

Figure 3.3.XRD pattern of ball milled Fe for a) 10 hr and b) 20 hr milling time

63

Milling time (hr)	Crystallite size (nm)
0	**44000** (Provided by the supplier)
1	**20(± 0.01nm)**
5	**15 („)**
10	**10(„)**
15	**7 („)**
20	**6 („)**

**Table 3.1.**Ball milling time and grain size of pure Fe measured using XRD.

Figure 3.3 represents the XRD pattern of milled iron milled for 10 hours and 20 hours. As milling time increases a corresponding crystallite size reduction occurs and line broadening effect is very clearly evident in XRD pattern of iron milled for 20 hours. Table 3.1 indicates the crystallite size reduction with milling time. An error of factor0.01nm is obtained in these Crystallite size measurements. Figure 3.4 shows the TEM images of iron milled for 1hour and 10hours. Particle size obtained for 1hourball milled Iron is 12nm and for 10 hr ball milled Iron is 8 nm.
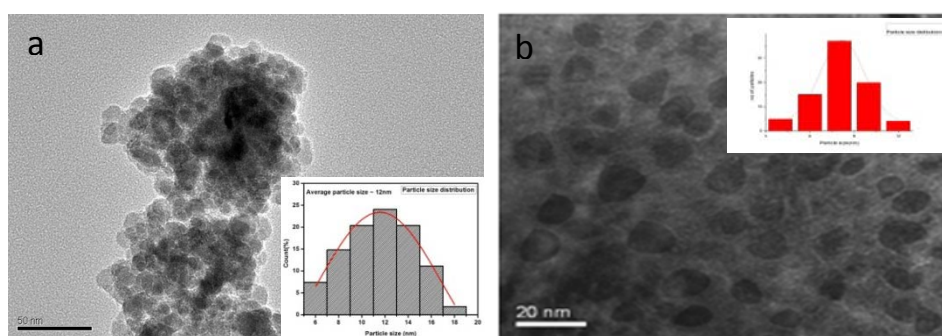

Figure 3.4.TEM images of a) 1 hour ball milled Fe powder and b) 10 hour ball milled Fe powder (size distribution is shown in the inset)

3.3.2. Magnetization studies

Figure 3.5shows the hysteresis loop for the samples with 1hr milled iron-rubber composites of different weight percentages. The value of saturation magnetization (M_s) increases with the loading of the filler in the matrix as expected [16, 17]. From figure 3.6 a)& 3.6 b), it is clear that an easy and earlier saturation is possible for samples with field assisted curing and anisotropy is evident in these samples. Figure 3.6a) & 3.6 b) and figure 3.7a) & 3.7 b) represent M-H loop plotted in plane and out of plane of MRE composites filled with 20 phr 1hr ball milled iron and 40 phr 5 hr ball milled iron cured under with field and without field conditions. Figure 3.8 represents the hysteresis loop of unmilled, 1hr and 5hr ball milled Iron powder. Saturation magnetization decreases with milling time.
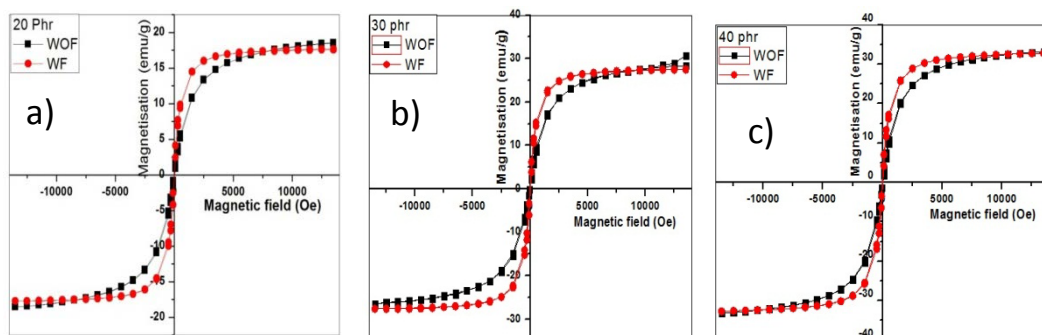
Figure 3.5. Hysteresis loop for the samples with 1 hr ball milled Fe WF and WOF of different weight percentages a) 20phr b) 30phr c) 40 phr
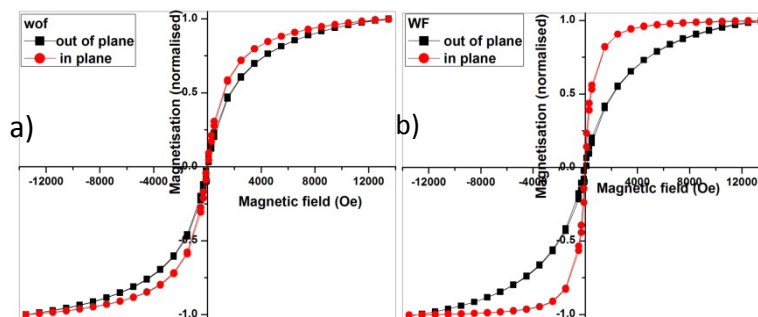
Figure 3.6. Hysteresis Loop -out of plane and in plane for representative elastomers of filler size 20 nm Fe 20phrcured a)without field and b) with field
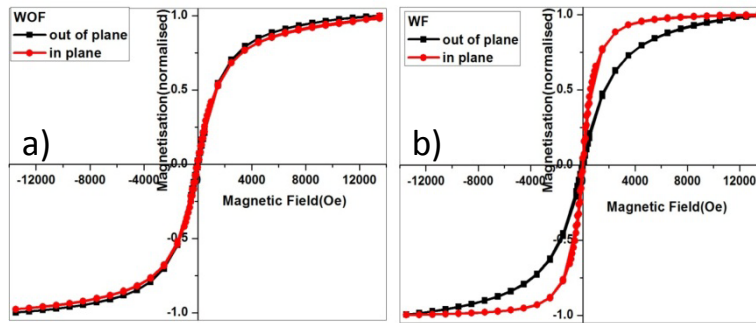
Figure 3.7. Hysteresis Loop-out of plane and in plane for representative elastomers of filler size 15 nm Fe 40phr cured a) without field (WOF) and b) with field (WF)
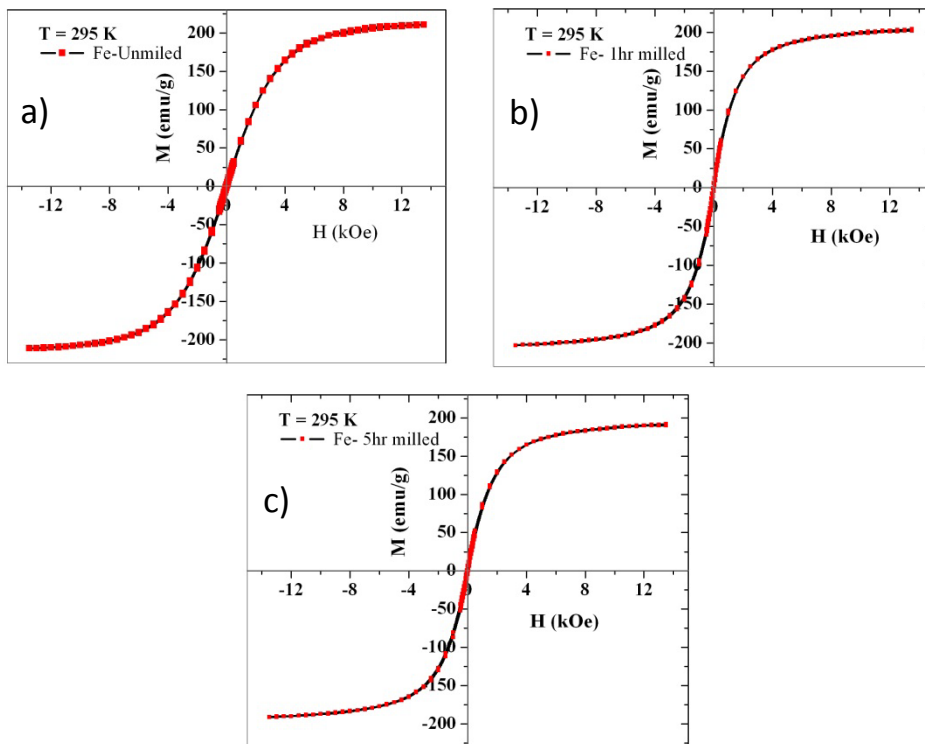
Figure3.8 Hysteresis Loopof Fe powder a) Un milled b) 1hr ball milled c) 5hr ball milled

Figure 3.9a) & 3.9b) gives the variation in saturation magnetization with loading of 5hr ball milled α-Iron under field assisted curing and zero field curing. In all cases magnetization increased with loading (Figure 3.10). From the shape of the MH loop of with field(WF) and without field(WOF) MR Rods, alignment and easy saturation of magnetic filler in the field direction of WF sample is clearly visible (Figures3.5, 3.6, 3.7).
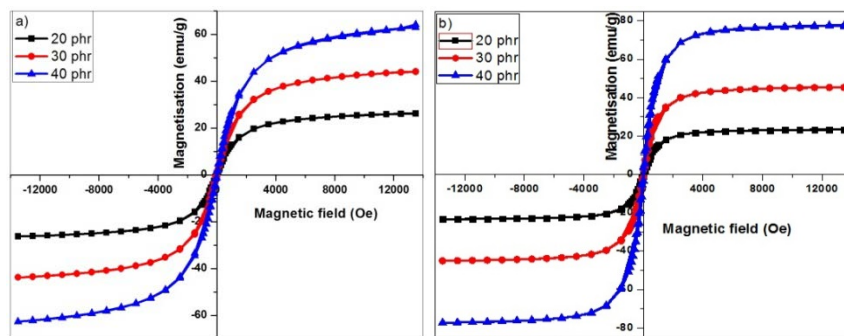
Figure 3.9.Magnetization studiesof Fe 5 hr ball milled with different loading a) WOF and b) WF
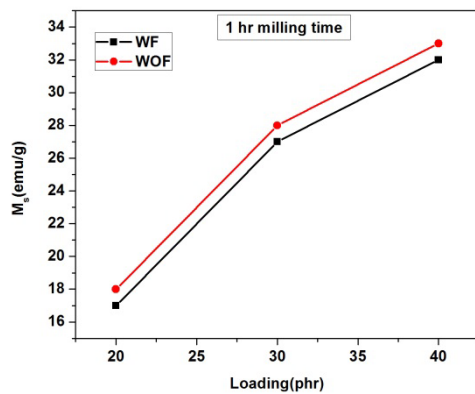
**Figure 3.10.**Loading vs Ms for 1hr milled WF and WOF sample

The saturation magnetisation and coercivity of samples have been tabulated in table 3.2. It may be noted that the saturation magnetization of the composite sample containing 40 phr (5hr WF) is unusually large. This is interesting and need further investigation. The coercivity almost remains the same for both field and zero field cured samples.

Powder	M_s (emu/g)	H_c Oe
Fe UM	210	30
Fe 1 hr	202	35
Fe 5hr	190	40

MRE rods	Loading	M_s (emu/g)		H_c (Oe)	
		WF	WOF	WF	WOF
FeUM	40 phr	36	37	25	30
Fe(1 hr)	40 phr	32	33	26	33
Fe(1 hr)	30 phr	27	28	25	53
Fe(1 hr)	20 phr	17	18	24	32
Fe(5 hr)	40 phr	77	63	38	44

Table 3.2. Magnetization Studies –Loop parameters of pure iron, ball milled Iron powder and MRE Rods (all are measured in plane)

3.3.3. Surface morphological studies
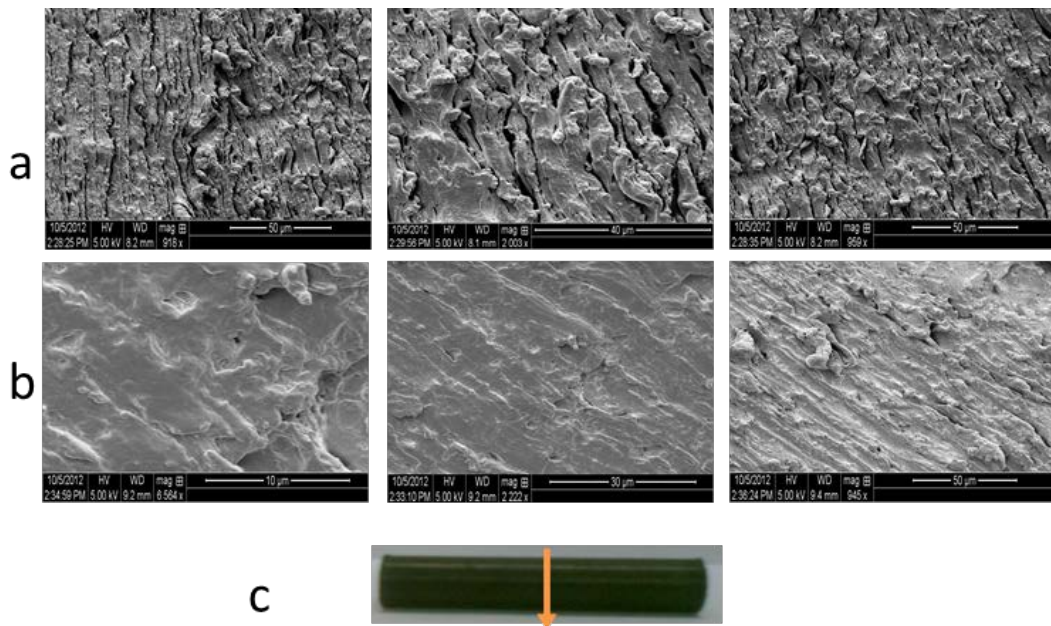
Figure 3.11. SEM images of (a) 5hr milled Fe 40 phrMR rod (WF)(b) 5hr milled Fe 40 phr MR rod (WOF)and (c)Arrow shows the direction of the cross section
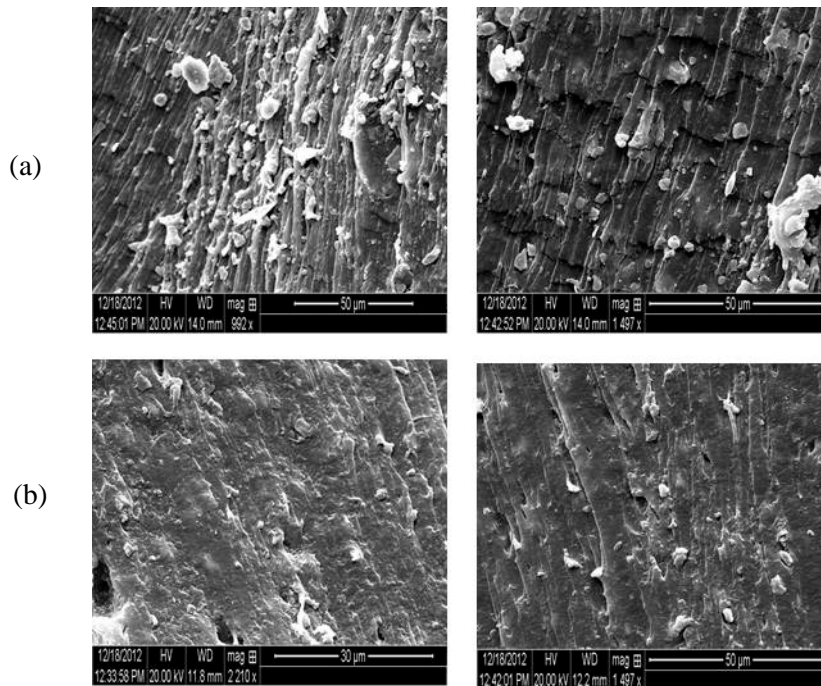
Figure 3.12. SEM images of a) 10 hr ball milled Fe 40phrMR rod (WF)

b) 10 hr ball milled Fe 40phr MR rod (WOF)

The morphology of Fe filled natural rubber (MR elastomer) is depicted in figures 3.11 and 3.12. Figure 3.11(c) represents MR elastomer rod and arrow indicates the cross sectionalview of the sample. In figure 3.11(a) layered structure formed due to field assisted curing is clearly seen and is not present in the case of samples with zero field curing figure 3.11(b). The existence of chain like or columnar structure of filler particles formed due to field assisted curing creating layers and voids are shown in figures 3.11(a)&3.12(a). However in thesecond case Figure 3.12(a)distance between different layers has reduced due to decrease in magnetisation values of iron in the 10 hours ball milled sample.Figure 3.13 (c) represents an MR elastomer rod and arrow indicating the axial direction and field direction. Figure 3.13 (a) and 3.13(b) represent SEM image of 5 hr ball milled 40 phr MRE rod both WF and WOF cut along the axial direction. Alignment of pure iron in the field direction is visible in the

case of field assisted curingFigure 3.13(a) while randomly oriented particles are seen in zero field samples Figure3.13(b).
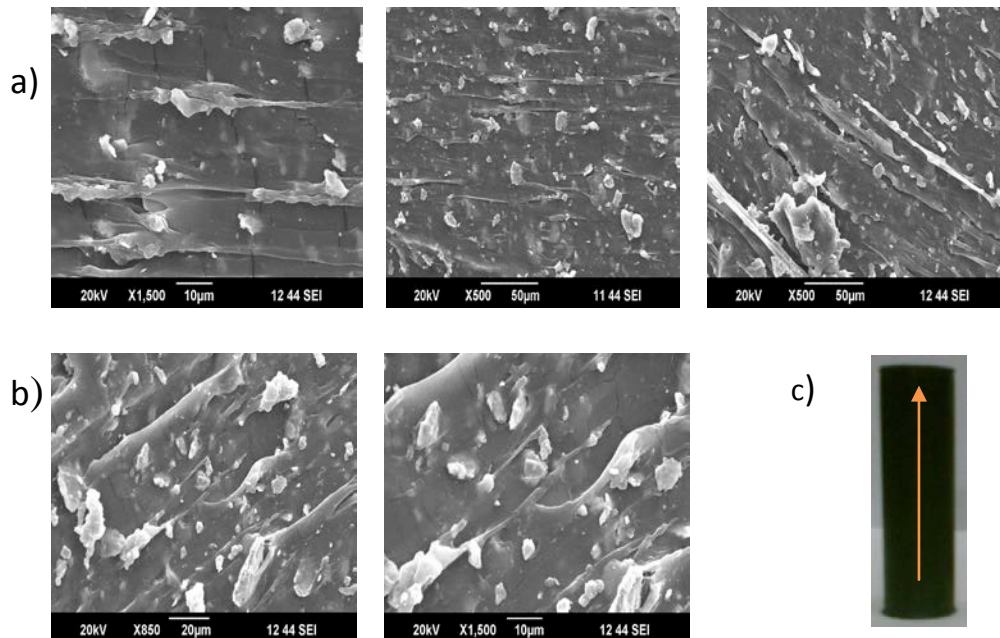
Figure 3.13.a) 5 hr ball milled Fe 40phr WF rod b) 5hr milled Fe 40phr WOF

c)   Arrow shows the direction of cross section and field direction

3.3.4. Microactuation studies

The micro actuation studies of MR elastomer rods of length 6 cm and diameter 1.8cm indicate an enhancement in actuation in field cured samples (Figure 3.14 and Figure 3.15). Maximum actuation of 0.1 mm was obtained for the 40 phr composite (5hr milled iron sample) at an ac magnetic field of strength 18.7 Oersted(figure 3.16).

Figure 3.14. Actuation curves for unmilled Fe 40 phr WF& WOF

Figure 3.15. Actuation curves for 1 hr ball milled Fe a) WOF & b) WF
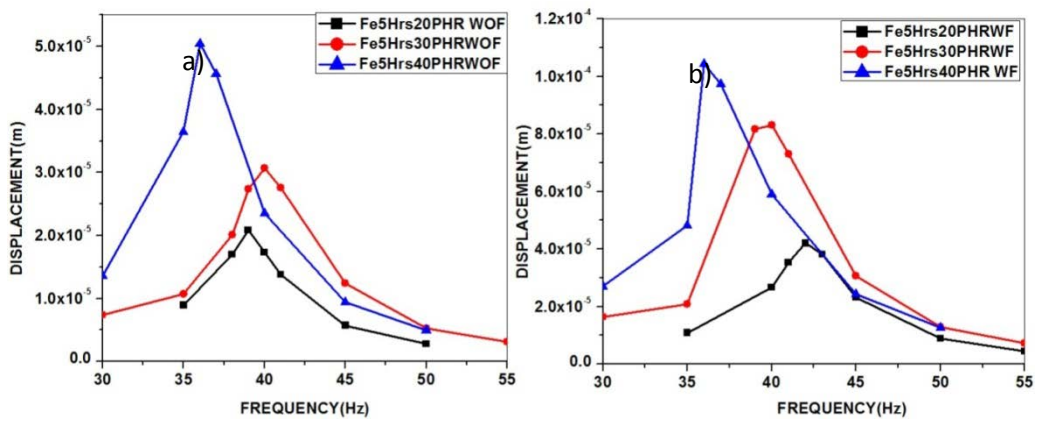
Figure 3.16. Actuation curves for 5 hr ball milled Fe a) WOF & b) WF
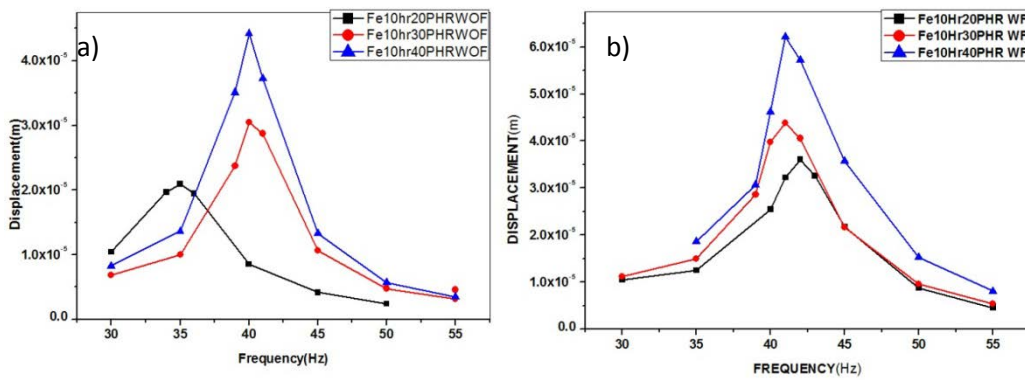
Figure 3.17. Actuation curves for 10hr ball milled Fe a) WOF & b) WF
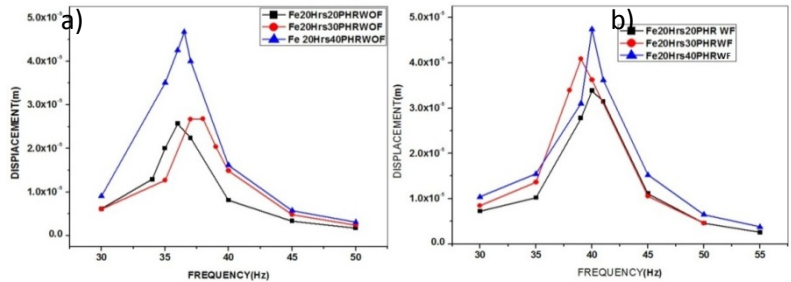
Figure 3.18. Actuation curves for 20 hr ball milled Fe a) WOF & b) WF
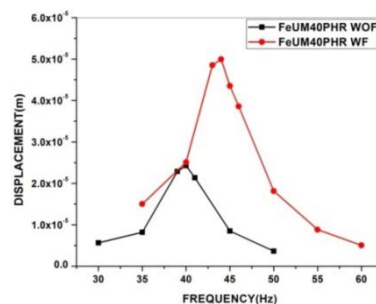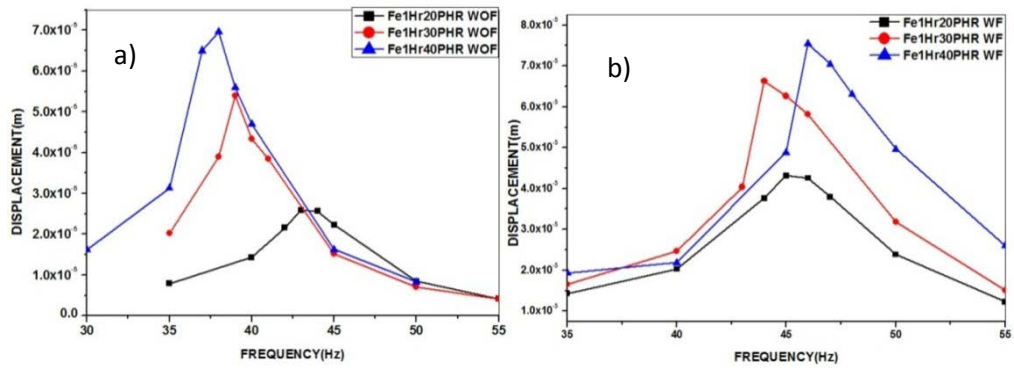
Viscoelastic nature of natural rubber, particle size and orientation of filler can affect the actuation of the rods [15, 20]. For 5hr milling, particle size, loading and magnetization of the filler was adequate for getting maximum alignment of filler in the field direction and hence enhanced micro actuation. Beyond 5 hr milling, magnetization of the filler reduces, but reinforcement of matrix increases. As a result micro actuation of these MR elastomer rods is reduced (figures3.18 and 3.19). For all samples there is a particular frequency of ac magnetic field for which the displacement have a maximum value. At this particular frequency,the effect of magnetostriction is maximum in the matrix, but for all other frequencies less than and greater than this value, the displacement produced by magnetostriction will be lesser due to the viscous component of complex tensile modulus of the composite [21,22].
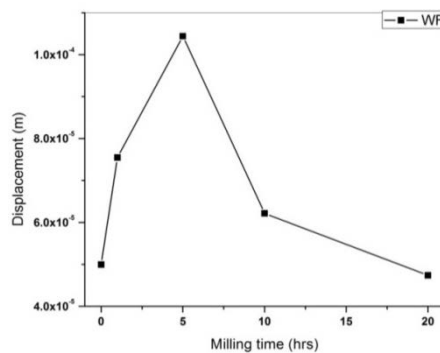
Figure 3.19. Ball milling time – displacement graph for 40 phr WF

72

a)   b)   c)   d)
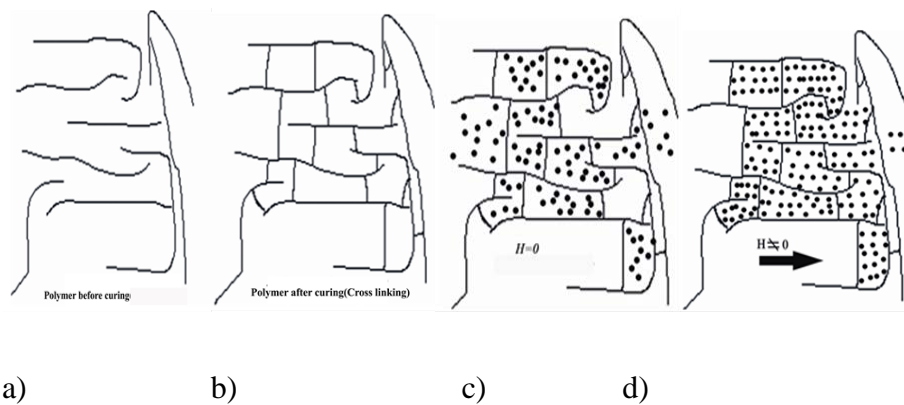
Figure 3.20. Schematic of the mechanism of field curing and alignment of filler

particles

Effect of magnetic alignment of filler particles in microactuation [22] is schematically represented in Fig 3.20. Polymer chains [23]have a usual tendency to slip away on the application of a force (Fig.3.20(a))**.**This can be controlled by cross linking the polymer chains (Fig.3.20(b)). The filler material fixed between the polymer chains further restricts this motion. But these filler materials are randomly oriented in the matrix (Fig.3.20(c)).The application of an external magnetic field while curing tends to align the initial random magnetization vectors of the filler particles along the direction of the applied field(Fig.3.20(d))**.** As a result the inter particle attractive magnetic forces reduce the average particle distance. SEM images of MRE rods with field and without field curing also indicate the above reduction in particle distance.

Figure 3.19 is the graph drawn between ball milling time and the displacement, and it can be seen that as the milling time increases displacement increases, reaches a maximum value at 5 hours milling, and then decreases. Figure 3.21 represents graphs drawn between displacement and loading of various samples. In all cases, displacement of samples increases with loading. An additional improvement in displacement is depicted for field cured samples. For isotropic

73

samples micro actuation produced will be lesser because of random rotation of magnetic domains which mutually cancel each other [23]. In anisotropic samples enhanced microactuation is evident because of the added effect of deformation of magnetic domains due to magnetostriction [24, 25].
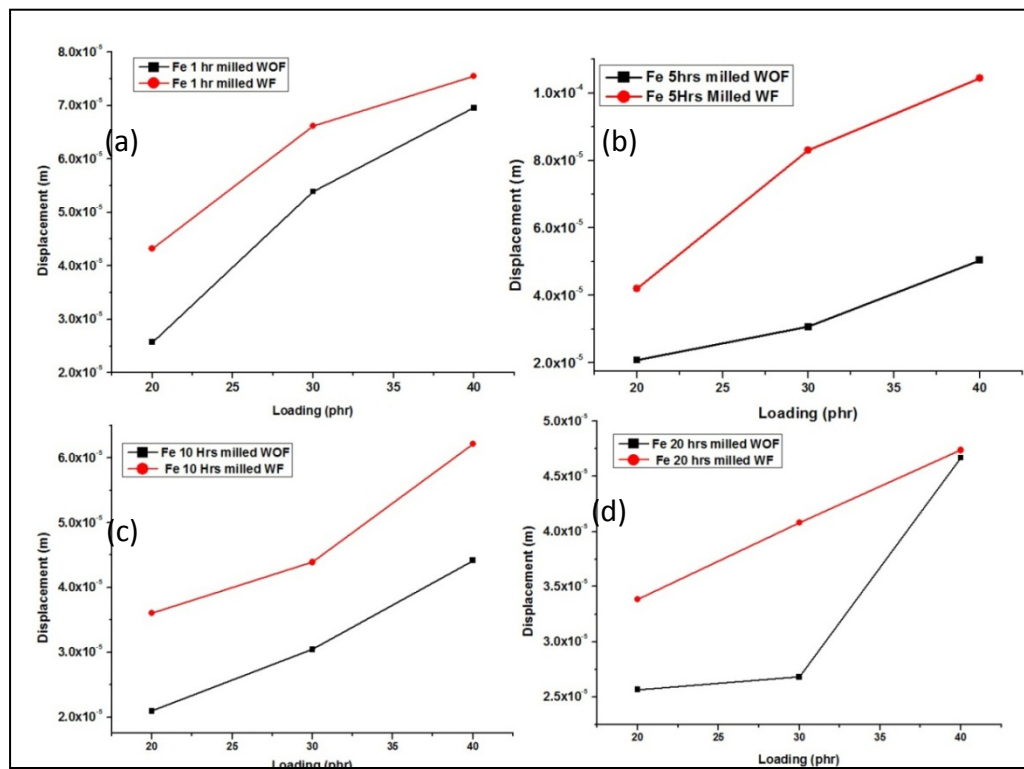
Figure 3.21. Displacement - loading curve a) Fe 1hr milled WF&WOF b) Fe 5hr milled WF &WOF c) Fe 10hr WF & WOF d) Fe 20hr milled WF&WOF

3.4. CONCLUSION

MRE rods of different weight percentage of filler were fabricated in a homemade field assisted and zero field curing setup.A detailed study on effect of loading and particle size of magnetic filler on the micro actuation of a MR elastomer based on natural rubber and ultra-fine Iron was carried out. Variation in loading and milling time of the filler particles influence the actuation of MR elastomers. The field

assisted curing of MR elastomer rods produce chain like /columnar structure of filler particles inside the polymer matrix due to anisotropy. A plausible model has been put forward to explain the observed enhanced micro actuation. These modified structures of magnetic domains enhance MR effects of field cured rods than isotropic samples. MR rods with5 hr milled pure iron of 40phr loading under field curing exhibit maximum actuation. Further studies are required to get the threshold of DC magnetic field for curing, AC magnetic field for actuation and particle size and volume fraction of filler generating optimized micro actuation. By properly maintaining all the above parameters, magneto rheological elastomers of desired properties for suitable applications can be fabricated. All passive and semi active systems available in this field can be replaced by smart magneto rheological elastomers which are efficient, reliable and cost effective.

REFERENCES

[1]. Advanced Elastomers - Technology, Properties and Applications-Publisher: InTech, ISBN 978-953-51-0739-2 (2012)412

[2]. NimaGhafoorianfa, Xiaojie Wang and FaramarzGordaninejad, Smart Mater. Struct., **23** (2014)055010

[3]. ZsoltVarga, Genove´vaFilipcsei, Miklo´sZrı´nyi-Polymer **46** (2005) 7779

[4]. Jeong-Hoi Koo, Fazeel Khan, Dong-Doo JangandHyung-Jo Jung-Smart Mater.Struct.**19**(2010) 117002

[5]. K. Danas, S.V.Kankanala ,N.Triantafyllidis-J. Mech. Phys. Solids **60** (2012) 120

[6]. Xinglong Gong, Guojiang Liao, and ShouhuXuan -Appl. Phys. Lett.,**100** (2012) 211909

[7]. Guangtao Du, Xiangdong Chen-Measurement,**45** (2012) 54

[8]. J. David Carlson, Mark R. Jolly-Mechatronics,**10** (2000) 555

[9]. Samir B. Kumbhar, Dr. Sanjay S. Gawade-International Journal of Engineering Research & Technology (IJERT), ISSN:2278-0181, **1(5)**(2012)

[10]. Wan-quan Jiang, Jing-jing Yao, Xing-long Gong, Lin Chen-Chin. J.Chem. Phys., **21**(2008)87

[11]. MattiasLokander,Torbjo¨rnReitberger, Bengt Stenberg-Polymer Degradation and Stability, **86** (2004) 467

[12]. Weihua Li, and Xianzhou Zhang-Recent Patents on Mechanical Engineering, **1**,(2008)161

[13]. Yi Han, Wei Hong, LeAnn E. Faidley- Int. J. Solids and Struct.**50**(2013) 2281

[14]. G J Liao, X L Gong, C J Kang and S H Xuan-Smart Mater. Struct.**20** (2011) 075015

[15]. S. A. Demchuk and V. A. Kuz'min-J.Eng. Phys. Thermophys. **75**(2002)3143

[16]. D Gunther, D Yu Borin, S Gunther and S Odenbach- Smart Mater.Struct. **21** (2012) 015005

[17]. B. Nayak, S. K. Dwivedy, K.S.R.K.Murthy, J. Sound Vib.**330** (2011) 1837

[18]. R. Li and L. Z. Sun- Appl. Phys. Lett.**99** (2011) 131912

[19]. WEI Ke-xiang, MENGGuang, ZHANG Wen-ming, ZHU Shi-sha-J. Cent. South Univ. Technol. **15**(2008) 239

[20]. Alan Fuchs, JokoSutrisno, FaramarzGordaninejad, MertBahadirCaglar, Liu Yanming, **117(2**)(2010)934

[21]. MemetUnsal, Christopher Niezrecki and Carl D. Crane III-J. Intell. Mater. Sys. Struct. **19** (2008) 1463

[22]. Xinchun Guan, Xufeng Dong, Jinping Ou- J. Magn. Magn. Mater. **320** (2008) 158

[23]. M.F. Winthrop, W.P. Baker, R.G. Cobb- J. Sound Vib. **287** (2005) 667

[24]. L. Lanotte,G. Ausanio ,C. Hison, V. Iannotti, C. Luponio, C. Luponio Jr.-J. Optoelectron. Adv. Mater. **6**(2004) 523

[25]. Luciano Lanotte,GiovanniAusanio, Cornelia Hison,VincenzoIannotti, Cesare Luponio-Sens. Actuators, A **106** (2003) 56

CHAPTER 4

MICROACTUATION STUDIES ON MAGNETO RHEOLOGICAL ELASTOMERS BASED ON CARBONYL IRON AND NATURAL RUBBER

4.1. INTRODUCTION

Magnetorheological elastomers, the solid state counter part of Magnetorheoloical(MR) fluids play an important role in the realm of smart and functional materials[1]. In the recent past MR fluids were used instead, but they have some drawbacks[2]. MR elastomers can take over from MR fluids as it can overcome the previously mentioned limitations like leakage and need of a container. They are cost effective too.MR technologyuses a non-contact type magnetic field, in contrast to electrorheology wherein, complicated arrangements are required for producing electric fields[3]. The magnetic field can be varied effectively by applying suitable current through the coil. By the exact application of appropriate ac/dc magnetic fields, mechanical properties of the elastomer can be controlled in a suitable manner.Magneto rheological elastomers of various shapes are required according to different device applications. Theyare very widely used in the field ofautomobiles, aerospace, mechanical engineering, sensors and actuators[4].For usein sensors and actuators,a rod type MR elastomer is required, while in vibration arrestors and engine mounts sheet type samples are utilised [5].

Carbonyl Iron is a specially made Iron of high purity (97%-99%) synthesised by chemical decomposition of purified Iron pentacarbonyl. Ironpentacarbonyl also known as Iron carbonyl is a compound with formula $Fe(CO)_5$.Under normal conditionsit is a free flowing liquid of pungent odour and straw colour[6].$Fe(CO)_5$ is manufactured by the reaction of the fine Iron particles with carbon monoxide and the major impurities are carbon, oxygen and nitrogen. It has very wide application in the field of electronics in the form of magnetic cores and microwave absorbers[7]. It is

also used in powder metallurgy and metal injection mould parts. In pharmaceutics Carbonyl Iron is used as a medicine to treat Iron deficiency [8]. Carbonyl Iron is a grey powder consisting of uniform spherical particles of size of the order of few microns. Because of the spherical shape Carbonyl Ironforms amajor component as suspended particles and fillers in Magnetorheological fluids and Magnetorheological elastomers respectively[9, 10].

In this chapter,studies on magneto rheological elastomer rods based on Carbonyl Iron and Natural Rubber is taken up.MR rods were fabricated and the microactuation were estimated with a view to employing them for actuator applications. For the fabrication of these rods ahomemade set up was designed which consist of a stainless steel mould and an electromagnet. Polymer matrix used in this case is natural rubber and magnetic filler incorporated wasCarbonyl Iron R10. For a comparison another set of MR elastomers are also fabricated using Carbonyl Iron R20 of a different particle size as filler.The experiment is repeated by changing the weight percentage of filler in natural rubber and thefabrication conditions. The rods werepreparedunder a zero magnetic field and an applied magnetic field.

4.2 EXPERIMENTAL

Carbonyl Iron was mixed withnatural rubber and other curing agents in aBrabenderPlastograph(PL 3S model) based on a recipe. It was then homogenized by passing through a two-roll mill (150mm ×300mm) for six times. Sample was kept as such in a dark room for 24 hours after which its cure characteristics were determined.Cure time is the time of vulcanization and is defined as the time taken to complete 90% of curing of the sample. It is also the time taken for fabrication or moulding.Arubber processing analyzer(RPA 2000) is utilised to determine the cure time of a small specimen and this time is used for actual fabrication with slight modification depending upon the size of the sample. Cure characteristic was plotted for each loading of Carbonyl Iron from which important cure parameters like scorch

value, minimumtorque and maximum torquewere found out [11].A homemade set up mentioned in the previous chapter was utilised in the fabrication of MR elastomers. The whole experiment is repeated as in the previous case with an additionalhigher loading of 80 phr of Carbonyl Iron in both with field and without field condition of fabrication. Magnetorheological elastomer rods of length 6cms and diameter 1.8cm were fabricated.

The structural characterization of the samples was performed using X-ray powder Diffractometer (XRD, RigakuDmax-C), with Cu Kα radiation λ=1.5418 A^0.The scanning speed was adjusted to 5ºmin^{-1} with a sampling interval of 0.05.Morphology of rod samples was studied using Scanning Electron Microscope (FEI Quanta 400 ESEM). Transmission Electron microscopy (JOEL TEM 2200 FS) was employed to determine the size of the Carbonyl Ironparticles R10 and R20. Vibrating Sample Magnetometry(VSM) was utilized for the magnetization studies of MR rods with Carbonyl Iron. This study was performed by applying a field parallel and perpendicular to the sample. By this the alignment of magnetic particles in the matrix during field curing was confirmed.MR rods with field assisted curing and zero field curing were used for measurement (VSM, model: DMS 1660).Micro actuations of these MR elastomers were studied by employing a specially designed LDV (OFV-5000 with OFV-505 Sensor Head, PolyTec) setup.

4.3 RESULTS AND DISCUSSIONS

4.3.1 Structural Characterization

Figure 4.1 shows the XRD pattern of R10 and R20 Carbonyl Iron and their composites. The peak corresponding to (110) plane of Carbonyl Iron was confirmed from the XRD pattern.
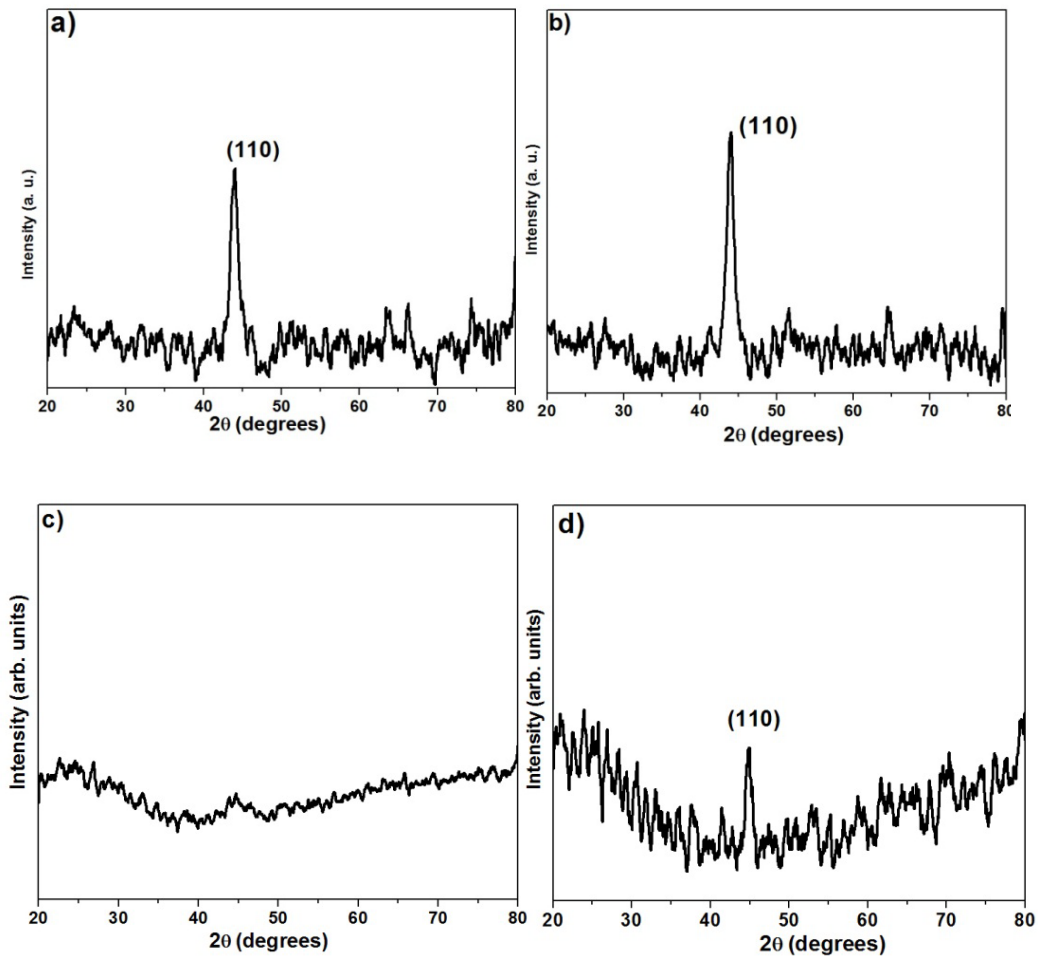
Figure 4.1.XRD pattern of Carbonyl Iron powder (a) R10 (b) R20 and Carbonyl Iron rubber composite (c) R10 and (d) R 20

TEM images of Carbonyl Ironis shown in figure 4.2.Figure 4.2 a) represent the TEM image of Carbonyl Iron R10 and Figure 4.2 b) represents that of R20. Uniform spherical spheres of Carbonyl Iron are clearly seen in TEM image. Particle size obtained for R10Carbonyl Iron was 0.4 μm and that for R20 was0.3 μm which was in agreement with the values provided by the manufacturer.
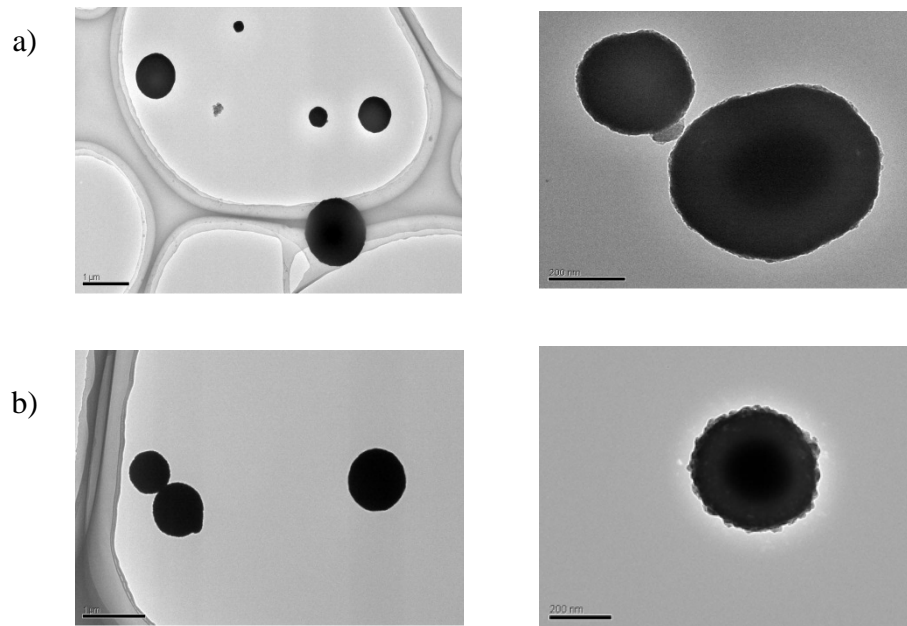
Figure 4.2.TEM images of a) Carbonyl Iron Powder R10 (b) Carbonyl Iron Powder R20

4.3.2. Magnetization studies

Figure 4.3 and4.4 show the hysteresis loop for the samples with Carbonyl Iron R10 of different weight percentages. Hysteresis loops of in plane and out of plane measurements are superimposed to show the effect of anisotropy and an easy and earlier saturation is obtained in all cases of samples under field assisted curing.Figure 4.5 and4.6 represent the hysteresis loop for the samples with Carbonyl Iron R20 of different weight percentages. The magnitude of saturation magnetization (M_s) increases with the loading of the filler in the matrix which is on expected lines [12].
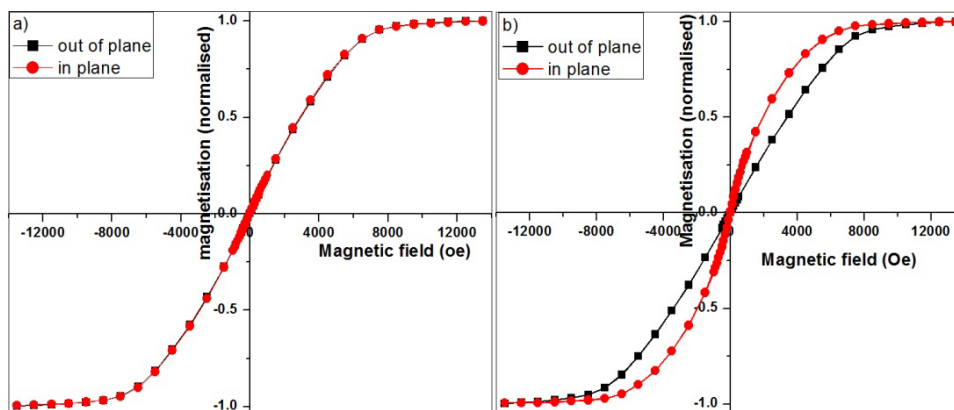
Figure 4.3. Hysteresis loop-in plane and out of plane for the samples with Carbonyl Iron R10-40phr (a) WOF (b) WF
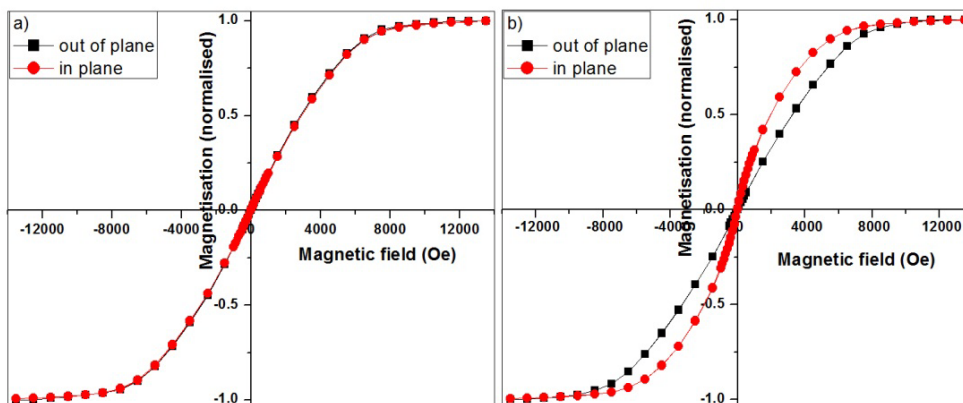
Figure 4.4. Hysteresis loop-in plane and out of plane for the samples with Carbonyl Iron R10-80phr (a) WOF (b) WF
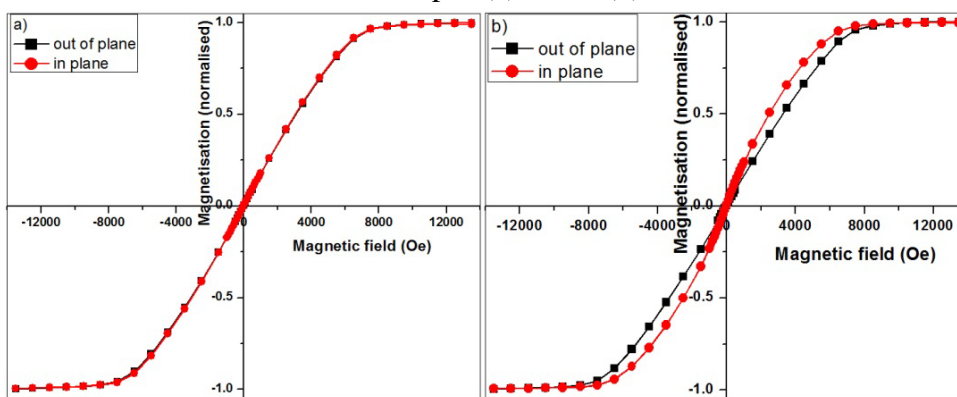
Figure 4.5. Hysteresis loop-in plane and out of plane for the samples with Carbonyl Iron R20 40phr a) WOF b) WF
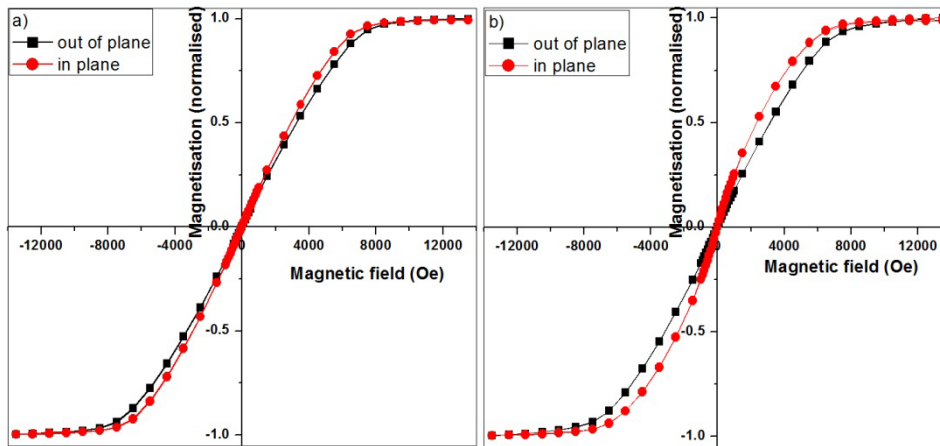
Figure 4.6. Hysteresis -in plane and out of plane for the samples with Carbonyl Iron R 20 80phr a) WOF b) WF

Hysteresis loop of the samples have been recorded under two different field orientation parallel and perpendicular to the plane of the sample. This is to find whether there is any change in the anisotropy energy with the application of amagnetic field during the curingof thecomposite sample [13, 14].
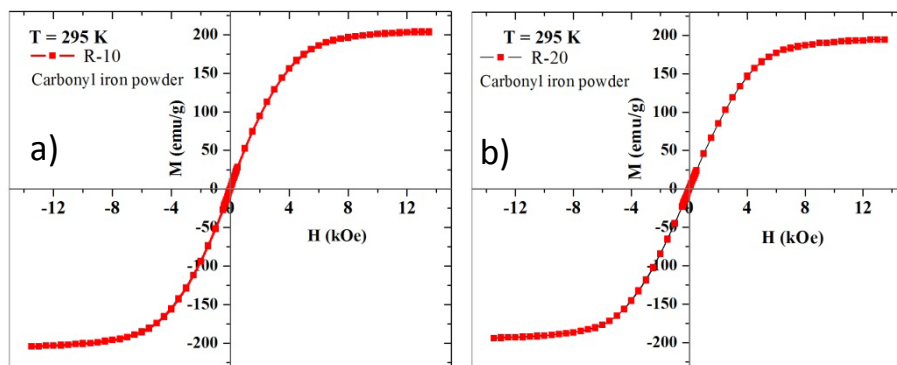
Figure4.7. Hysteresis loop of Carbonyl Iron powders a) R10 b) R20

From Figure 4.3 - 4.6, it is clear that the area between the parallel and perpendicular loop is least for the one which is cured in zero magnetic field. In WOF samples, since the fillers are randomly oriented no anisotropy is exhibited along in plane or out of plane directions.While for WF sample,due to alignment of fillers an

easy axis is obtained,which is in the direction of magnetic field applied for curing.Thus field cured sample exhibits anisotropy[15].
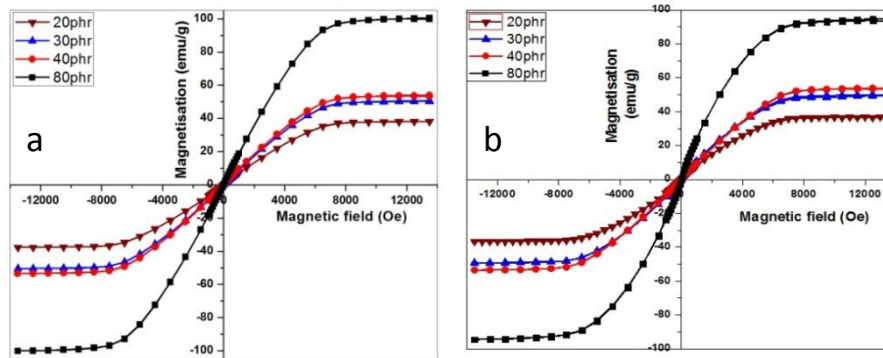
Figure 4.8. Hysteresis loop of R10 MR rods a) WOF and b) WF for different loading

Figure 4.7 represents hysteresis loops of R10 and R20 powders. Value of saturation magnetization of R10 is higher than that of R20.Same trend is observed in MRE rods also.Figure 4.8 and Figure 4.9 gives hysteresis loop of R10 and R20 MR rods of various loading with field and without field curing conditions. Saturation magnetization of all samples increases with increase of filler loading. Effect of field assisted curing is very clear in MH loop of WF MR rods. Figure 4.10 shows the variation of saturation magnetization with loading and it is clear that there is a gradual increase in magnetization with the increase in weight percentage which is in expected lines. The loop parameters are tabulated and shown in table 4.1.
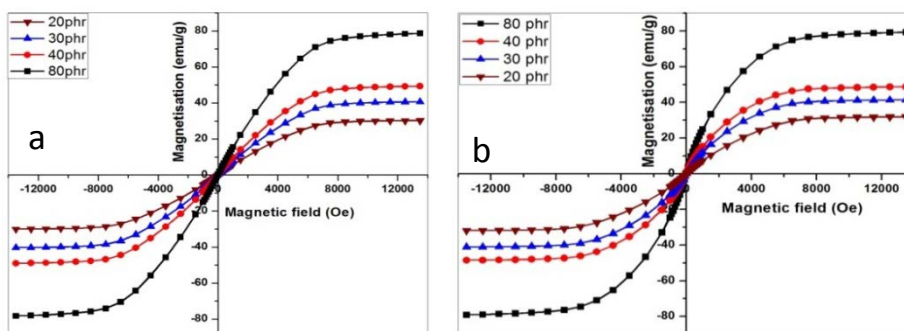
Figure 4.9. Hysteresis loop of R20 MR rods a)WOF and b)WF for different loading

Powder	M_s (emu/g)	H_c (Oe)
R10	201	7
R20	193	6

Table 4.1(a) Magnetization Measurements – Carbonyl Iron

MRE rods	Loading	M_s (emu/g)		H_c (Oe)	
		WF	WOF	WF	WOF
R10	80phr	94	99	6	12
	40phr	52	52	21	19
	30phr	48	49	21	4
	20phr	33	36	4	29
R20	80phr	79	77	6	9
	40phr	48	49	8	15
	30phr	41	40	12	19
	20phr	31	28	6	19

Table4.1(b) Magnetization Measurements -MRE rods

The saturation magnetization and coercivity values of all samples are tabulated and shown in table 4.1 (a) & (b).Here it may be mentioned that the coercivity of samples cured with and without field is not much different.The loading versus M_s is plotted and is shown in the figure 4.10.
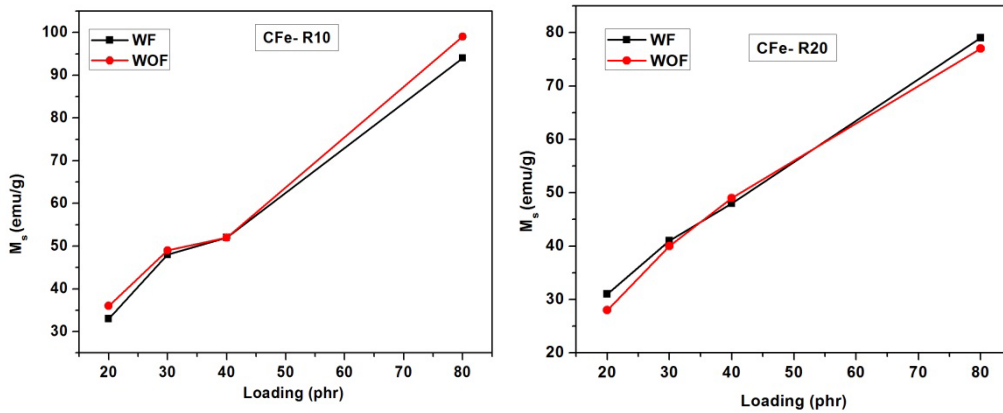
Figure 4.10. Loading vs Ms graph for a) R10 and b) R20

4.3.3. Morphological studies

The morphology of Carbonyl Ironfilled natural rubber (MR elastomer) is given in Figure 4.11. Spherical Carbonyl Ironfiller in the Natural rubber matrix is clearly visible in the cross section.
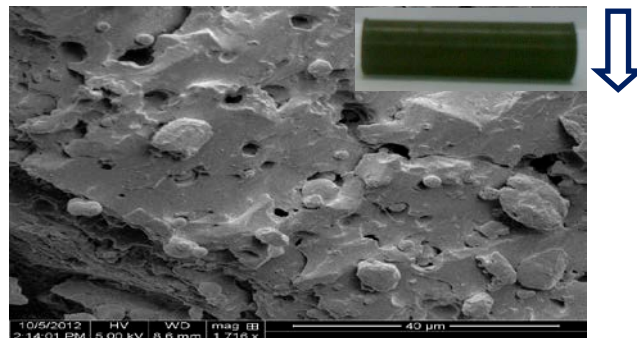
Figure 4.11.SEM of Carbonyl Iron R10-80 phr MR rod (WF)

Figure 4.12represents the morphology of MR elastomer rods along the axial direction. The alignment of magnetic particle along the field direction is established in the SEM image of field cured sample(figure 4.13). For zero field cured samples, spherical Carbonyl Iron particles are randomly distributed (figure 4.12).For morphology studies, MRE rods were cut along both transverse and longitudinal

directions. On close observation of these SEM images it is clear that filler free areas and voids are largely seen in field cured samples.These voids and layers are formed because of the particle-particle interaction between magnetic fillers. On field assisted curing Iron nano particles come closer and closer in the field direction creating chain like and columnar structures.
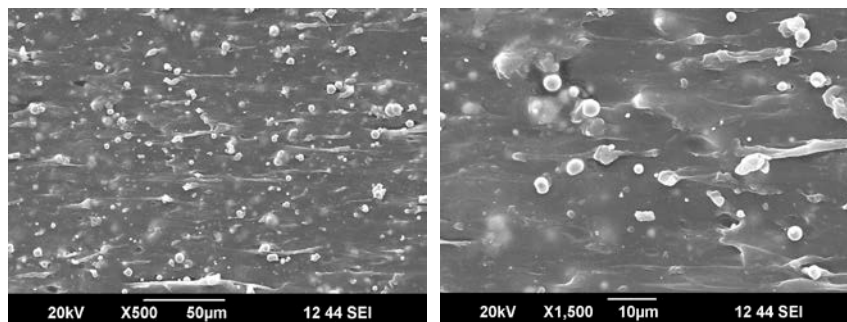
Figure 4.12.SEM of Carbonyl Iron R10-80phrMR rod WOF

This rearrangement of magnetic nano particles gives rise to formation of filler free areas, layered structure and voids. All these structures are very clearly visible in cross sectional SEM and axial SEM.Correspondingly this will reduce the stiffness of theMRE rod under field assisted curing and can be considered as a reason for enhanced micro actuation.
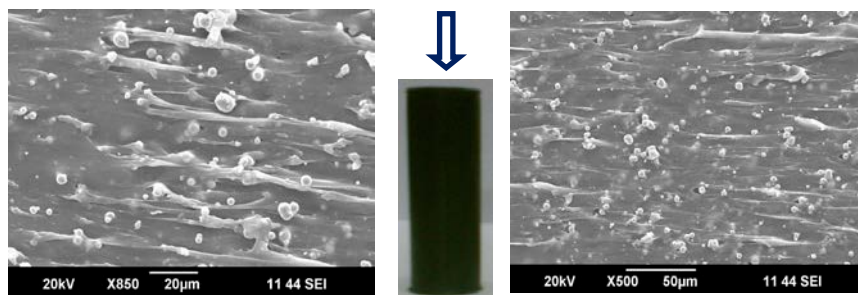
Figure 4.13. Carbonyl Iron R10-80phr MR rod WF (Field direction is shown in between)

4.3.4. Microactuation Studies

MREs of different weight percentages of Carbonyl Iron R10 and R20 under field assisted curing and zero field curing were fabricated. Micro actuation of all the samples exhibit positive(increasing) trend with loading.For R10 sample of 80 phr loading actuation produced was maximum for field cured samples. But forR20 samples of same loading actuation obtained was minimum. Comparing the actuation of anisotropic rods and isotropicrods, anisotropic rods have an additional advantage due to field assisted curing(Figure 4.14 and4.15).Viscoelastic nature ofnatural rubber, particle size and alignment of filler in matrix can also influence the actuation of the rods[16, 17]. For R10 samples, particle size,loading and magnetization of the filler was conducive for achieving maximumalignment of filler in the field direction and hence enhanced micro actuation is obtainedin an alternating magnetic field.For each sample there is a particular frequency of ac magnetic field for which rotation of magnetic domains inside the polymer matrix on either direction due to magnetostriction has a maximum value. This results in maximum actuation/displacement of the sample for that frequency[18, 19].
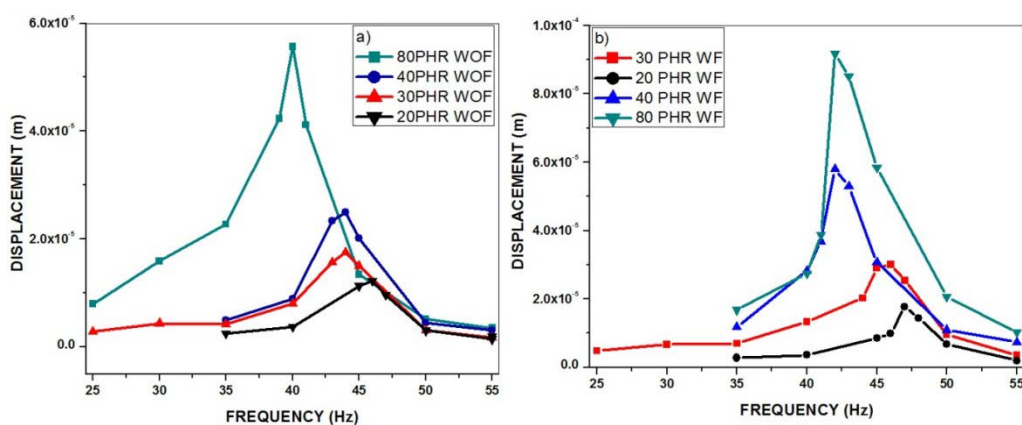
Figure 4.14. Actuation curve for Carbonyl Iron-NR rods R10a) WOF b)WF
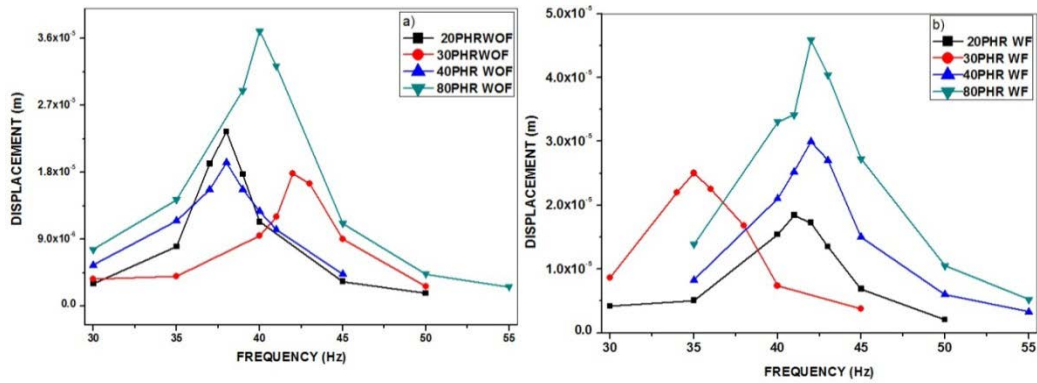
Figure 4.15. Actuation curve for Carbonyl Iron-NR rods R20a) WOF b)WF

At the frequency corresponding to maximum displacement, magnetic domains have maximum mobility and therefore theresultant displacement is also maximum. But for other frequencies less than or greater than this value, added effect of displacement will be somewhat lesser depending upon therelaxation time and viscoelastic nature of the composite[20,21]. The displacement of samples increases with loading. An additional improvement in displacement is observed for field cured samples. The layers of wavy chain like structures of magnetic particles create some columns of filler free regions inside the matrix. This in turn decreases the storage modulus and effects a corresponding reduction in stiffness [22]. This is the reason for enhanced micro actuation of MRE due to field assisted curing. Actuation produced is maximum for MR rods filled with Carbonyl Iron R10 at 80 phr loading under field curing. For isotropic samples micro actuation produced will be lesser because of randomly oriented magnetic moments. Zero field curing has no special effect on magnetic fillers and therefore they get dispersed as such. This will improve the stiffness of the MRE rod and hence reduce microactuation.For anisotropic samples, due to the presence of chainlike structure of magnetic filler,deformation of magnetic domains due to magnetostrictionin the aligned direction will be maximumand results in an enhancedmicroactuation.

89

4.4. CONCLUSION

MRE rods of different weight percentages of Carbonyl Iron R10 and R20 were fabricated in a homemade setup for field assisted curing and zero field curing.A study on micro actuation of these rodswas performed.Anincrease in loading and particle size of the filler enhance the micro actuation of MR elastomers. Field assisted curing of MR elastomer rods produced chain like /columnar structure of filler particles inside the polymer matrix whichenhanced the MR effects of field cured samplescompared to zero field samples.MR rods with Carbonyl Iron R10 of 80 phr loading under field curing show maximum actuation. In all cases magnetization values increases with loading. Actuation obtained also indicates the same tendency. With field assisted curing,an enhancedactuation is observed. Out of two Carbonyl Iron powders R10 and R20, R10 of 80 phr loading under field curing is the best candidate for magnetorheological elastomers.MREs can be tailored for various applications by suitably varying the filler concentration, particle size/crystallite size, base matrix and magnetic field applied during curing and testing.

REFERENCES

[1]. Jinkui Wu, Xinglong Gong, Yanceng Fan and Hesheng Xia - Smart Mater. Struct. **19** (2010) 105007

[2]. S R Gorodkin, R O James and W I Kordonski-J. Phys.: Conference Series **149** (2009) 012051

[3]. YupingDuan, Guofang Li, Lidong Liu and Shunhua Liu- Bull. Mater. Sci. **33** (2010) 633

[4]. Seyyed M Hasheminejad and MaysamShabanimotlagh- Smart Mater. Struct. **19** (2010) 035006

[5]. Hua-xia Deng, Xing-long Gong and Lian-hua Wang- Smart Mater. Struct. **15** (2006)111

[6]. Anna Boczkowska, Stefan F. Awietjan- J. Mater. Sci. **44** (2009)4104

[7]. Lin Chen, Xing-long Gong , Wan-quan Jiang ,Jing-jing Yao , Hua-xia Deng ,Wei-hua Li- J. Mater. Sci. **42** (2007)5483

[8]. Marcelo J. Dapino , Ralph C. Smith , LeAnn E. Faidley , Alison B. Flatau – J. Intell. Mater. Sys. Struct. **11** (2000) 135

[9]. Cornelia Lorelai Hison- PhD thesis (2005)

[10]. Hua-xia Deng, Xing-long Gong and Lian-hua Wang-Smart Mater. Struct. **15**(2006) 111

[11]. Xiushou Lu, XiuyingQiao, Hiroshi Watanabe, Xinglong Gong, Tao Yang, Wei Li. Kang Sun, Meng Li, Kang Yang, HongenXie, Qi Yin, Dong Wang, Xiaodong Chen- RheolActa**51** (2012) 37

[12]. Jae Lim You, Bong Jun Park, and HyoungJin Choi-IEEE Trans. Magn. **11** (2008) 44

[13]. Miao Yu, BenxiangJu, Jie Fu, Xueqin Liu, Qi Yang –J. Magn. Magn. Mater. **324** (2012) 2147

[14]. L. Chen, X.L. Gong, W.H. Li-Polym. Test. **27(3)**(2008)340

[15]. Won Jun Choi- Ph.D thesis (2009)

[16]. Baoshan Zhang, Yong Feng, JieXiong, Yi Yang, and Huaixian Lu-IEEE Trans. Magn. **7** (2006) 42

[17]. B. Nayak, S.K. Dwivedy , K.S.R.K. Murthy-Int. J. Non Linear Mech., **47**(2012)448

[18]. T Borbath, S Gunther¨, D Yu Borin, ThGundermann and S Odenbach-Smart Mater. Struct. **21** (2012) 105018

[19]. ÍvarGuðmundsson-Ph.Dthesis (2011)

[20]. MattiasLokander- Ph.D thesis (2002)

[21]. X.L. Gong, X.Z. Zhang, P.Q. Zhang- Polym. Test. **24** (2005) 669

[22]. W. Zhang, X. L. Gong, S. H. Xuan, and Y. G. Xu-Ind. Eng. Chem. Res. **49** (2010) 12471

CHAPTER 5

ON THE MECHANICAL PROPERTIES OF MAGNETO RHEOLOGICAL ELASTOMER RODS AND SHEETS BASED ON NATURAL RUBBER AND IRON

5.1. INTRODUCTION

Mechanical Properties of Magnetorheological (MR) elastomers have an important role to play in the engineering applications of these elastomers. MREsare polymer composites in which magnetic fillers are embedded orderly or randomly.Natural rubber, polyurethane and silicone rubber can serve as matrices while the magnetic fillers can be soft or hard, usually used are high energy ball milled iron, carbonyl Iron and Terfenol–D [1-4]. These elastomeric composites can undergo instantaneous strain or change in dimension when placed in a magnetic field according to a property called magnetostriction[5]. Their stiffness can be varied by applying a varying magnetic field which makes them suitable candidates in the field of actuators.Similarly a stress on a magnetically oriented sample can produce a change in overall magnetization [6]. This behaviour of MR elastomers can be utilized in the area of sensors. In automobile industry, these materials have enormous applications in the form of vibration arrestors, clutches, brakes and suspension system. In aerospace engineering they are used to control vibration and failure free sealing [7-8]. Due to their flexibility and adaptability MR elastomers can be fabricated into objects of any size or shape.

MR elastomer sheets are smart materials which exhibit viscoelasticity: a property of exhibitingboth elastic and viscous nature [9-10].Iron in micron regime and nanoregime can serve as useful fillers.These fillers are to be incorporated in an appropriate matrix to fabricate MR elastomers. The matrix chosen in this study is inexpensive natural rubber. The fillers are incorporated to make rods and sheets

according to a specific recipe. The alignment of magnetic fillers during curing has a profound influence on the mechanical properties of these MR elastomers. For this a specially made field curing set up is necessary. This has been fabricated in house and the details are provided in Chapter 2.The curing of MRE sheets and rods are performed for two different directions of magnetizations.For this, a setup employing a coil and permanent magnet is made (see chapter 2 for details).

The micron sized fillers are reduced to nano dimensions by high energy ball milling and nano composites are made with different loading of fillers. The effect of size,loading and magnetic field during curing on the mechanical properties is studied in this chapter.Shear modulus of a viscoelastic material is a complex entity. It consists of a real part representing storage modulus and an imaginary part giving loss modulus. Storage modulus of the material is its capacity to store energy while deforming and loss modulus represents the amount of energy dissipated when the material is undergoing a strain [11,12]. These properties are studied in details for different loading and sizes of the filler. Their magnetic properties are also evaluated.

5.2. EXPERIMENTAL

Magnetorheological elastomer rods of different weight percentage and particle size of iron were fabricated by employing a field assisted curing set up. Thematrix used wasnatural rubber. High energy ball milling was employed to reduce the grain size of pure Iron with different milling times of 1hr, 5hr, 10hr and 20 hr. The first set of rods was prepared under isotropic conditions, that is in the absence of any magnetic field and for the next batch anisotropy is produced by field assisted curing. MR sheets were prepared by applying a field normal to the plane of the sample during mouldingfor which a special type of mould was designed. By placing an electromagnet around the mould, a normal field can be generated along the axial direction. For the second set of anisotropic samples a set up was used in which a horizontal field was applied to the sample during curing. Thus fivesets of samples in

the form of rods and sheets of various weightpercentages and milling times were prepared. They are named as with field coil or WF(C), with field magnet or WF (M) and without field or WOF samples. Loading of ball milled iron was varied as20phr (parts per hundred grams of rubber), 30phr and 40phr.

For the fabrication of sheet type samples, a specially made pre heated mould was used. Appropriate amount of mixture was placed inside the preheated mould and the electromagnet was placed around the mould to produce a magnetic field normal to the plane of the sample. It was then placed on the hydraulic press kept at a temperature of 150^0 C and a high pressure of 200 kg/cc was applied using a hydraulic press. Electromagnet was switched on during curing. Cure time was predetermined using Rubber Processing Analyser (RPA).After the completion of curing, sample was removed from the mould and immersed in cold water for some time. This is named asWF(C) (anisotropic samples).

For the preparation of WF (M) sheets, permanent magnets were placed on either side of the mould so that a near uniform magnetic field was produced in a direction parallel to the plane of the sample. The details are described in chapter 2. Ina similar manner isotropic samples were prepared under zero field condition and they are named (WOF).

5.3. RESULTS AND DISCUSSIONS

5.3.1. Structural Studies

Figure 5.1 shows the XRD patterns of MRsheets. These sheets contain 40 phr of milled Iron (1hr), (5hr), (10hr) and (20hr).The pattern is identifiable with a prominent peak at $2\theta = 44.3°$. The amorphous peaksare due to the natural rubber present in the composites. Traces of Iron Oxide are visible in the XRD pattern. The peak at $2\theta = 44.3°$ is due to reflections from (110) plane of bcc -Fe. As seen in the

powder samples here also the line broadening isclearly seen with sufficient reduction in grain size.
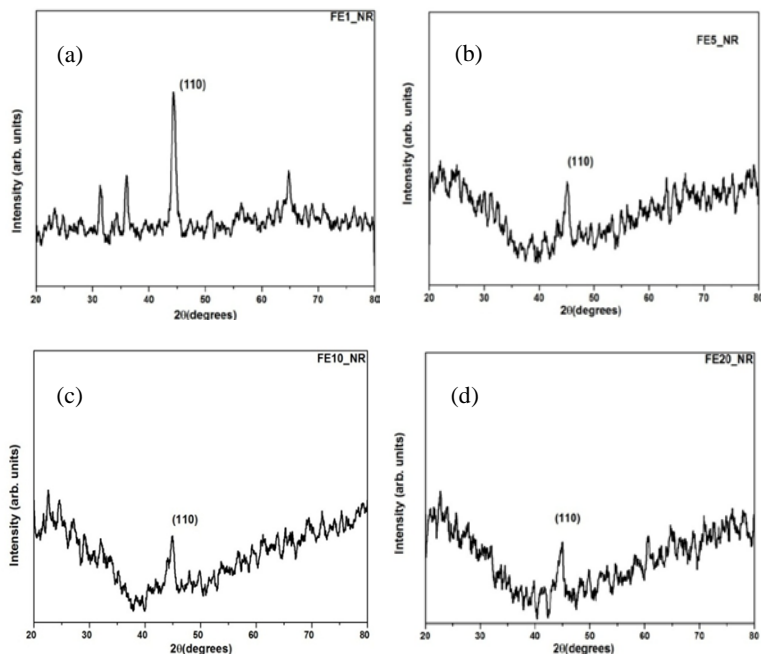
Figure 5.1.XRD pattern of nano composite containing ball milled iron (a) 1 hr (b) 5 hr (c)10hr(d) 20hr
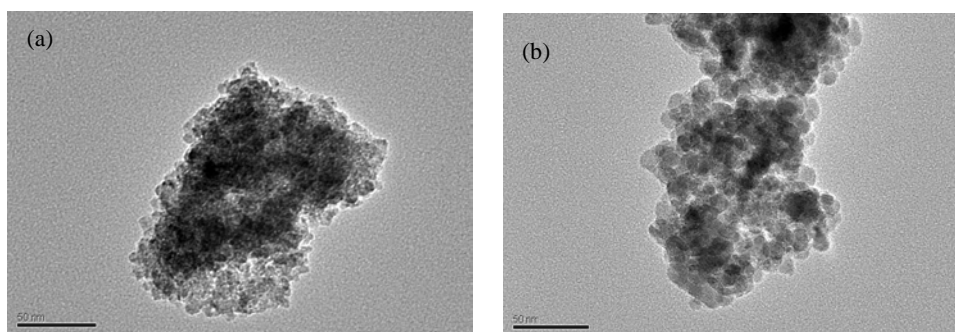
Figure 5.2.TEM images of (a) 10 hr (b) 1hr ball milled iron powder

Figure 5.2represent TEM images of pure Iron powder milled for 10hr and 1hr.Particle size reduction due to high energy ball milling is clearly evident from the micrographs and particle size is 12nm for 1hr milled and 6nm for 10hr milled.

96

5.3.2. Magnetisation studies

Hysteresis loops of MRE samples are shown in figure 5.3. Measurements were performed for both parallel and perpendicular field directions. For WF(C) samples, out of plane measurement exhibit a saturation magnetization indicating the alignment of magnetic particles in the normal direction. For all the other samples a saturation magnetization is obtained for in plane measurement. This is a clear evidence for the orientation of magnetic fillers in a direction perpendicular to the plane of the sheet for WF(C) samples. The parameters are typical of anisotropic samples.
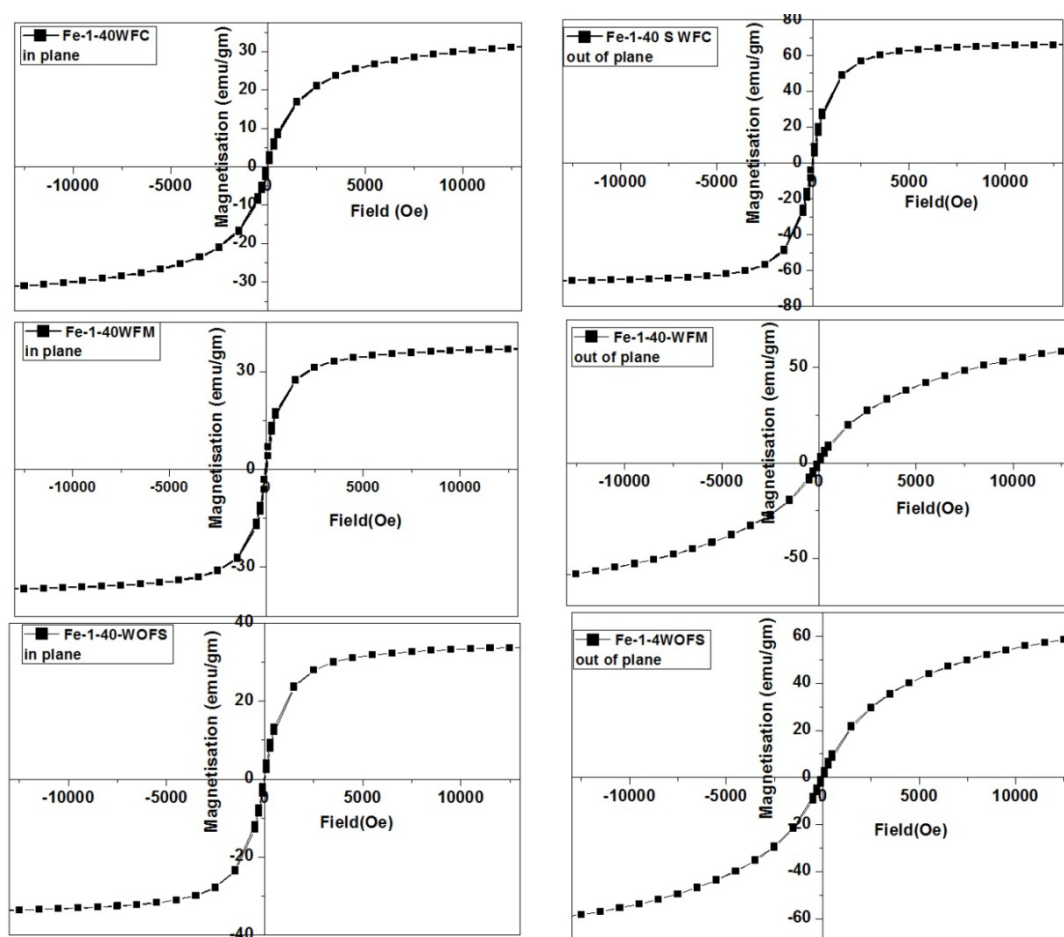
Figure 5.3.In plane and out of plane hysteresis loop of MR sheets with 1 hr ball milled IroninWF(C),WF (M), WOF
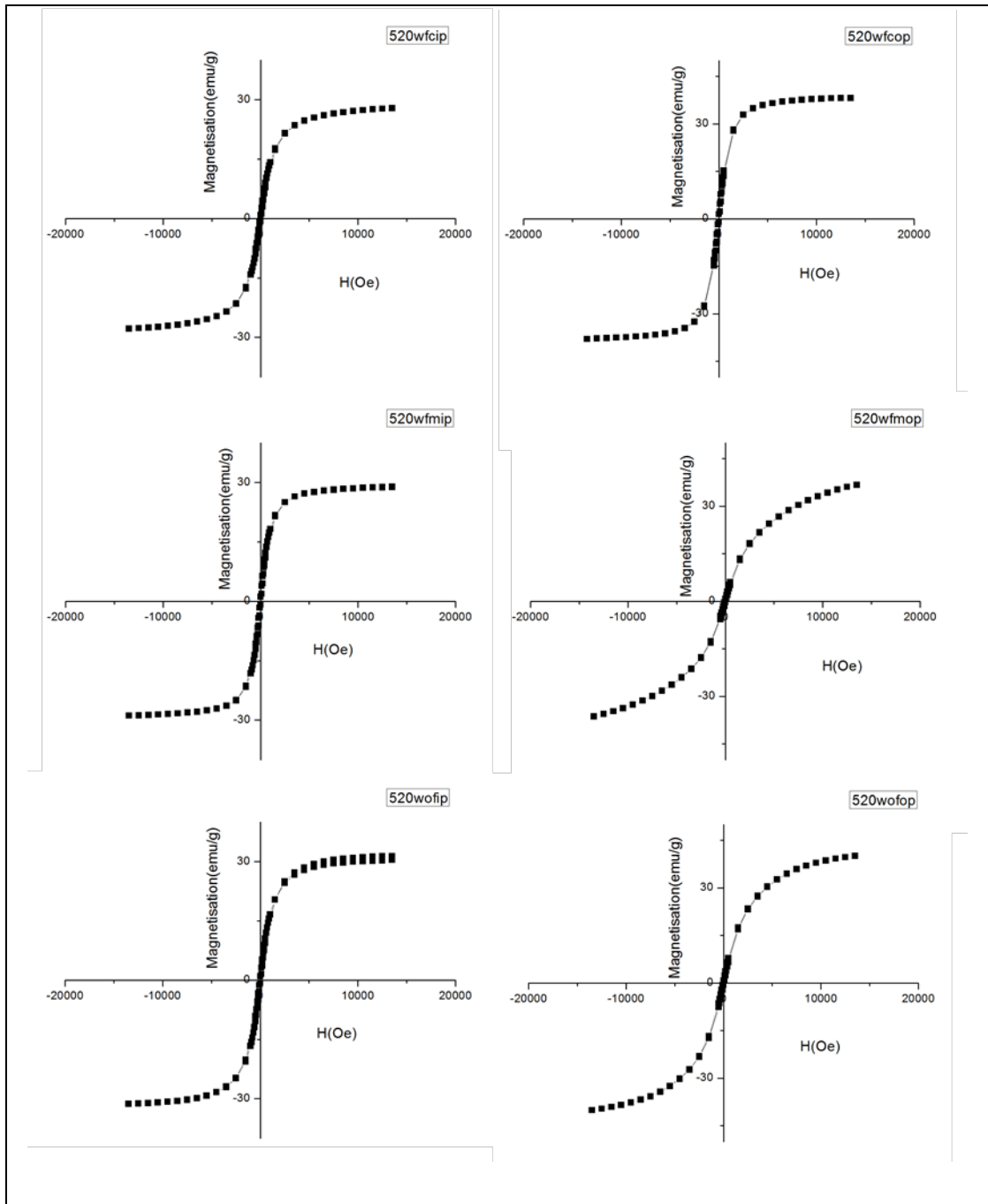
Figure 5. 4. In plane and out of plane hysteresis loop of MR sheets with 5 hr ball milled 20phr Iron inWF(C),WF (M), WOF
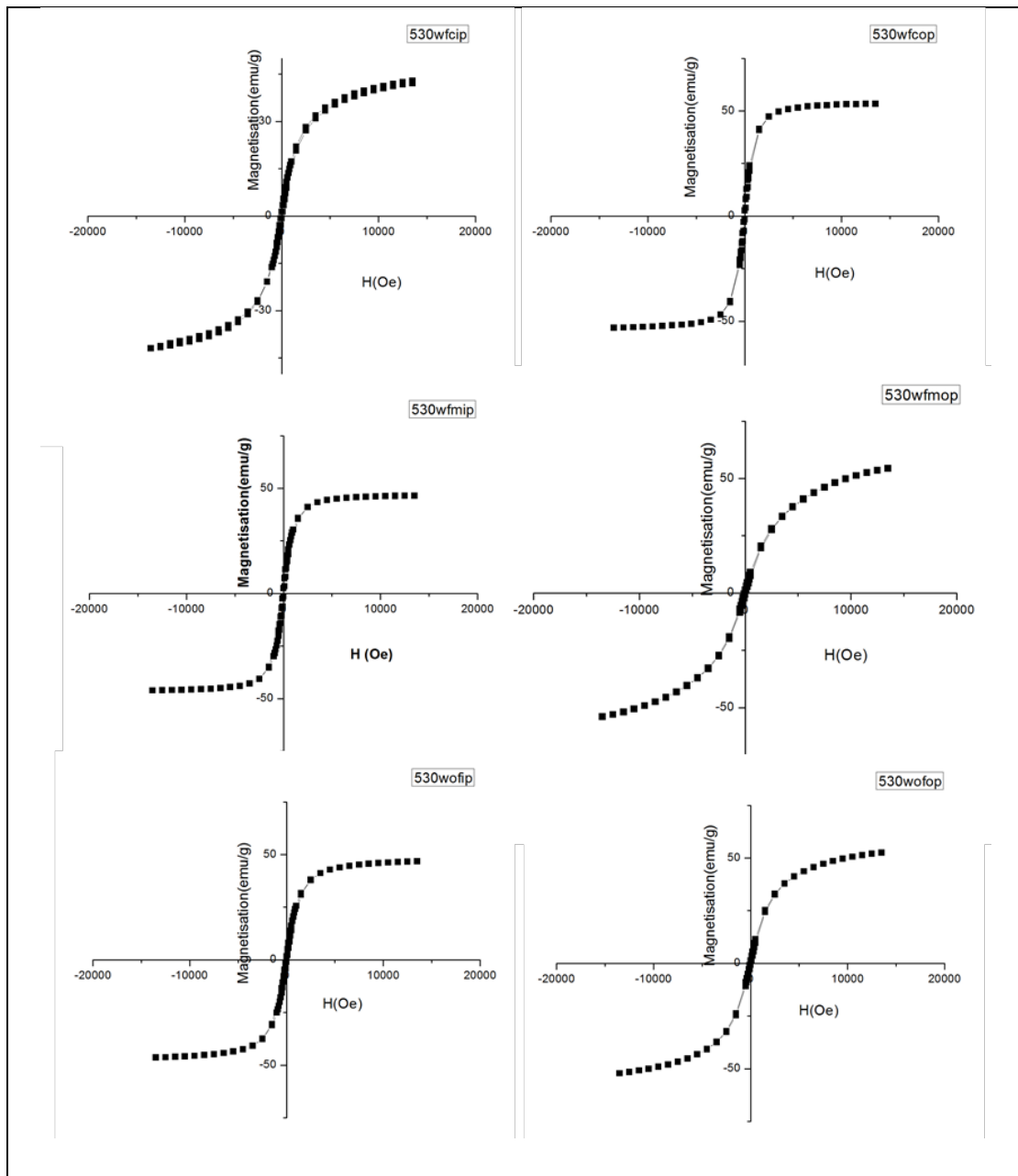
Figure 5.5.In plane and out of plane hysteresis loop of MR sheets with 5 hr ball milled
30phr Iron inWF(C),WF (M), WOF
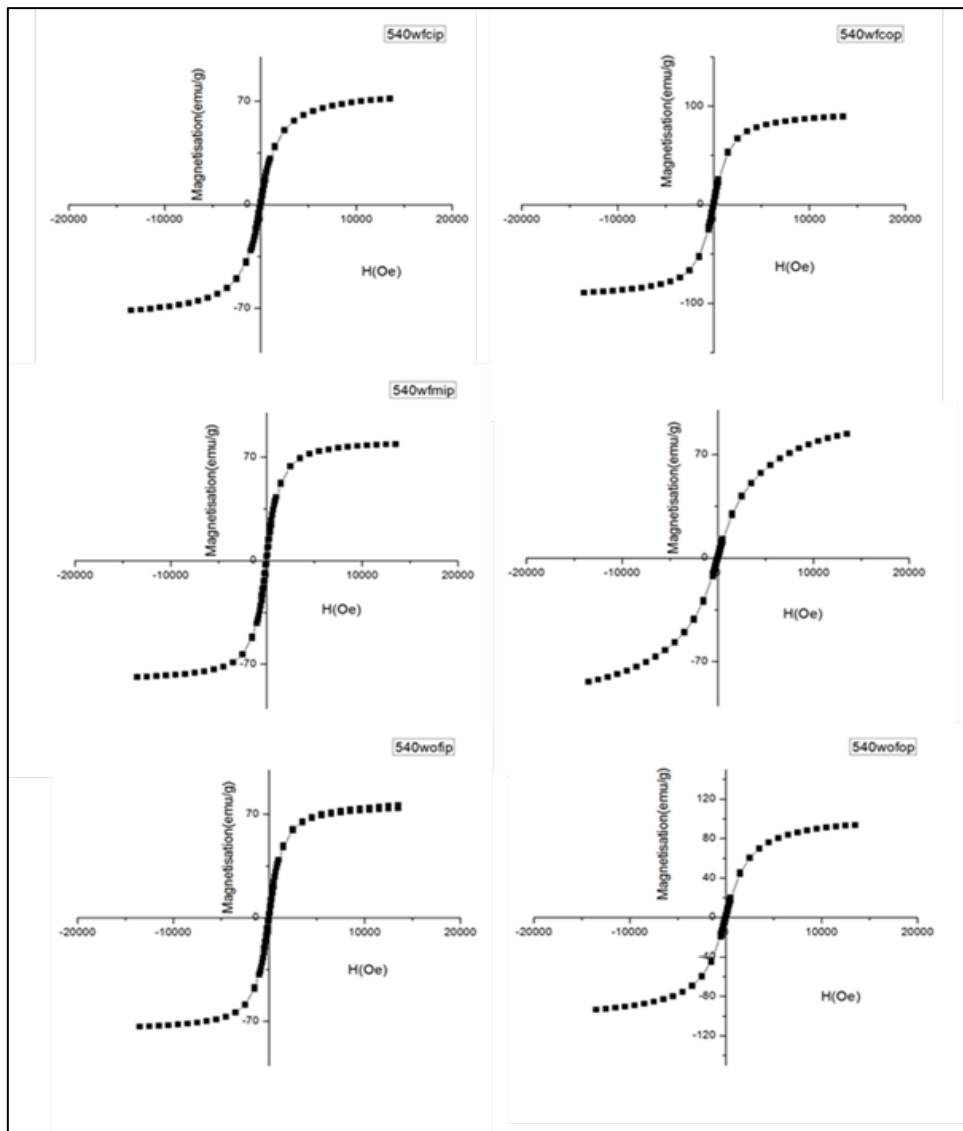
Figure 5.6. In plane and out of plane hysteresis loop of MR sheets with 5 hr ball milled 40phr Iron inWF(C),WF (M), WOF

The loop parameters are tabulated and shown in table 5.1. The saturation magnetization M_s of sheets increases with loading of magnetic filler which is on expected lines. The H_c with respect to in plane and out of plane measurements is evidence for anisotropy. H_c increases with loading of filler.

	Fe 1 hr MRE					
	40 phr					
	WF(C)		WF(M)		WOF	
	Out of Plane		In Plane			
	M_s (emu/g)	H_c (Oe)	M_s (emu/g)	H_c (Oe)	M_s (emu/g)	H_c (Oe)
	66.1	30.72	36.82	29.26	33.36	32.17
Error		±1		±1		±1

	Fe 5 hr MRE																	
	20 phr						30 phr						40 phr					
	WF(C)		WF(M)		WOF		WF(C)		WF(M)		WOF		WF(C)		WF(M)		WOF	
	Out of Plane		In Plane				Out of Plane		In Plane				Out of Plane		In Plane			
	M_s	H_c	M_s	H_c	M_s	H_c	M_s	H_c	M_s	H_c	M_s	H_c	M_s	H_c	M_s	H_c	M_s	H_c
	emu/g	Oe	emu/g	Oe	emu/g	Oe	emu/g	Oe	emu/g	Oe	emu/g	Oe	emu/g	Oe	emu/g	Oe	emu/g	Oe
	38	52	29	51	31	47	53	49	46	46	46	49	89	47	79	50	76	49
Error		±1		±1		±1		±1		±1		±1		±1		±1		±1

Table 5.1. Magnetization studies–Loop parameters of 1 hour and 5 hour milled Fe (20phr, 30phr & 40phr loading) MRE sheets WF(C), WF (M) and WOF samples

5.3.3. Surface morphological studies
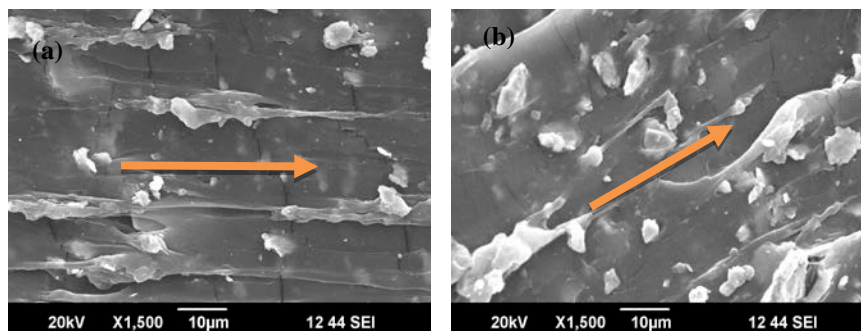
Figure 5.7.SEM images of (a) MRE rod 5 hr milled Fe 40phrWF (arrow- axial direction of the rod and field direction H≠0) (b) MRE rod 5hr milled Fe 40phr WOF (arrow- axial direction of the rod and field H=0)

SEM images of WF(C), WF (M) and WOF samples are shown in figure5.8.In WF(C) samples a magnetic field is applied normal to the plane of the sheet. Corresponding SEM micrograph shows evidence for orientation of fillers in the applied magnetic field direction (Figure5.8 a).
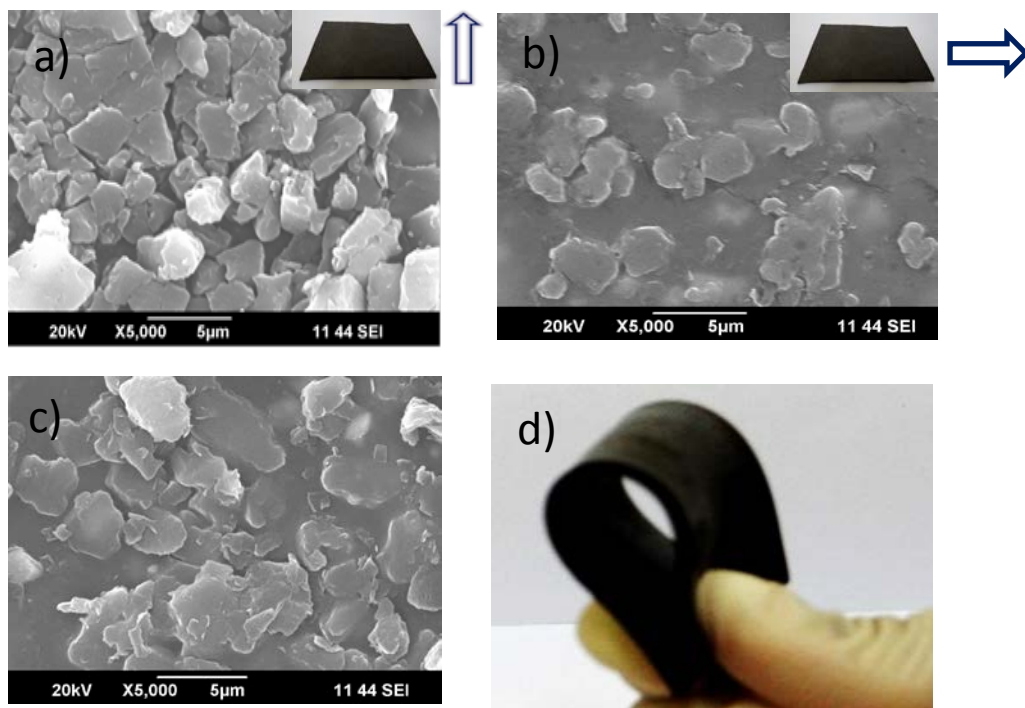
Figure 5.8.SEM images of MRE sheet a) WF(C), b) WF(M) and c) WOF (MRE sheet and field direction shown in inset) d) Photograph of MRE sheets based on NR and ball milled Iron

A normal projection of filled Iron particles is also visible from the SEM micrographs. For samples cured with magnets WF (M) SEM micrograph indicates a horizontal orientation of particles along the field direction. No normal projection of filler particles is seen in this case (figure 5.8 b). From the micrographs of zero field cured samples, random orientation of filler particles are clearly visible(figure5.8 c). Magnetorheological elastomer sheets fabricated are highly flexible as shown in the

figure 5.8 d). They can be utilised as sandwhich beams in many vibration isolation systems.

5.3.4. Study on Mechanical Properties of MR Elastomers using Instron Mechanical Analyser and modified DMA

Instron mechanical analyser was employed to study the mechanical properties of MR rods based on milled iron and natural rubber. Two types of rods with field assisted curing and zero field curing were tested separately. This was repeated for all samples of various loading and particle size including blank rubber. From these studies important parameters like Young's modulus, resonant frequency, Stiffness, tan δ, loss angle, compliance and transmissibility of test samples were obtained. Being viscoelastic in nature a few more quantities like complex modulus, storage modulus and loss modulus were also generated [13-15]. The findings are shown in figure 5.9.

From figure 5.9 it is clear that Young's modulus, resonant frequency and stiffness of the rods increase with loading. However MRE rods which underwent field curing exhibited decreased young's modulus, resonant frequency, Stiffness, tan δ, loss angle, compliance and transmissibility with respect to zero field samples. This is mainly because of (dimension of the rod) the shape of the particles and the non-uniform nature of the applied field [16]. Due to the application of a magnetic field during curing chain like structures are created which is evident from the micrographs [17-18]. Non uniformity creates differently destructive regions where in one case there are voids which are devoid of any particle. As a result, the stiffness of the sample is reduced. As a result resonant frequency and young's modulus of anisotropic samples decrease with field curing. For zero field samples where random distribution of filler particles were seen in micrographs are more stiffer (Figure 5.7 b).
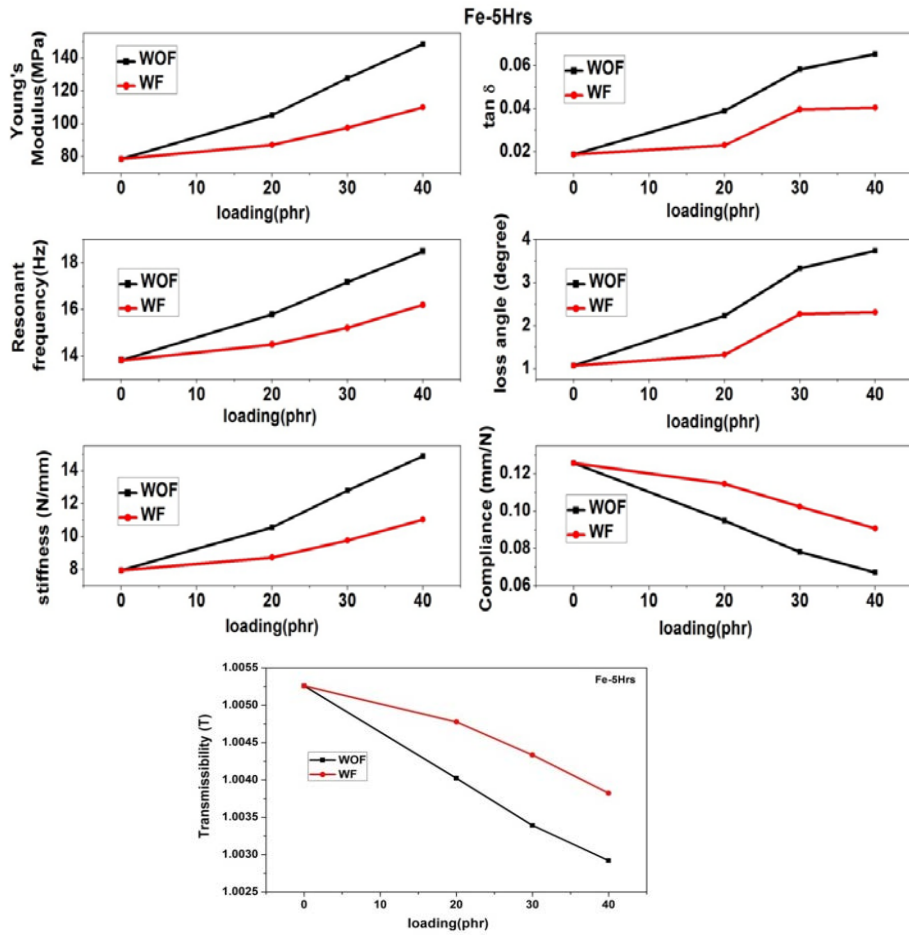
Figure.5.9. Variation of different mechanicalproperties with loading of MRE Rods based on NR-5hr ball milled Iron

Blank rubber rod, always possess low value for young's modulus, stiffness and resonant frequency [19]. In this study also values obtained for rods are the same and exhibit a minimum for both with-field curing and zero field curing. Presence of magnetic filler modifies the mechanical properties of samples in both cases.

The angle δ, which is the phase lag between the applied strain and the resultant stress is known as loss angle or phase angle. Tangent of this angle, Tan δ, is the ratio of loss modulus to storage modulus [20,21]. As the filler loading increases more interfaces are created resulting in increased loss of energy. This results in the increase of loss

angle and Tan δ. Reduction in the extent of rubber - particle interface in the field assisted samples may be the reason for reduced loss angle and tan δ observed in these samples.

For compliance and transmissibility of the rod the trend obtained is different and it is reversed. Compliance of the rod is the reciprocal of its stiffness. It decreases with loading in each case but always has a higher value for samples cured under a field. Similarly transmissibility depends on stiffness of the sample and is the measure of energy transfer through the material. Hence similar behaviour is exhibited in this case also. The highest value of compliance and transmissibility was obtained for blank natural rubber or for zero loading because of its lowest value of stiffness (Figure5.9).
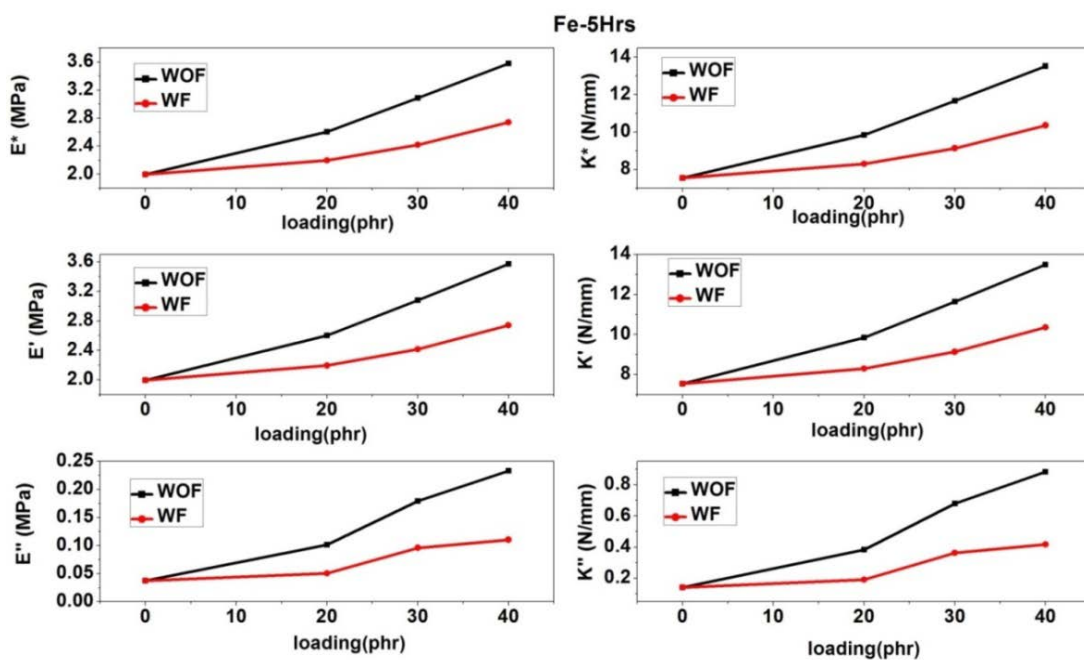
Figure 5.10. Mechanicalproperties (Compression mode) of MRE rods based on NR with 5hr ballmilled Ironusing-Instron mechanical analyser

The complex modulus E* can be written as

$$E^* = E' + iE'' \qquad (5.1)$$

Being viscoelastic in nature an elastomer has a complex modulus having a real part and imaginary part. The real part E′ represents the storage component and imaginary part E″consists of loss component. Similarly spring constant of viscoelastic polymer composite is also a complex entity which is represented as,

$$K^* = K' + iK'' \qquad (5.2)$$

Where K′ measures the stored energy representing the elastic part and K″ indicates the energy lost or the viscous part. In Fig.5.6, the variation of these physical quantities with loading is plotted. When the finely powdered iron particles are dispersed homogeneously in the matrix the rubber molecules are increasingly restrained which reduces the relative motion of molecules with one another. This causes the composite to be more elastic increasing the modulus and stiffness which is reflected in the increased storage components, E′ and K′ respectively. With increase in loading of iron the composites become stiffer increasing E′ and K′. In the case of samples cured under a field, the iron particles are aligned along the magnetic lines of force, in effect, reducing the homogeneous dispersion in the matrix. This increases the possibility of relative motion of molecules, lowering the modulus and stiffness compared to samples moulded without magnetic field. The distribution of iron particles in the matrix produces considerable amount of interfaces where stress transfer between the matrix and particles takes place. Insufficient interfacial adhesion between the iron particles and the matrix results in energy being dissipated at the interface increasing the lossy part of both modulus and stiffness i.e. E″ and K″ respectively. With increase in loading more interfaces are created increasing E″ and K″.

5.3.5. Effect of magnetic field on mechanical properties ofMREsheets based on natural rubber with 5hr ball milled iron

The effect of magnetic field on mechanical properties of MR elastomers are shown in figure 5.11.A modified Dynamic Mechanical Analyser (DMA) was employed to study the storage modulus, loss modulus and tanδ of MRE sheets. Here

in this case an external magnetic field was applied during testing. Readings were recorded for three types of sheets namely WF(C), WF (M) and WOF and field applied was categorized as high field, zerofield and a moderate field. In all these cases storage modulus increase with frequency having a maximum value at 15 Hz and thereafter remain almost constant. Increase in frequency can be equated to decreasing the temperature in dynamic measurements. An increase in storage modulus is observed beyond 10 Hz. This sort of behaviour has parallel when storage modulus is plotted against temperature.Similar behaviour is exhibited in loss modulus and tan δ graphs both showing a peak at the particular frequency. Application of a magnetic field during measurement affects these values according to the orientation of magnetic particles in the samples. WF (C) samples, where orientation is parallel to the magnetic lines of force, exhibits highest values for the storage modulus. This may be due to a pinning effect exerted by the magnets on the samples during the measurements which make the samples stiffer. When the strength of the magnetic field is increased storage modulus is also increased. WF (M) samples with orientation of magnetic particles in a direction perpendicular to the magnetic field applied during measurements show the lowest values for storage modulus. In this case, probable change in the orientation of magnetic particles, because of the applied magnetic field, causes a reduction in stiffness of the samples. As the field strength increases storage modulus also decreases. WOF samples with random orientation of magnetic particles in the matrix show values in between that of WF (C) and WF (M) samples. Here also an increase in storage modulus with the strength of magnetic field is observed. Almost similar trend is observed in loss modulus and tan δ values.
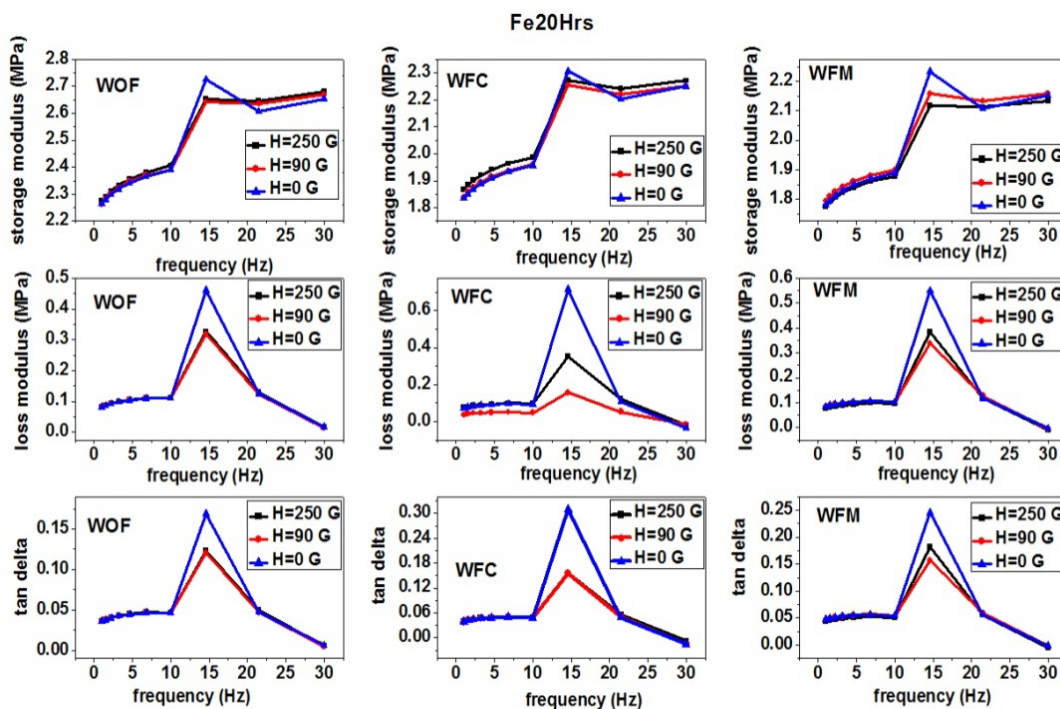
Figure 5.11. Effect of magnetic field on mechanical properties of MREsheets based on NR with5hr ball milled Iron

5.3.6. Mechanical properties of MRE sheets based on natural rubber with 5hr ball milled iron-shear mode

Dynamic mechanical studies in the shear mode of these MR sheets were carried out in DMA using appropriate clamps. Schematic of setup for shear studies is shown in the figure 5.14.MR sheets of proper size are placed on either sides of a platform which is moving between two fixed platforms. Thus a tangential stress is applied to the top layers of the sheet and bottom layers are kept fixed.

In these studies WF (C) samples with magnetic particles aligned normal to the plane of the sheet exhibit a maximum value for storage modulus. Correspondingly loss modulus and tan δ of these samples were also higher. High shear value produced in this case is due to the pinning effect of normally oriented magnetic particles in the sample. Theoretically, high values of loss modulus and tan δ of these samples are not

possible, but the presence of interfaces without proper adhesion or bonding between filler particles and matrix results inefficient stress transfer leading to the dissipation of energy in that region causing high loss modulus [22].WOF samples with random orientation of magnetic particles show better storage modulus values than WF (M) samples in which filler particles are aligned parallel to the plane of the sheet. In this case a pining effect is not possible and this produces low storage modulus. Same behaviour is observed for loss modulus and tan δ of WF (M) sample.
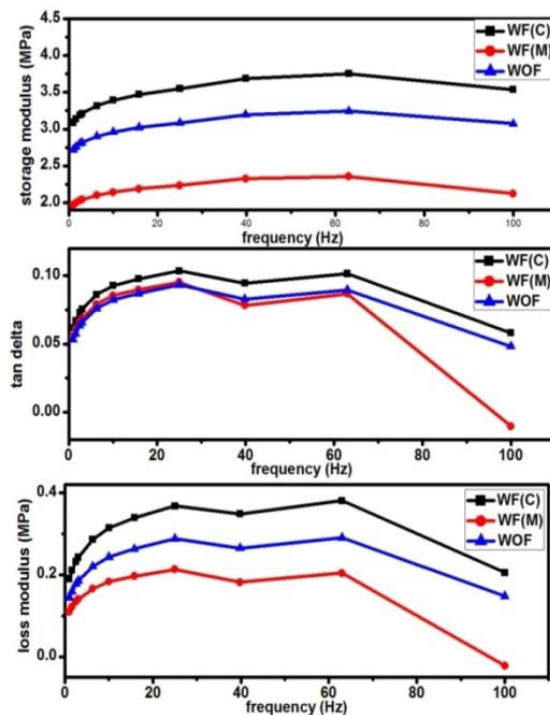
Figure 5.12. Mechanical properties (shear) of MRE sheets based on NR with 5hr ball milled Iron
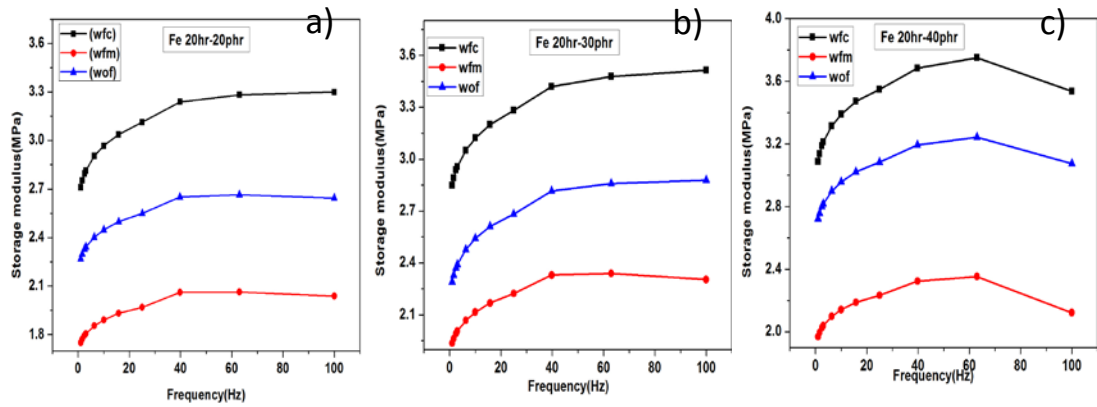
Figure 5.13. Storage Modulus of MRE sheets based on NR with 20 hr ball milled a) 20phr Ironb) 30phr and c) 40phr
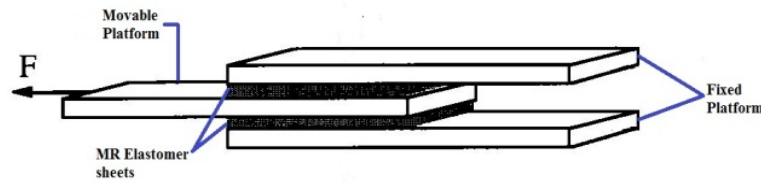
Figure 5.14. Schematic of setup for shear studies

5.4. CONCLUSION

MRE rods and sheets based on milled Iron and natural rubber were fabricated. Mechanical properties of elastomer rods were examined using an Instron mechanical analyser in compression mode. A rod with field assisted curing show a reduction in stiffness, resonant frequency and Young'smodulus. In all cases mechanical properties increases with loading and were lowered by field assisted curing. Complex modulus E*, storage modulus and loss modulus of the rod also follow the same trend. Compliance and transmissibility of the rods show a reverse trend, both of them being inversely proportional to stiffness which is higher for WOF samples. A modified DMA set up was employed for the study of complex modulus of MRE sheets. The storage modulus, loss modulus and tan δ have maximum value at resonant frequency of 15 Hz. Application of a magnetic field reduces the values and a high value is obtained in all cases for a zero magnetic field. In the shear mode,WF(C) samples

110

exhibit maximum storage modulus. A very low value for it was obtained in the case of WF (M) sheets. So WF(C) sheets are the best candidate for MR sheets in shear mode.

REFERENCES

[1]. Guoliang Hu, Miao Guo, Weihua Li, Haiping Du, and GurselAlici, Smart Mater.Struct.,**20** (2011) 1.

[2]. Li, W. H., Zhang, X. Z. & Du, H. Advances in Elastomers I: Blends and Interpenetrating Networks Berlin, Germany: Springer **11** (2013) 357.

[3]. J Fu, M Yu, X M Dong and L X Zhu, J. Phys.: Conf. Series **412** (2013) 012032

[4]. Jie Yang, XinglongGon, LuhangZong , Chao Peng, ShouhuXuan, Polymer Engineering and Science (2013) 2615

[5]. Jason P. Rich · Patrick S. Doyle · Gareth H. McKinley, RheolActa, **51** (2012) 579

[6]. Wan-quanJiang, Jing-jing Yao, Xing-long Gong, Lin Chen, Chin. J. Chem. Phys.**21**(2008) 87

[7]. P. Ponte Castaneda, E. Galipeau-J. Mech. Phys. Solids **59**(2011) 194

[8]. Gausanio, C Campana, C Hison, V Iannotti and L Lanotte-Smart Mater. Struct. **16** (2007) 570

[9]. ZsoltVarga, Genove´vaFilipcsei, Miklo´sZrı´nyi - Polymer **47** (2006) 227

[10]. Weike-xiang, MengGuang, Zhang Wen-ming, Zhu Shi-sha-J.Cent. South Univ. Technol. **15** (2008) 239

[11]. G.V. Stepanov , A.V. Chertovich , E.Y. Kramarenko -J. Magn. Magn. Mater.

[12]. AnnaBoczkowska , Stefan F. Awietjan, StanisławPietrzko , Krzysztof . Kurzydłowski- Composites Part B**43** (2012) 636

[13]. YinlingWang , Yuan Hu ,Lin Chen , Xinglong Gong ,WanquanJiang ,Peiqiang Zhang , Zuyao Chen –Polym. Test. **25** (2006) 262

[14]. Miao Yu , Benxiang Ju , Jie Fu , Xueqin Liu , Qi Yang –J. Magn.Magn. Mater.**324** (2012) 2147

[15]. L Chen, X L Gong and W H Li-Smart Mater.Struct.**16**(2007) 1

[16]. W H Li, G Chen and S H Yeo-Smart Mater. Struct. **8** (1999) 460

[17]. Hyung-Jo Jung , Sung-Jin Lee , Dong-Doo Jang , In-Ho Kim , Jeong-Hoi Koo, and Fazeel Khan-IEEE trans. magn. **45** (2009) 3930

[18]. Li, W. H., Zhang, X. Z. & Du, H. Advances in Elastomers I: Blends and Interpenetrating Networks (2013) 357.

[19]. W. Zhang, X. L. Gong, S. H. Xuan, and Y. G. Xu-Ind. Eng. Chem. Res. **49** (2010)12471

[20]. ZsoltVarga, Genove´vaFilipcsei, Miklo´sZrı´nyi- Polymer **46** (2005) 7779

[21]. Mark R Jolly, J David Carlson and Beth C Mu˜noz- Smart Mater.Struct.**5** (1996) 607.

[22]. Un-ChangJeong, Ji-Hyun Yoon, In-Hyung Yang, Jae-EunJeong,Jin-Su Kim, Kyung-Ho Chung and Jae-Eung Oh-Smart Mater.Struct;, **22**, (2013) 115007

CHAPTER 6

MECHANICAL PROPERTIES OF MAGNETO RHEOLOGICAL ELASTOMER RODS AND SHEETS BASED ON CARBONYL IRON AND NATURAL RUBBER

6.1. INTRODUCTION

Polymer nanocomposites are macroscopically coherent masses that exhibit interesting physical, mechanical and rheological properties.Their properties are a result of theinteractions taking place between the matrix and the dispersed phase or the filler. MR elastomers coming under this category of engineering materials find potential applicationsin various fields. Fillers are added into a polymer in order to improve certain key properties of the resultant composite like modulus, stiffness and viscosity[1'2'3].Magnetic fillers are incorporated in matrixes like rubber in order to fabricate MR Elastomers. During curing a magnetic field can be applied to align the particles in a particular direction which influences the MR properties as well as its mechanical properties[4,5]. In the previous chapter MREs were made by incorporating iron of varying sizes. The magnetic and mechanical properties of both rods and sheets were evaluated and the influence of external magnetic field during curing on various properties was estimated.

This chapter takes a look at MREs made by incorporating carbonyl iron of two different particle sizes (R10 and R20) in varying weight percentages in a matrix of natural rubber. The method of preparation remains the same and is described in detail in chapter 2.Carbonyl iron of high purity (99%) is synthesised by chemical decomposition of purified Iron pentacarbonyl$Fe(CO)_5$.Carbonyl Iron is a grey powder consisting of uniform spherical particles of size a few microns. It has immense applications in the field of electronics, powder metallurgy and pharmaceuticals [11]. Carbonyl Iron powder is an important filler in MR fluids and

MRelastomers. Both, field cured sheets and rods were fabricated. For comparison a zero field cured samples were also made. It is presumed that incorporation of a magnetic filler not only imparts magnetic properties to the matrix but also improves its various mechanical properties namely storage modulus, loss modulus and tanδ. The influence of an external magnetic field during curing on the mechanical properties is also an intended study.

It is anticipated that shear properties of these composites can be modified by the application of an external magnetic field during testing. An external magnetic field during measurement would rearrange the pre-arranged chain like structure of filler particles and produce inter particle interaction of these structures. This imparts additional strength to the elastomer [8,9].Thus the storage modulus which is related to the stiffness of the elastomer can be properly controlled by an external magnetic field. This mechanism can be utilised for applicationinvolving variable stiffness applications [10].

6.2. EXPERIMENTAL

MRE sheets and rods with carbonyl iron for different loading were prepared. The details are exactly the same as described in the previous chapter and hence not repeated here. Here in this case MRE rods and sheets were made for varying concentration of two different mesh sizes of Carbonyl Iron. The recipe, mould and curing conditions are described in chapter 2.Rods and sheets were moulded after determining the cure characteristics of the samples in a Rubber Processing Analyser.

## 6.3.RESULTS AND DISCUSSIONS

6.3.1. Structural Studies

XRD patterns of MRE sheets are shown in figure 6.1. These sheets contain 40 phr of Carbonyl Iron R10 and R20.The amorphous peaks corespond to the natural

rubber present in the composites. Traces of iron oxide and other oxides are also visible in the pattern. This may be from the residue of ingredients which were used for curing. The diffraction peak at $2\Theta = 44.3^\circ$ is dueto reflections from (110) plane of bcc -Fe.
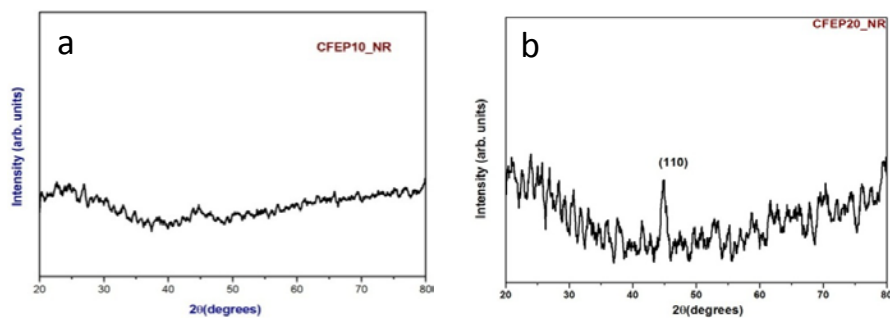
Figure 6.1.XRD pattern of Carbonyl Iron embedded in natural rubber(a)R10 (b)R20
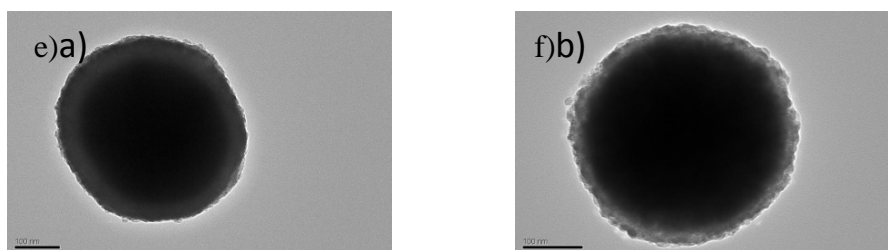
Figure 6.2.TEM images of Carbonyl Iron powder (a) R10 (b) R20

Figure 6.2represents TEM images of Carbonyl Iron powders R 10 and R 20. Particle size obtained for R10 Carbonyl iron was 0.4 µm and that for R20 was0.3 µm.

6.3.2. Magnetisation studies

The hysteresis loop of MRE sheets are shown in figures 6.3, 6.4 and 6.5 for both in plane and out of plane measurements. The loops are typical of a soft magnetic material with a large saturation magnetization (Ms) and very small Coercivity (Hc). The Ms and Hc are seperately tabulated and shown in table. The saturation magnetisation (Ms) of sheets increases with the increase in loading of Carbonyl Iron.
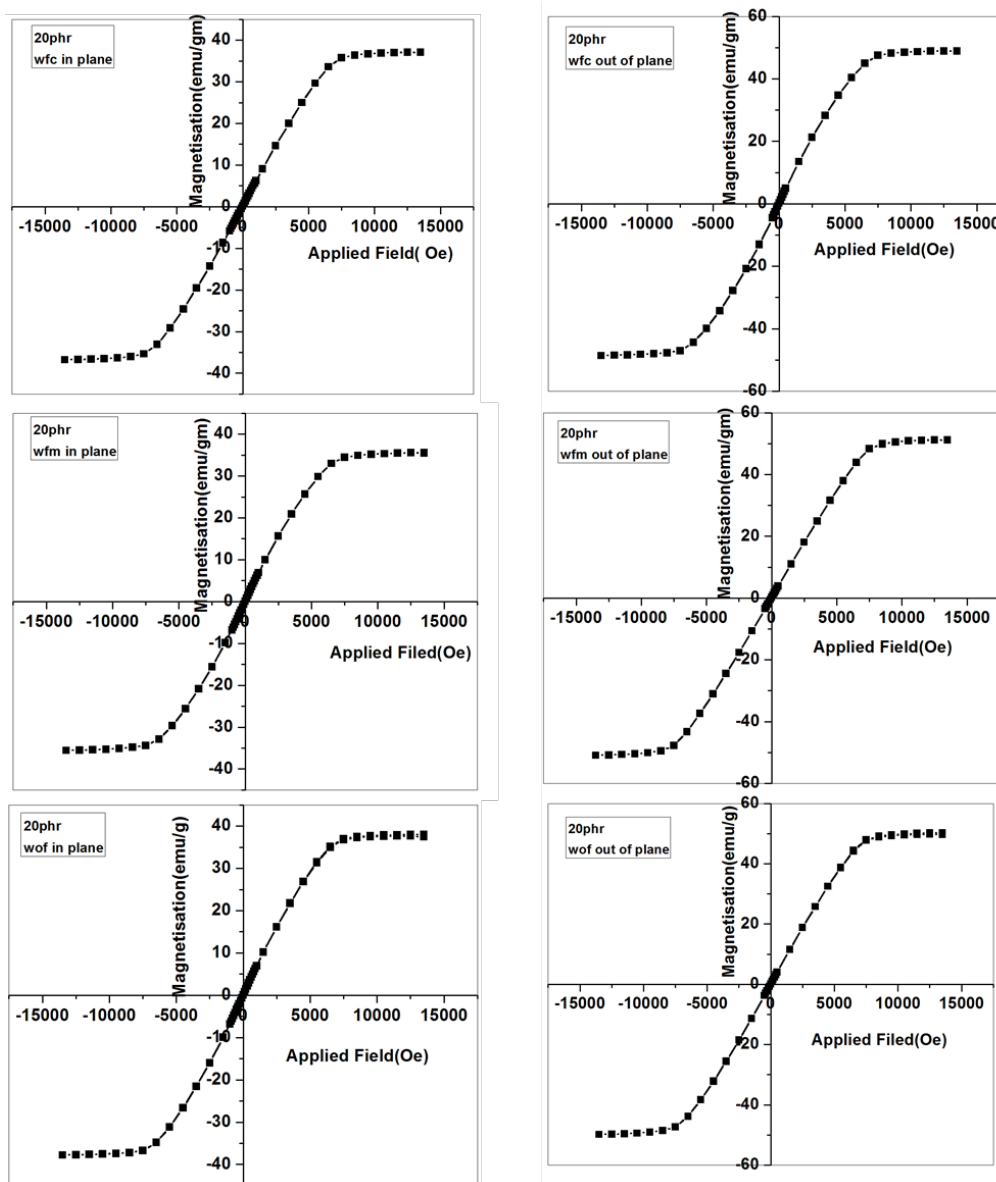
Figure 6.3. In plane and out of plane VSM graphs of MR sheets with 20phr Carbonyl Iron R20 in WF(C), WF (M) and WOF samples.

A maximum of 95 emu/g was obtained for a loading of 80 phr of Carbonyl Iron. The in plane and out of plane measurements provided proof for the anisotropy present in the samples during the curing process. However the coercivity of these sheets decreased with increase in iron concentration. It showed a maximum of 31Oe for 20 phr samples and a minimum of 12 Oe for 80 phr samples. This is perhaps a case of agglomeration induced phenomenon. This is for WF(C) MRE sheets. However in the case of WF(M) no such pattern were forthcoming. Isotropic samples

exhibited a minimum of 12 Oe for 20phr and a maximum of 19 for 40 phr. The coercivity further reduced to 10Oe for 80 phr.
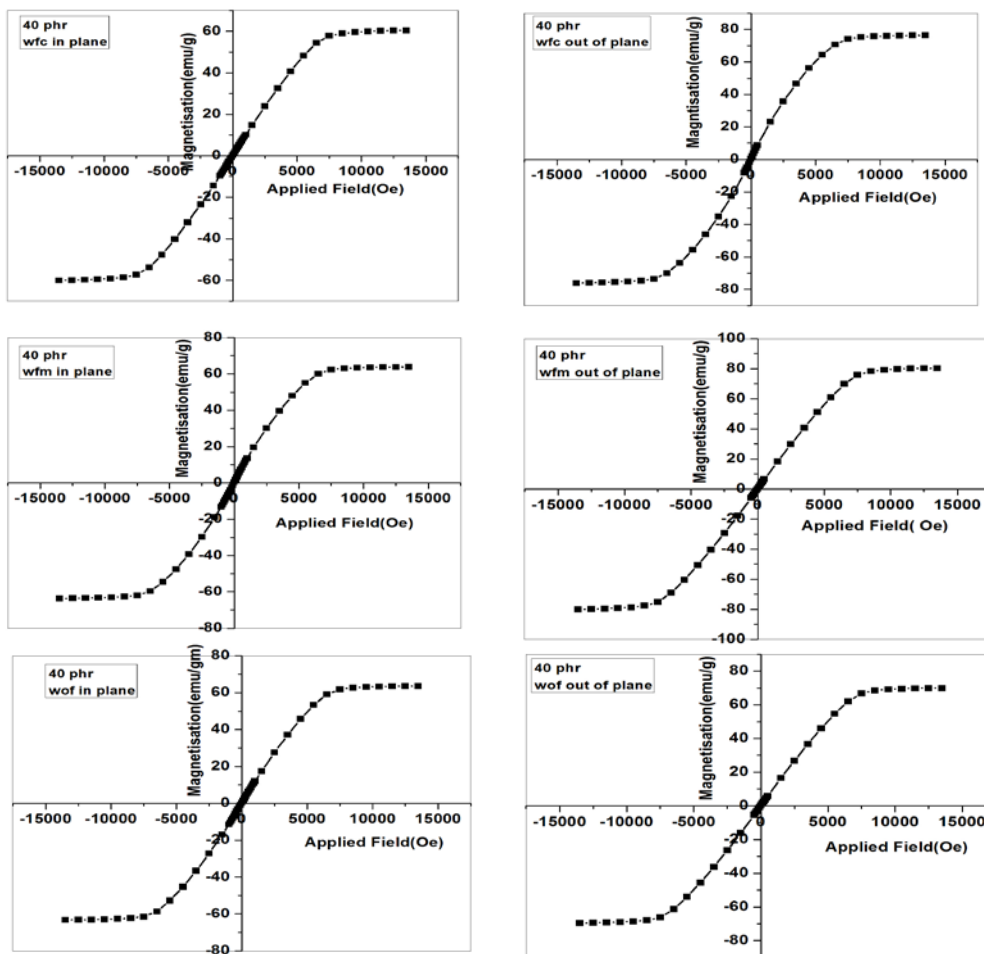
Figure 6.4. In plane and out of plane VSM graphs of MR sheets with 40phr Carbonyl Iron R20 in WF(C), WF (M) and WOF samples

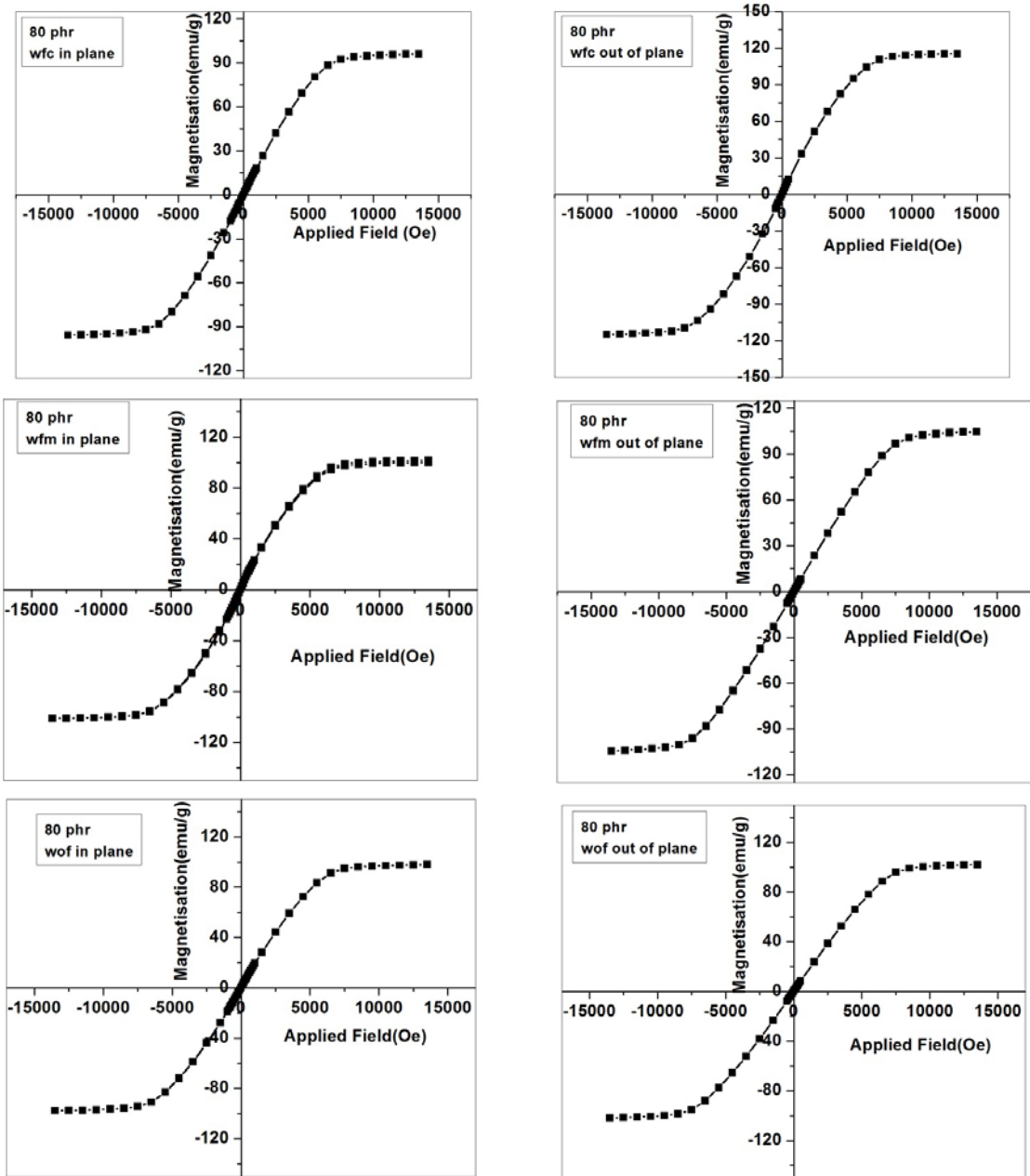**Figure 6.5.** In plane and out of plane VSM graphs of MR sheets with 80phr Carbonyl Iron R20 in WF(C), WF (M) and WOF samples

Loading		Sample		M_s(emu/g)			H_c (Oe)	
	MRE Sheets	WF(C)	WF(M)	WOF	WF(C)	WF(M)	WOF	
80phr		95	101	95	12	9	10	
40phr	R20	59	62	62	21	15	19	
20phr	(in plane)	37	35	37	31	5	12	
80phr		115	104	100	11	24	11	
40phr	R20	75	80	69	21	16	21	
20phr	(out of plane)	48	51	49	21	26	12	

Table 6.1. Magnetization studies–Loop parameters of Carbonyl Iron powder R20 and MRE sheetsWF(C),WF (M) and WOF samples (R20)

6.3.3. Surface morphological studies

Photographs of MRE sheets are shown as inset of SEM micrographs of MRE samples in Figure 6.7. The alignment of magnetic particles along the field direction is clearly visible in the micrographs.The difference in the isotrophic and anisotropic samples are very clearly noticeable from their respective micrographs.in the case of zero field cured samples carbonyl Iron is seen distributed randomly.
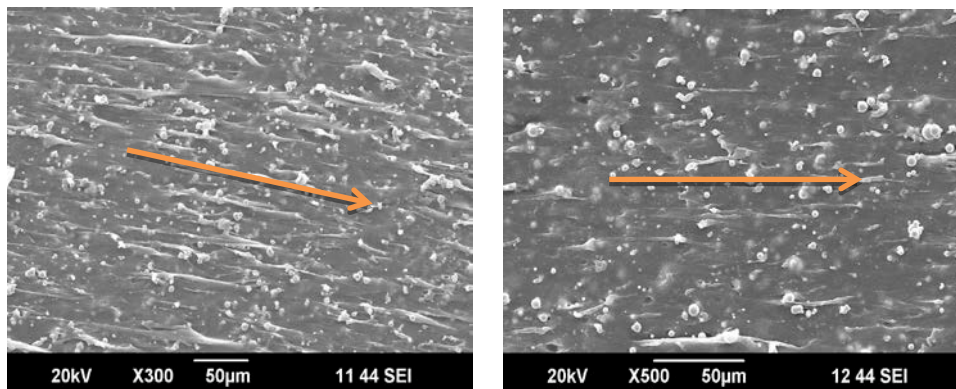
Figure 6.6.SEM images of (a)MRE rod with Carbonyl Iron 80phr WF (arrow- axial direction of the rod and field direction; H>0)(b)MRE rod with Carbonyl Iron 80phr WOF (arrow- axial direction of the rod and field; H=0)
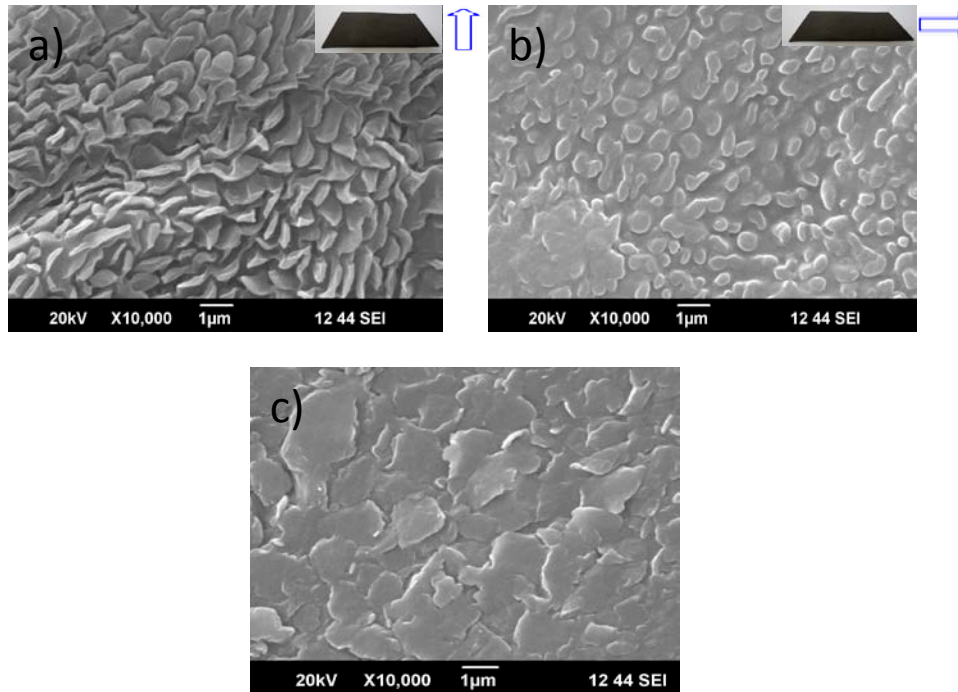
Figure 6.7.SEM images ofMRE sheet a) WF(C) b) WF(M)(Field direction shown in the inset; H>0)and c) WOF

Figure 6.7show SEM images of WF(C), WF (M)   and WOF samples. During the fabrication of WF(C) samples a magnetic field was applied normal to the plane of the sample. Corresponding SEM micrograph shows a clear alignment of filler particle in the applied field direction (figure6.7 a)). Nano flowers can be seen in the case of samples cured under an applied field. This is quite interesting and a possible correlation of such structures with the mechanical properties would help in identifying structures for specific applications.

6.3.4. Study on Mechanical properties of MRElastomer Rods and Sheets using InstronMechanical Analyser (rods) and modified DMA (sheets)
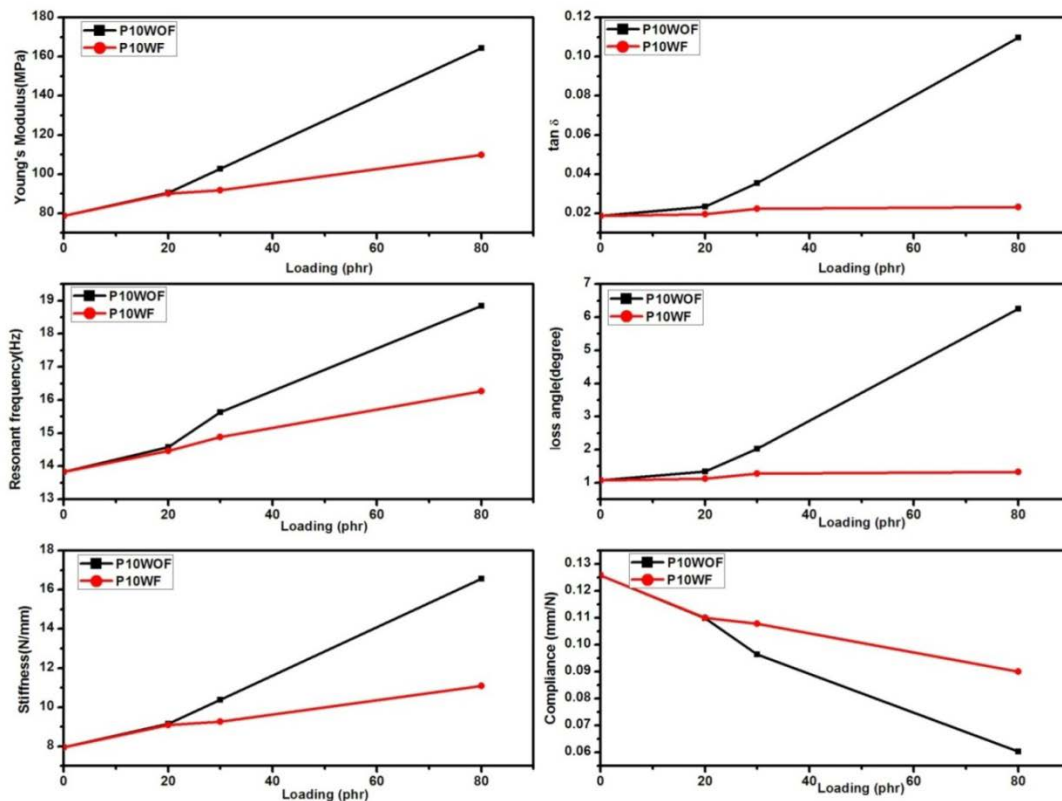
Figure 6.8.Mechanical properties of MRE rods based on NR and Carbonyl IronR10 WF&WOF-Instron mechanical analyser

Instron mechanical analyser was utilised to study the mechanical properties of MRelastomer rods based on Carbonyl Iron and natural rubber. Two kinds of rods of field assisted curing and zero field curing were tested separately. This was repeated for all samples of loading 20,30,40 and 80phr of R10 and R20. Parameters namelyYoung's modulus, resonant frequency, Stiffness, tanδ, loss angle, compliance and transmissibility of rod samples were thenobtained. The variation of all parameters with loading is shown in Figure6.8. Another set of important physical quantities of

these samples like complex modulus, storage modulus and loss modulus were also determined. They are depicted in figure 6.9.
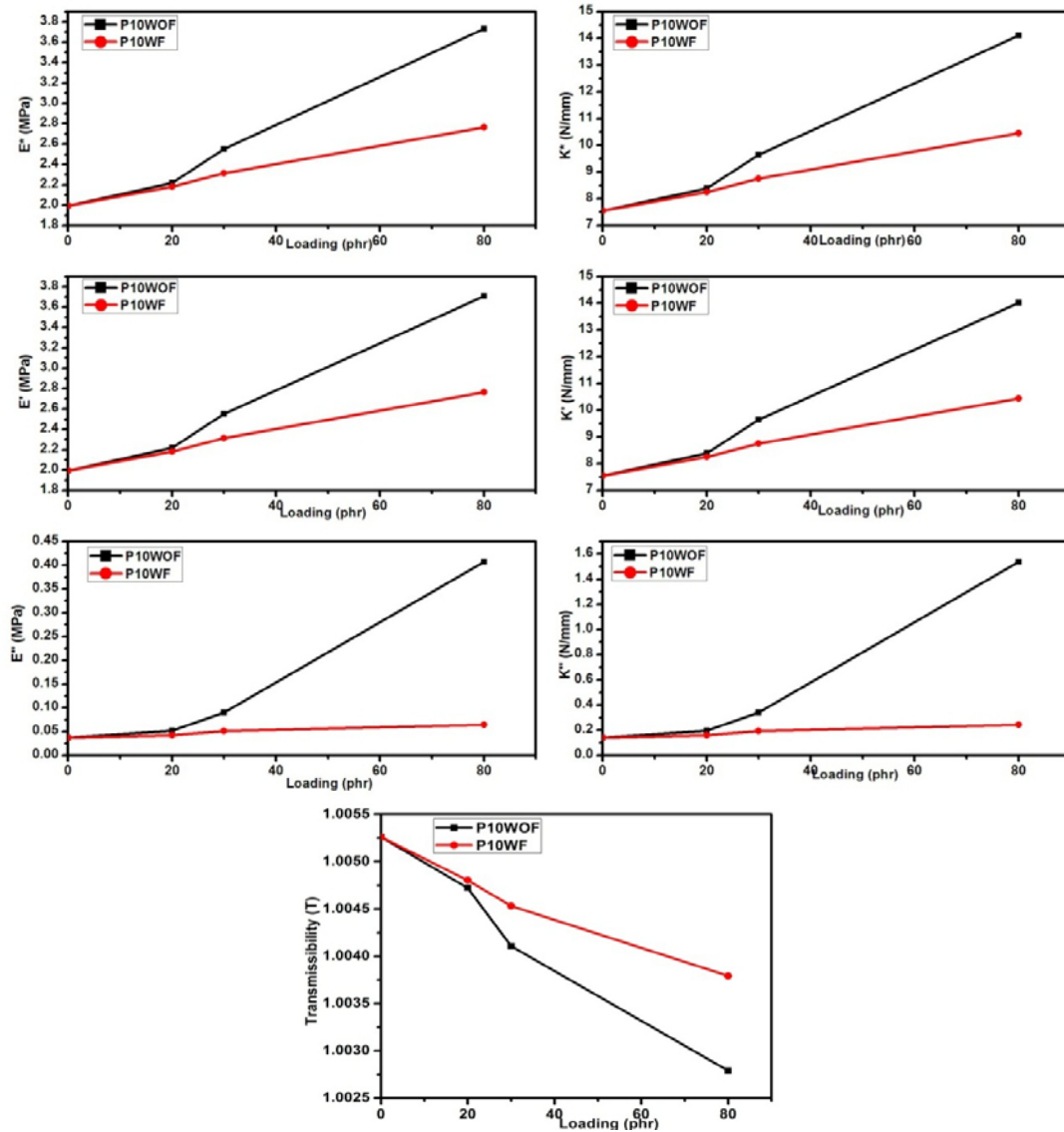
Figure 6.9. Mechanical properties ofMRErods based on NR and Carbonyl Iron R10
WF&WOF-Instron mechanical analyser

122

From the figure.6.9, it is clear thatcomplex modulus, storage modulus and loss modulusare related to each other. Young's modulus, resonant frequency and stiffness of the rods increase with loading. The stiffness of the samples was affected by the following factors like thenon-uniform field applied during curing, formation of unfilled area in the matrix and the dimension of the rod.As a result stiffness of the sample isreduced. For isotropic samples, random distribution of filler particles were seen in SEM micrographs (Figure 6.6)and no voids are visible and this will improve their stiffness. For blank rubber rod, complex modulus, storage modulus and loss modulus was relatively lower.Addition of magnetic filler and field applied curing improve the properties of samples and gave an advantage to anisotropic samples in actuation.

Storage modulus and loss modulus of the samples increase with loading in all cases.A higher value is obtained for isotropic samples. A similar trend has been noticed in the case of MREs based on Natural Rubber and has been explained in chapter 5. Complex modulus of a viscoelastic matter consists of storage modulus and loss modulus[12]. Tanδ is the ratio of loss modulus to storage modulus[13]. So in this study all the above quantites including loss angle exhibit same behaviour showing a decrease in stiffness of field cured samples.

Compliance and Transmissibility depend on stiffness of the sample[14]. Compliance is defined asthe reciprocal of stiffness[15]. It decreases with loading in each case and always has a higher value for WF samples. Similarly transmissibility which represents the trasfer of energy through samples depends on the stiffness of the sample[16].Similar behaviour is obtained in this case also. The maximum value of compliance and transmissibility was obtained for blank natural rubber because of low stiffnessand zero loading(figure 6.8& 6.9)[17]. The complex modulus E* and complex spring constant K* of carbonyl iron rods follow the same behaviour as that of MRE rods based on Natural Rubber and Iron.

6.3.5.Mechanical properties of MRE Sheets based on Natural Rubber and Carbonyl Iron(R10) –-Modified DMA

A modified Dynamic mechanical Analyser set up was used to measure the Storage modulus, loss modulus and tan δ of MRE sheets based on Carbonyl Iron. An external magnetic field was appliedduring testingby means of two permanent magnets.

Readings were recorded in each case and field applied was a high field, zerofield and a moderate field. Three types of sheetswere used for this study namely WF(C),WF(M) and WOF. The Storage modulus was found to increase steadly with frequency and attains a maximum value at 15hz, then decreases at 20 Hz and almost remains as a constant for all other frequencies.At this stage(about 15Hz) the natural frequency of the polymer chain is equal to the frequency of oscillation giving rise to a resonance.Here stiffness attain a maximum value[18].

Same behaviour is observed in the case of loss modulus and tanδ for all samples. Application of a magnetic field during measurement also has a profound inflouence on these parameters. Orientations of magnetic filler in these samples were different and a high value for storage modulus, loss modulus and tanδwas obtained for zero field measurement.In WF (M) sample, filler particles were aligned parallel to the plane of the sheet.Thus the orientation of magnetic particles and direction of magnetic field applied are mutually perpendicular to each other. Because of this WF (M) samples record lowest value for storage modulus and highest value for loss modulus and tanδ.But for WF(C)samples, direction of external magnetic field is along the orientation of magnetic filler and therefore they have maximum value for storage modulus and minimum values for loss modulus and tanδ.

Without field (WOF)   **With field magnet WF(M)**   **With field coil WF(C)**
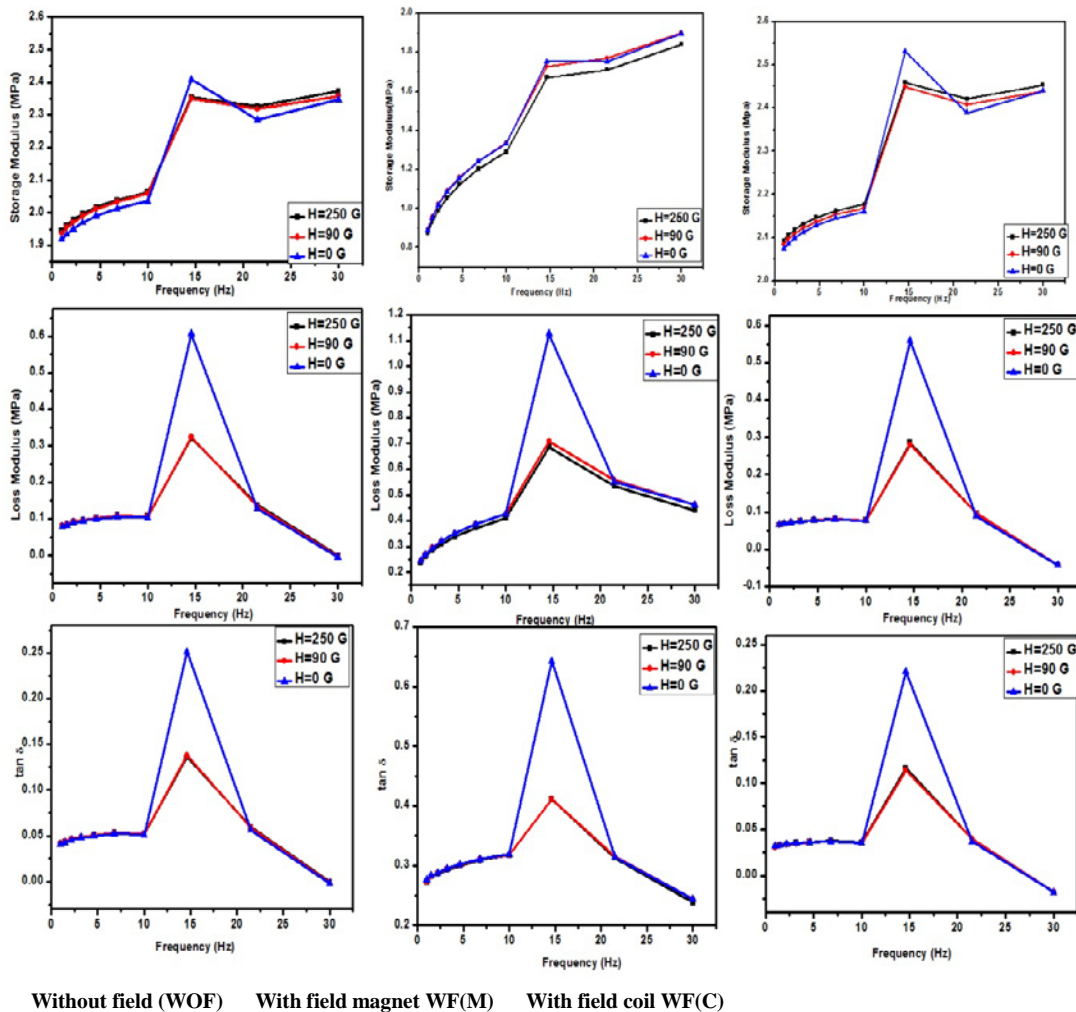
Figure 6.10. Mechanical properties MRE sheets based on NR and Carbonyl IronR10) - Modified DMA

DMA studies of sheets with field and with out field R20 samples were carried out. They are shown in figure 6.11. Here also WF(C)is the best candidate and values obtained were slightly less than R10 samples because of smaller particle size and low magnetization values. (Refer figure 6.10)
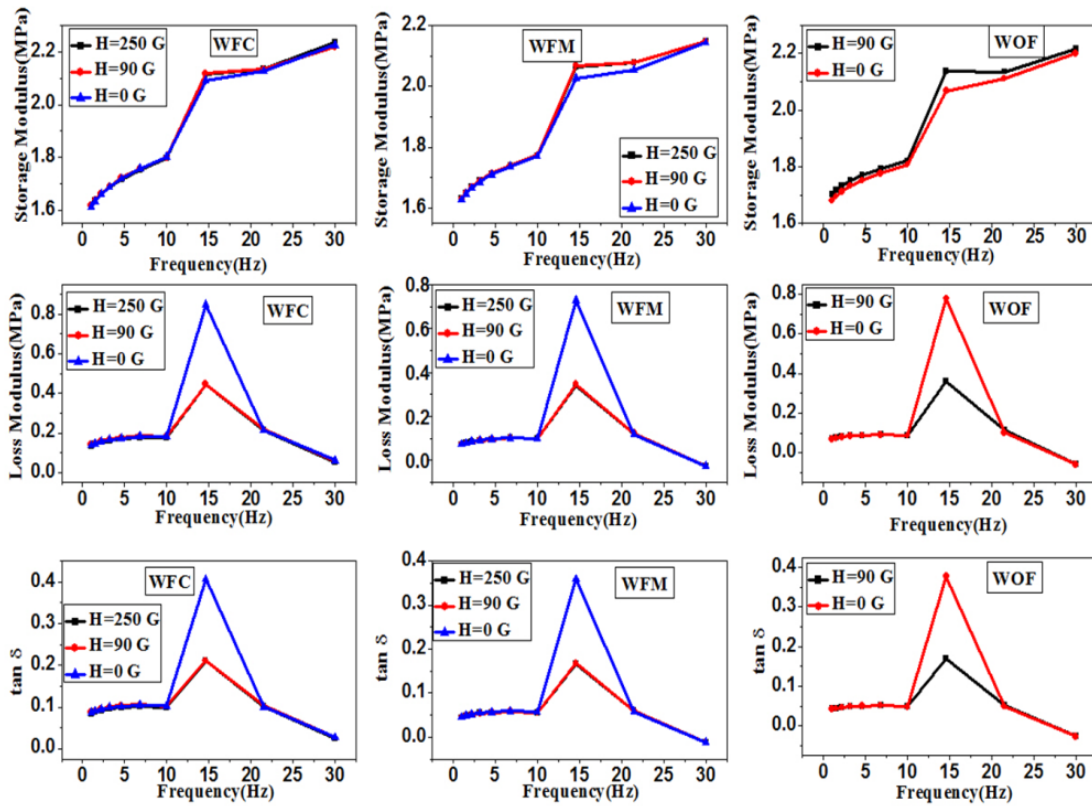
Figure 6.11. Mechanical properties MRE sheets based on NR and Carbonyl Iron R20
- Modified DMA

6.3.6.Mechanical properties of MRE Sheets based on NRand Carbonyl Iron-Shear Studies- DMA

Shear properties of MR elastomer sheets were studied by utilising a dynamic mechanical analyser whose bottom was fixed and corresponding shearing strain was measured.In this measurement,a clamp with two fixed plates and a moving plate in between them was used which is described in the chapter 5.Using this special type of clamp a tangential stress was applied to the top surfaces of two pieces of sample placed on either side of the moving plate. In this case also WF(C) samples acquire maximum values for storage modulus,loss modulus and tanδ(fig.6.12). In the absence of a magnetic field, filler particles are more free at the interfaces and thus dissipate more energy[19]. This is the reason for high value of loss modulus and tanδ of these

samples.InWF(M) samples chainlike structure of filler particles were formed parallel to the plane of the sample and move along the tangential force's direction.Thus storage modulus will be lesser in this case.But for WOF samples no chain like structure was available and because of random orientation of magnetic filler,it has high values of storage modulus than WF(M) sample.Figure 6.13 and 6.14 depicts the variation of storage modulus with frequency and loading of MRE sheets.Storage modulus increases with loading in all cases.Field assisted curing in normal direction to the plane of sample increases the storage modulus of the sheets. But for an infield curing in horizontal direction,storage modulus of the sheet decreases.A zero field curing has a better result than field assisted curing with permanant magnets.
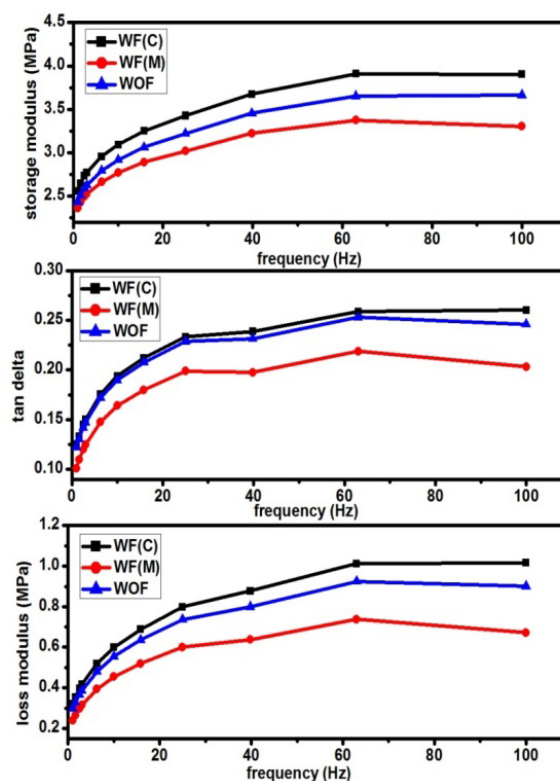
Figure 6.12. Mechanical properties of MRE sheets based on NR and Carbonyl Iron-Shear studies- DMA

127
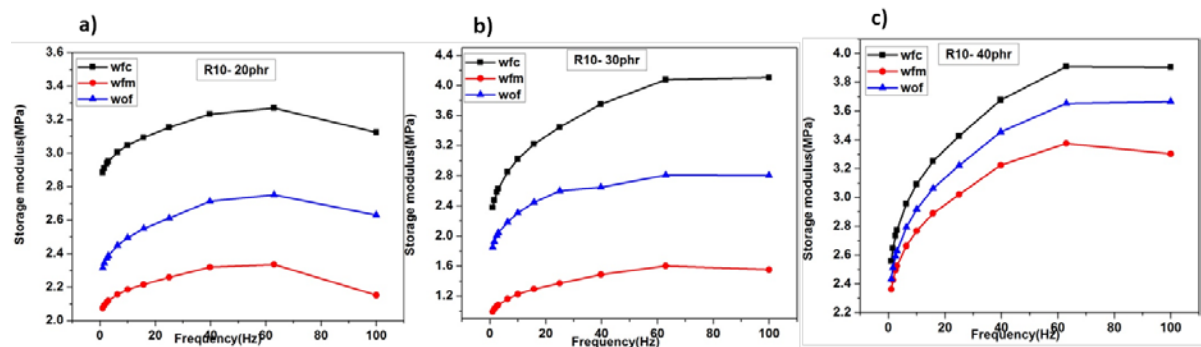
Figure 6.13. Shear Modulus of MRE sheets based on NR and Carbonyl Iron R10
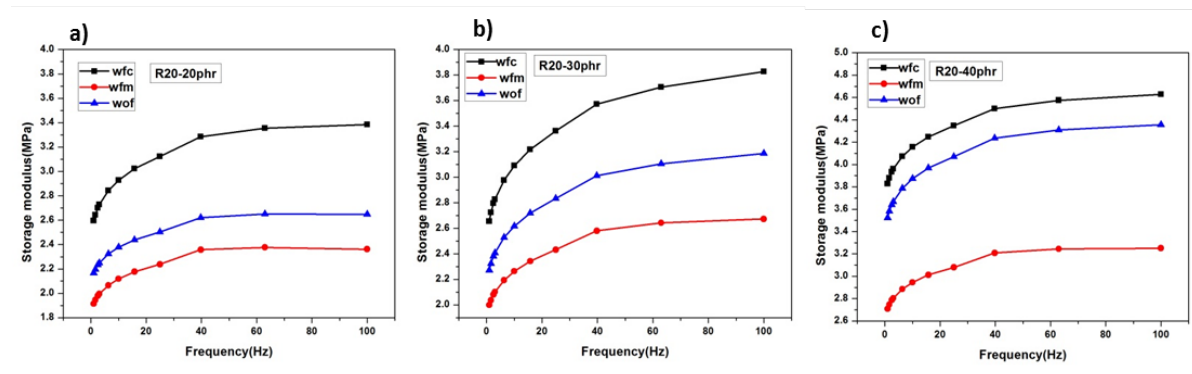
Figure 6.14. Shear Modulus of MRE sheets based on NR and Carbonyl Iron R20

6.4.CONCLUSION

MR elastomer rods and sheets based on Carbonyl Iron and natural rubber were moulded. Using Instron Mechanical analyser a compression test was carried out for MR rods. Mechanical properties show a marked improvement with loading in both cases. Field curing decreases the mechanical strength of the rod.

For MR sheets a modified DMA is used and WF (C) samples exhibit improved mechanical properties in zero magnetic field. Application of a magnetic field decreases the values which depend on the orientation of magnetic particles in the filler. Storage modulus of WF(C) samples increased with frequency and a maximum

128

value was obtained for 15Hz. For MR sheets field assisted curing enhances the mechanical strength.

In shear studies of the MR sheets, WF(C) samples acquire high storage modulus, loss modulus and tanδ. WF (M) samples record low values and WOF samples come with moderate values in this case.

REFERENCES

[1]. S.Q. Abu-Ein, S.M. Fayyad, Waleed Momani, Aiman Al-Alawin and Muntaser Momani, Res.J.Appl.Sci., Eng.Tech. **2**(2010) 159

[2]. W H Li, G Chen and S H Yeo-Smart Mater.Struct.**8**(1999) 460

[3]. Jeongwon Park, Jepil Lee, and Junhong Park, Acoustical Society of America, **130(6)**(2011)3729

[4]. ArefNaimzad ,MojtabaGhodsi , Yousef Hojjat and AliasgharMaddah-International Conference on Advanced Materials Engineering(IPCSIT) **15** (2011)

[5]. Xianzhou Zhang, SuiliPeng,WeijiaWenandWeihua Li.- Smart Mater. Struct.**17**(2008) 045001

[6]. P. Ponte Castaneda, E.Galipeau , Proc R Soc A,**469**(2013)385

[7]. T Borb´ath, S G¨unther, D Yu Borin, ThGundermannand S Odenbach- Smart Mater.Struct. **21** (2012) 105018

[8]. Hu, G., Guo, M., Li, W., Du, H. &Alici, G.SmartMater.Struct.**20** (2011) 1.

[9]. W. Zhang, X. L. Gong, S. H. Xuan, and Y. G. Xu-Ind. Eng. Chem. Res. **49**, (2010)12471

[10]. J Fu, M Yu, X M Dongand L X Zhu-J. Phys.: Conference Series **412**(2013) 012032

[11]. Yancheng Li, Jianchun Li, WeihuaLiandHaiping Du-Smart Mater.Struct. **23**(2014)123001

[12]. Jinkui Wu, Xinglong Gong, Yanceng Fan and Hesheng Xia-Smart Mater.Struct. **19** (2010) 105007

[13]. G.V. Stepanov, S.S. Abramchuk , D.A. Grishin , L.V. Nikitin ,E.Yu. Kramarenko , A.R. Khokhlov -Polymer **48** (2007) 488e495

[14]. Yi Han, Wei Hong , LeAnn E. Faidley-Int. J. Solids Struct.**50** (2013) 2281

[15]. E Yu Kramarenko, A V Chertovich'G V Stepanov, A S Semisalova, L A Makarova, N S Perov and A R Khokhlov-Smart Mater,Struct., **24**(2015)035002

[16]. G. V. Stepanov, D. Yu. Borin, E. Yu.Kramarenko, V. V. Bogdanov,D. A. Semerenko, and P. A. Storozhenko-Polymer Science, Ser. A, **56** (2014) 603

[17]. Omar A. Al-Hartomy, Ahmed A. Al-Ghamdi, Falleh Al-Salamy, Nikolay Dishovsky, DesislavaSlavcheva and Farid El-Tantawy-Int.J. Polymer Science, **2012**(2012)8

[18]. T F Tian, X Z Zhang, W H Li, G Alici and J Ding-J. Phys.: Conference Series **412**(2013) 012038

[19]. JánKruželák, Richard Sýkora, RastislavDosoudiland Ivan Hudec-Polym.Adv.Tech., **25(9)**(2014)995

CHAPTER 7

MAGNETO DIELECTRIC PROPERTIES OF MAGNETO RHEOLOGICAL ELASTOMER SHEETS BASED ON CARBONYL IRON AND NATURAL RUBBER

7.1. INTRODUCTION

The dielectric permittivity of composites containing ferromagnetic particles at different frequencies is interesting not only from an applied angle but also assume significance from a fundamental perspective. The dielectric permittivity and dielectric loss are dependent on the individual permittivity of the components. Factors like grain size, grain boundary, agglomeration of particles, the nature of polymers, cross linkage, polar or non-polar all decides the overall permittivity of the composite [1, 2, 3].

In the case of MREs, the influence of an applied magnetic field on the dielectric permittivity and dielectric loss of these composites is of great significance from an application point of view. The phenomenon of modification of dielectric properties of a MRE is called magneto dielectric effect [4, 5].

7.2. EXPERIMENTAL

Here, MREs were prepared for various concentration of Carbonyl Iron R20and were cured under an influence of a magnetic field. In order to align the particles along two different directions, a solenoid and a permanent magnet was employed separately to apply the magnetic field. For comparison, a third sample containing similar loading percentage was also made. All the samples were made in the form of sheets. The details as regard to the moulding of sheets are provided in chapter 2.

The dielectric permittivity, dielectric loss and ac conductivity of these sheets were evaluated with and without the application of an external magnetic field by

employing an LCR meter and a homemade dielectric cell with provision for applying an external magnetic field. A full description of the dielectric set up is provided in chapter 2 and hence not repeated here. This chapter discusses the magneto dielectric properties of MREs with differently aligned magnetic fillers.

7.3. RESULTS AND DISCUSSION

The variation of dielectric constant, dielectric loss and ac conductivity with frequency is plotted for three samples with different weight percentage of Carbonyl Iron are shown in figures 7.1, 7.2 and 7.3.
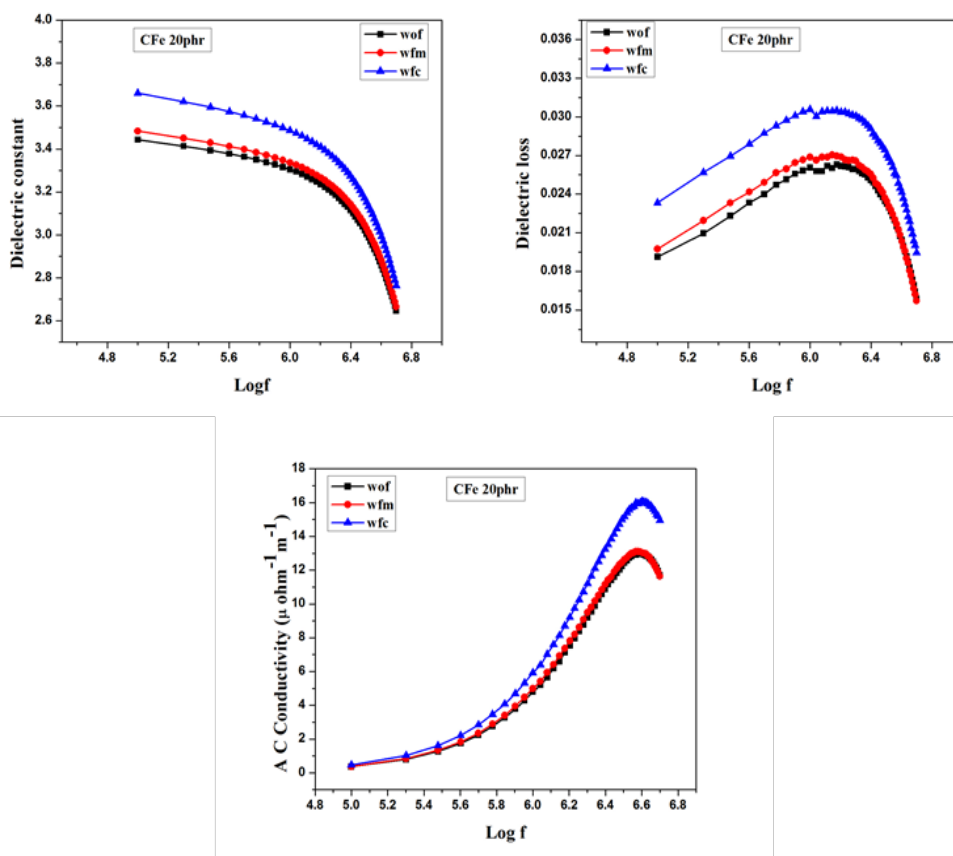
Figure 7.1 *Dielectric constant, Dielectric loss, AC conductivity of MRE sheets based on NR and Carbonyl Iron R20 for WF(C),WF(M).WOF samples at 20 phr loading(a) Dielectric constant(b)Dielectric loss(c) AC conductivity*
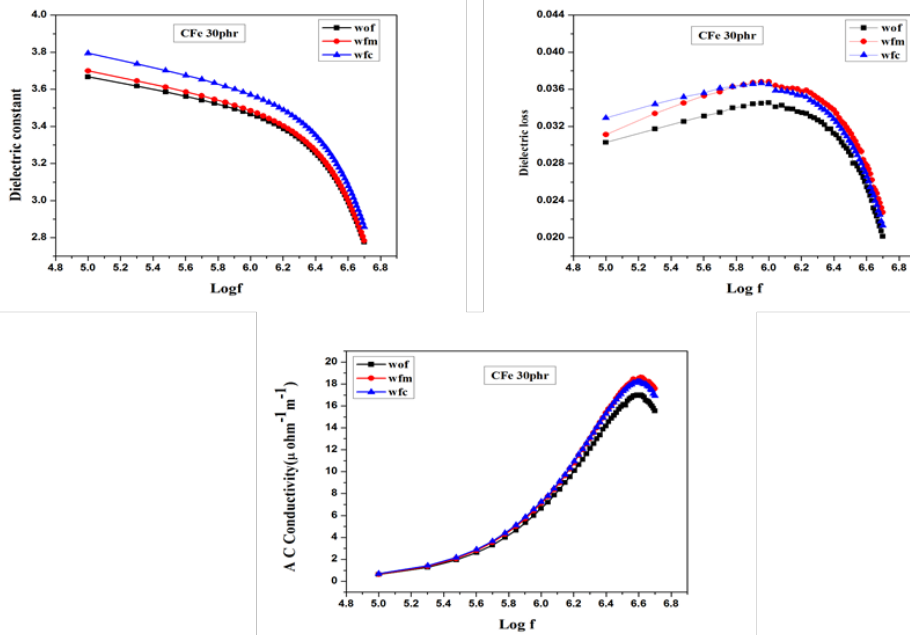
Figure 7.2 *Dielectric constant, Dielectric loss, AC conductivity of MRE sheets based on NR and Carbonyl Iron R20 for WF(C),WF(M).WOF samples at 30 phr loading(a) Dielectric constant(b)Dielectric loss(c) AC conductivity*
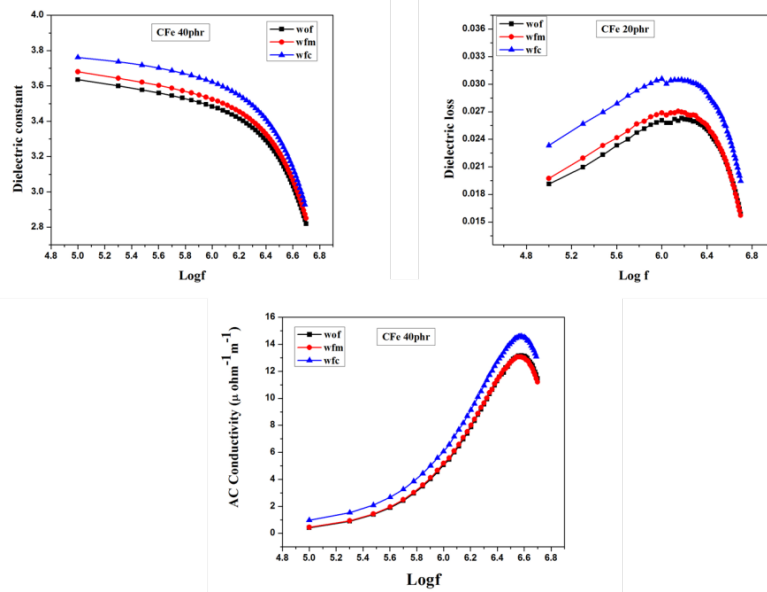
Figure 7.3 *Dielectric constant, Dielectric loss, AC conductivity of MRE sheets based on NR and Carbonyl Iron R20for WF(C),WF(M).WOF samples at40 phr loading(a) Dielectric constant(b)Dielectric loss(c) AC conductivity*

The variation of dielectric constant with different weight percentages of Carbonyl IronR20 and are depicted in figure 7.4. The dielectric loss (tanδ) is also plotted for different loading and is shown in figure 7.5.
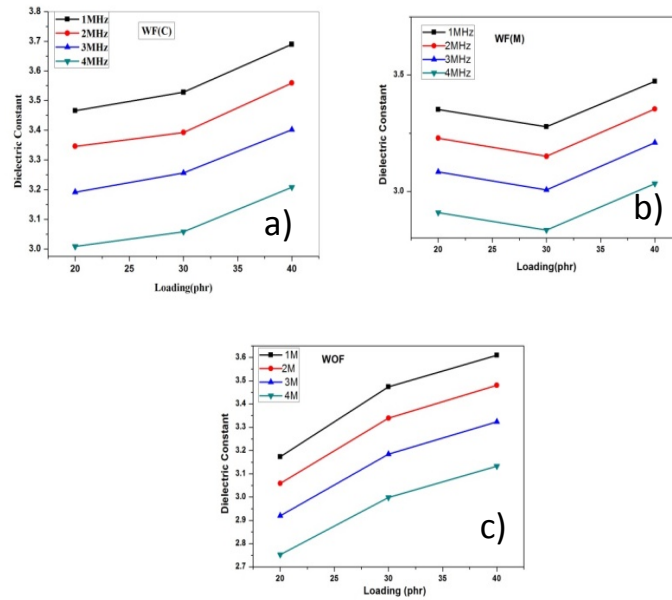
Figure 7.4 *Variation of Dielectric constant with different loading of Carbonyl Iron R20 (a) WF(C), (b) WF(M) and (c)WOF*
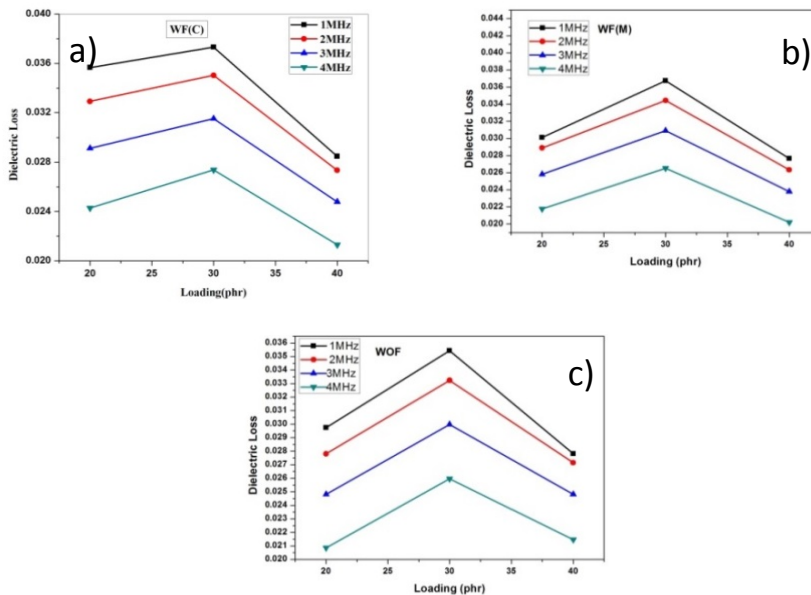
Figure 7.5*Dielectric loss with different loading of Carbonyl Iron R20 (a) WF(C), (b) WF(M) and (c)WOF*

The variation of dielectric permittivity with frequency is akin to the Maxwell Wagner model where interfacial polarization plays a crucial role in determining the overall permittivity of the composite. The incorporation of solid conducting particles in a rubber matrix can trigger polarizations which might contribute to the overall permittivity of the composite. As discussed in the previous section, the phenomenon can be explained on the basis of Maxwell Wagner model of interfacial polarization and Koops phenomenological theory. In this model, it is assumed that the dielectric structure is imagined to be consisting of well conducting grains which are separated by poorly conducting grain boundaries. It is reported that the high value of dielectric constant at lower frequencies can be accounted by this theory for heterogeneous double layer dielectric structures [6, 7, 8]. Here in MREs the filler present in the elastomer matrix could act as a minute capacitor and can contribute to Maxwell Wagner type interfacial polarization. Considering that the material has a single relaxation time in the frequency regime under test, it is possible to write the equations for complex dielectric permittivity as

$$\varepsilon^*(\omega) - \varepsilon_\alpha = \frac{\varepsilon_s - \varepsilon_\alpha}{1 + i\omega\tau} \tag{7.1}$$

where $\varepsilon^*(\omega)$ is the complex permittivity at the frequency ω and ε_α is the permittivity at optical frequencies. The above equation can be written as real and imaginary parts separated as

$$\varepsilon'(\omega) = \varepsilon_\alpha + \frac{\varepsilon_s - \varepsilon_\alpha}{1 + \omega^2\tau^2} \tag{7.2}$$

And $$\varepsilon''(\omega) = (\varepsilon_s - \varepsilon_\alpha)\frac{\omega\tau}{1 + \omega^2\tau^2} \tag{7.3}$$

This is Debye equations. The decrease in dielectric permittivity with increase in applied frequency is therefore understood according to equation 7.2 [9, 10].

A decrease in dielectric permittivity with increase in frequency is on expected lines as in the case of lossy dielectric materials. This is due to the dielectric relaxation of the isoprene molecule or the combined effect of the matrix and the filler [11, 12]. The speed of dipole rotation at high frequencies is unable to match the variation in the applied ac bias during measurements. The decrease in dielectric constant could be because of the reduced polarization with increase in frequency. The dielectric polarization is the sum of contribution arising from electronic, ionic, orientational and interfacial/space charge.

$$\alpha = \alpha_e + \alpha_i + \alpha_o \qquad (7.4)$$

Each of these three types of polarizations is a function of frequency of the applied field. But in a non-polar molecule the polarization arises from two effects. The electric field will cause a displacement of the electrons relative to the nucleus in each atom (electronic polarization) and also a displacement of the atomic nuclei relative to one another (atomic polarization), the former effect being generally the greater. Hence the equation becomes

$$\alpha = \alpha_e + \alpha_i \qquad (7.5)$$

In the system under study, dielectric dispersion is mainly due to the electronic polarization. At lower frequencies, the variation of dielectric constant is insignificant whereas at high frequencies, comparatively sharp decrease is observed. It is presumed that at low frequencies, polarizations respond favourably with the applied electric field.

The dielectric constant increases with the loading of the filler (Carbonyl Iron) and is linear in nature (figure 7.4). This behaviour obeys the rule of mixtures and can be fitted to near perfection with any of the following equations[13, 14].

In a mixture containing m components, the dielectric constant ε^* is connected by a relation, where log ε^* is given by

$$\sum_{i=1}^{m} Y_i log\varepsilon_i$$

Whereε^* is the dielectric constant of the mixture and y is the volume fraction of the component. For a two component system, the relationship can be written as

$$\log \varepsilon^* = y_1 log\varepsilon_1 + y_2 log\varepsilon_2 \qquad (7.6)$$

whereε^* is the dielectric constant of the composite, ε_1, y_1 and ε_2, y_2 are the dielectric constants and the volume fractions of the matrix and the filler components respectively.

Another mixture equation, which is used to calculate the dielectric constant of the mixture, is given by

$$\varepsilon^* A = {\varepsilon_1}/{(1-y)^3} \qquad (7.7)$$

Hereε_1 is the permittivity of the matrix and y is the volume fraction of the inclusion or filler. These formulae have their own limitations. Equation 7.7 is applicable for a composite containing conducting filler and cannot be applied to a composite containing an insulating filler. For a two component system consisting of a non-polar matrix and insulating filler of the ferrite type, the relationship can be written with the help of an equation of the form

$$\varepsilon^* = \varepsilon_1\{[2\varepsilon_1 + \varepsilon_2 + 2y(\varepsilon_2 - \varepsilon_1)]/[2\varepsilon_1 + \varepsilon_2 - 2y(\varepsilon_2 - \varepsilon_1)]\} \quad (7.8)$$

Where $\varepsilon_1$isthe dielectric constant of the blank matrix, ε_2 is the dielectric constant of the uniformly distributed (by volume) spherical inclusions and let y be the volume

fraction of the inclusion and ε^* is the dielectric constant of the matrix mixture or the composite.

However, we have not attempted a calculation to see which one of them exactly fits the observed values because of the non-availability of experimental values of dielectric permittivity of the filler. It can be seen that the variation pattern remains the same for field cured samples. Samples cured with a solenoid WF(C) shows the highest dielectric permittivity while the samples cured under a permanent magnet WF(M) has permittivity values in between that of WF(C) and WOF. The enhancement of dielectric permittivity arises from the orientation of Carbonyl particles within the rubber matrix. Perhaps, the formation of conductive layers of Carbonyl Iron inside the matrix as is evident from SEM micrographs also influences the dielectric permittivity. At low frequencies a value of 3.7 was obtained for samples cured under a permanent magnet.
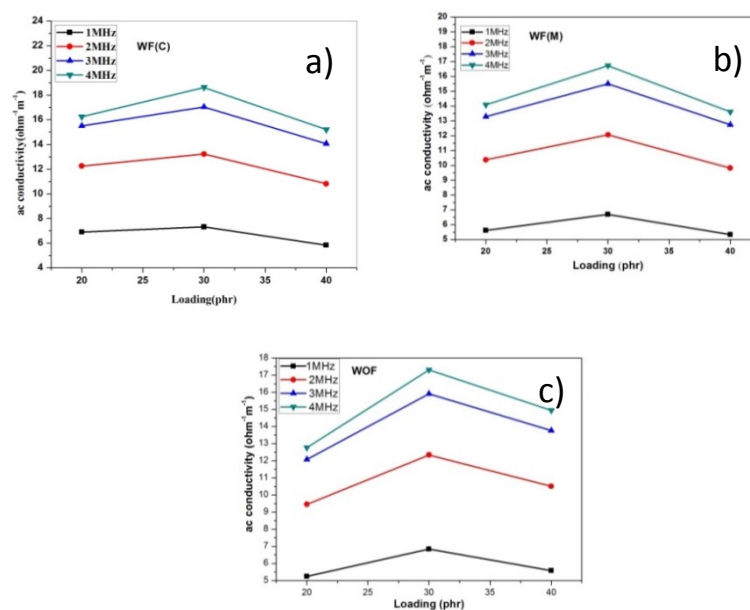
Figure 7.6. Variation in ac conductivity of MRE sheets with different loading of Carbonyl Iron R20 (a) WF(C), (b)WF(M) & (c)WOF

The dielectric loss and ac conductivity was evaluated using the formula

138

$$\sigma_{ac} = \varepsilon_0 \varepsilon' \omega tan\delta \qquad (7.9)$$

It may be noticed that the dielectric loss is relatively less and augurs well for applications. The variations of ac conductivity with loading are shown in figure 7.6.Initially the loss increases with loading and it reaches maximum value at 30 phr and then decreases for 40 phr. This is interesting and needs further investigations.

To investigate the effect of a magnetic field on dielectric constant, dielectric loss and ac conductivity of MR elastomer, a special type sample holder was utilized. By means of set of permanent magnets a magnetic field was produced and above values was estimated as in the previous cases. A magnetic field of 0.2 T was applied during measurements. The variation of permittivity and loss with frequency are shown in figure 7.7 and7.9 respectively.

(a)   (b)
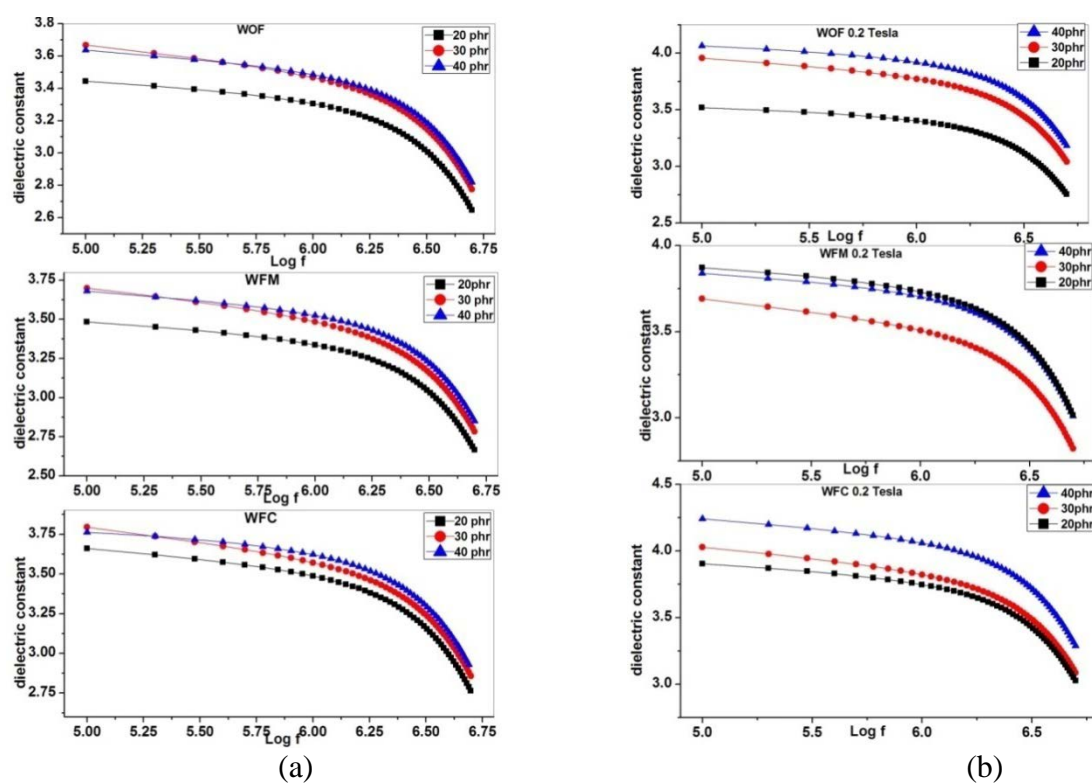
Figure7.7. Change in dielectric constant of WF(C), WF (M) and WOF samples with frequencies in a magnetic field (a) without field (b) in a magnetic field of 0.2 T
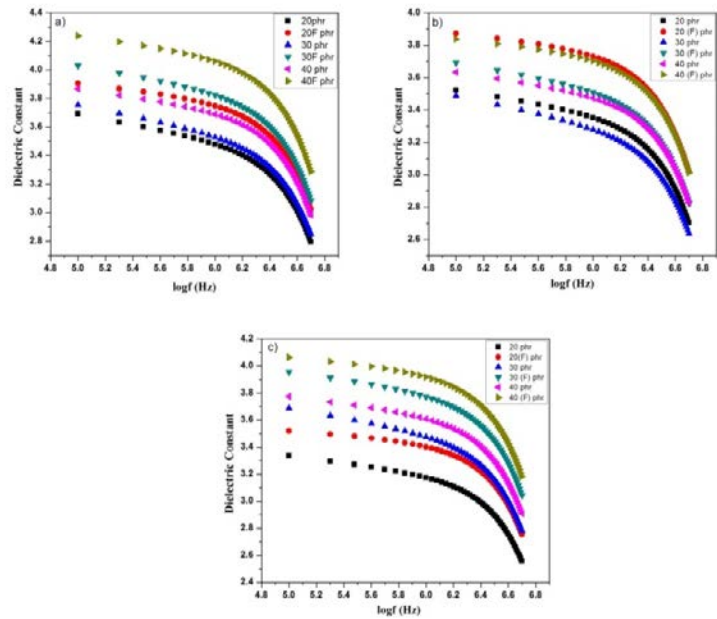
Figure 7.8. Change in dielectric constant of MR elastomer sheets with frequency in accordance with different loading, in the presence and absence of magnetic field for all the samples a) WF(C), b) WF(M) and c) WOF

(a)   (b)
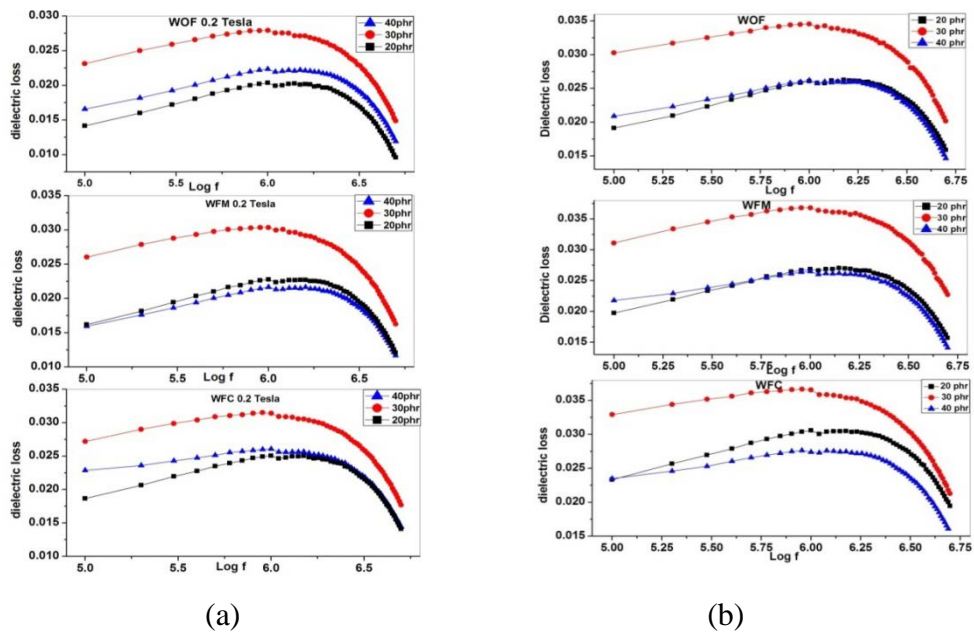
Figure 7.9. Change in dielectric loss of WF(C), WF (M) and WOF samples with frequencies in a magnetic field (a) without field (b) in a magnetic field of 0.2 T

140

From figure 7.7, it can be seen that the dielectric constant increases in the case of MR elastomer in a magnetic field of 0.2 T. The maximum value of dielectric constant obtained is 4.25and for WF (C) samples. This increase in dielectric constant is less in WOF samples to WF (M) samples. Dielectric constant increases with loading in all cases and a corresponding increase in dielectric constant can be seen in measurements taken in the presence of magnetic field is as shown in figure 7.8.

Dielectric loss of all samples increases from 20phr loading to 30 phr and then decreases at 40 phr. With respect to frequency, dielectric loss increases and reaches a maximum value for a particular frequency and then decreases. Application of a magnetic field during test decreases dielectric loss of the sample and the maximum reduction was observed for WF (M) samples as shown in Figure 7.9

(a)   (b)

Figure 7.10. Change in ac conductivity of WF(C),WF (M) and WOF samples with frequencies in a magnetic field (a) without field (b) in a magnetic field of 0.2 T

141
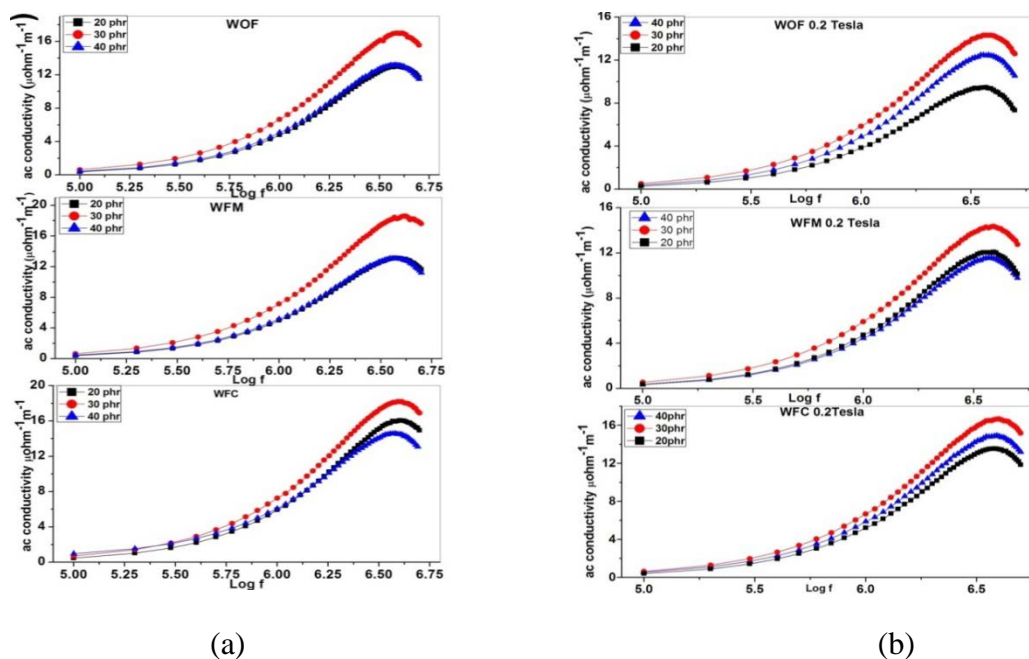
For all samples ac conductivity increases with frequency, attains a maximum value for a particular frequency and then decreases which is depicted in Figure 7.10. This particular frequency is somewhat different from that for dielectric loss. Application of a magnetic field during the test diminishes the ac conductivity. The observed change in dielectric permittivity of isotropic MR elastomers can be attributed to the structural reorganization of the magnetic filler within the polymer matrix under the action of the field.

To describe this observed effect of magnetic field on dielectric constant we can consider the plane capacitor-MRE model proposed by Anna *et al* [15].
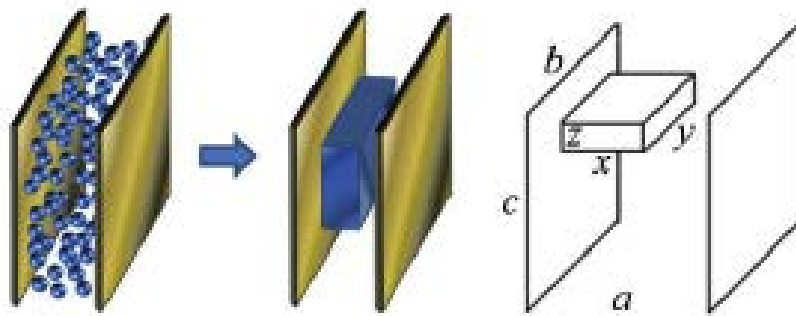
Figure7.11. Plane capacitor with a metal parallelopiped particle placed inside the capacitor.

It has been proposed that in the absence of an external magnetic field the MRE sample represents a dielectric medium with homogeneously distributed metal particles where its capacitance can be estimated as the capacitance of a capacitor with a parallelopiped metal particle placed between its plates and the dimensions of this metal parallelepiped are defined by the total volume concentration of the magnetic filler within the MRE.

If $c_{vol} = \eta^3$ then,

$$x = \eta a, \; y = \eta b, \; z = \eta c \qquad (7.10)$$

and the effective capacity of the capacitor $a \times b \times c$ with the metal particle x $\times y \times z$ (x, y, z < a) is calculated.

Thus the final capacitance reads

$$C_{final} = \varepsilon_0 \varepsilon \frac{abc + xyz - bcx}{a(a-x)} \qquad (7.11)$$

The value of C_{final} depends on the size x of the metal parallelepiped particle.

This simple consideration shows that the capacity of a plane capacitor partly filled with a conducting material depends not only on the volume fraction of the metal part but also on its spatial distribution. Thus when a uniform magnetic field is applied to a piece of a MRE the magnetic moments of the filler particles tend to orient with the magnetic field lines, and the particles try to organize themselves into chains parallel to the magnetic field[5]. In the course of this structuring, the particle density in the direction of the field increases while that in the perpendicular direction decreases.

Thus, we can say that the particle structuring does not change the volume of the equivalent metal parallelepiped V= xyz, instead it changes the size of the parallelepiped, in particular, the size x, thus, changing the capacitance according to equation 7.11. When the magnetic field is directed perpendicular to the plane of the capacitor, the size x' of the equivalent metal parallelepiped becomes larger and the sizes y' and z' become smaller in comparison with those for the homogeneous distribution of particles without the magnetic field (x, y, z). Let x'=βx, β> 1. As a result, the capacity of the capacitor increases. In the case of a magnetic field applied parallel to the capacitor plane y'= yβ, x'= yβ$^{-1/2}$ and the sign of the effect would be opposite and hence the result.

7.4. CONCLUSION

Dielectric properties of MR elastomer sheets were studied. The dielectric constant of all samples increases with loading and decreases with frequency.Dielectric loss and ac conductivity increases from 20 phr loading to 30 phr and decrease at 40 phr.Dielectric loss and ac conductivity initally increase with frequency reach a maximum value and then decreases.Application of a magnetic field enhances the dielectric constant of all samples and a moderate value is obtained for WF(C) samples.Dielectric loss and ac conductivity decreases with the application of a magnetic field keeping the same trend of loading for zero field measurement.These MREs can be thought of as potential magneto capacitors or even for making sensors based on the principle of magnetocapacitance.

REFERENCES

[1]. IoanBica, J. Ind. Eng. Chem. **15**(2009), 605

[2]. N Kchit, G Bossis, J. Phys. D: Appl. Phys.**42**(2009), 105505

[3]. N Kchit, P Lancon and G Bossis, J. Phys. D: Appl. Phys.,**42**(2009) 105506

[4]. Guangtao Du, Xiangdong Chen, Measurement,**45** (2012) 54

[5]. N Kchit and G BossisJ. Phys.: Condens. Matter **20**(2008) 204136

[6]. C. G. Koops, Phys. Rev.83, **121**(1957).

[7]. J. Maxwell, Electricity and magnetism, 1(1873)

[8]. K. Wagner, Ann.Phys. **40**(1913), 817

[9]. E Muhammad Abdul Jamal, D SakthiKumarand M R Anantharaman, Bull. Mater. Sci. **34**(2011), 251

[10]. M.R.Anantharaman, K.A.Malini, S.Sindhu, E.M.Mohammed, S K Date, S D Kulkarni, P A Joy, and Philip Kurian, Bull. Mater. Science, **24**(2001) 623

[11]. GVStepanov,DYuBorin, Yu L Raikher, P V Melenev and NSPerov-J. Phys.: Condens. Matter-**20**(2008) 204121

[12]. S. Devikala, P. Kamarajand M. Arthanareeswari-Chem. Sci. Trans.,**2(S1)**(2013)129

[13]. M R Anantharaman,S Sindhu,S jagatheesan,K A Malini and P Kurian-J.Phys.D:Appl.Phys.**32**(1999)1801

[14]. K.A.Malini, E.M.Mohammed P. Kurian,M.R.Anantharaman, Mater. Res. Bull.,**37**(2002)753

[15]. Anna S. Semisalova, Nikolai S. Perov, Gennady V. Stepanov, Elena Yu. Kramarenko and Alexey R. Khokhlov, Soft Matter. **9**(2013) 11318

CHAPTER 8

CONCLUSION AND FUTURE PROSPECTS

Research is perennial in nature and no work is cent percent perfect, though nature is an embodiment of perfection. She does not bestow that attribute to her worshippers. This piece of investigation is not above that rule. So there exists room for improvement and perfection. This is what gives rise to removal of obsolescence in technological jargons and in scientific terms it is called the 'constant endeavor' to change, improvise and innovate. As the old saying goes it is this 'constant' which is called 'change' which drives research, innovation and lead to incremental science.

The field of magnetorheological elastomers is nascent and is constantly updated by researchers on a day to day basis. They are the solid state analogues of the much familiar rheological fluid which are in vogue for many engineering applications including automobile, aerospace and biomedical.

However, the main drawback of rheological fluids is that they are to be contained safely in a container and this limits its applications. Though, as a substitute, electrorheological materials came up, they lost their sheen because of the necessity to apply a large electric field as an external stimuli. These lacunae caught the imagination of scientists and engineers and people started thinking of a soft material which can be manipulated by a noncontact external stimulus. This eventually evolved in to magnetorheological elastomers. This piece of work is also to be seen as another attempt in fabricating magnetorheological elastomers under the influence of an external magnetic field during curing/moulding.

The primary task in the first phase of this thesis was to design and fabricate instrumentation and other accessories. This particular task was accomplished with near perfection. Setups for moulding MRE sheets and rods were fabricated in house.

Two separate setups were made for providing a field parallel to the plane of the sheet/rod and perpendicular to the plane of the sheet.

A fully automated system for the measurement of magnetostriction was made based on the principle of Laser Doppler Vibrometry. Power amplifiers and solenoid assemblies were specially designed and made for this. A cell for evaluating the magnetocapacitance of MREs with provision for applying an external magnetic field was also designed and fabricated which was integrated to an LCR meter for automatic data acquisition system.

In the second phase, MREs (both rods and sheets) were made by incorporating Iron and Carbonyl Iron fillers in different weight percentages in a matrix of Natural Rubber. The quality of rods and sheets are almost factory made grade. This process of moulding can be scaled up for mass production.

The evaluation of microactuation of these MREs revealed that MREs based on Natural Rubber and Iron exhibited enhanced actuation and the results were explained based on stiffness and morphology. Comparable results were obtained for MREs based on Carbonyl Iron and Natural Rubber.

The evaluation of mechanical properties of MRE sheets and rods were also conducted and the findings are encouraging. Loading always enhanced the mechanical properties. Stiffness, which is a very important parameter in the performance of an MRE determines the vibration absorbing property of a device, is found to be decreasing on field cured rod/sheet samples. The application of a magnetic field modifies parameters like storage modulus, loss modulus, loss factor (tanδ), Young's modulus, stiffness, and resonant frequency.

The magneto dielectric properties of MREs were evaluated and the results are quite promising. The dielectric constant of MRE cured under the application of a field

perpendicular to the plane of the sheet was found to be the maximum. Loading always improved the magnetic as well as the magneto dielectric properties of these MREs.

Huge scope exists for improvement. The explanation provided for the modified mechanical properties of MREs is quite tentative and requires further studies to fit the results based on a mathematical model. The interaction process taking place between the polymer and an aligned filler is quite complex and demands a separate investigation. It is a good idea to link morphology with the properties of field cured MREs.

As far as tensile and hardness of MREs are concerned, scope exists to make MREs with reinforcing fillers like carbon black or carbon nano tubes. It is known that carbon black and carbon nano tubes reinforce the mechanical properties of elastomers substantially. The advantage of using carbon nano tubes is that the loading percentage need not be very high to achieve superlative strengths. This is a futuristic proposition.

An altogether different matrix like silicone rubber can be a replacement for Natural Rubber. In the event of employing Silicone Rubber a transparent MRE can be realized by incorporating small amounts of hard magnetic materials like TERFENOL-D or Samarium Cobalt.

The prospects of a transparent MRE which can be externally manipulated by light as well as a magnetic field are quite bright as far as applications are concerned. From an application point of view an active vibration control can be designed with an MRE having the required mechanical and magnetic properties. A force sensor can also be designed and demonstrated.

The magneto dielectric measurements carried out on MRE sheets are quite promising in the sense that they exhibit low loss as well as reasonable dielectric constant. However, as of now, no idea about the dielectric breakdown is available. An

earth quake resistant device could be made with these MREs which can be active and self-controllable. The design of such a system needs modeling based on finite element analysis and is earmarked for the future. Altogether the results are encouraging and have opened up further avenues for future research.